



UNIVERSITY OF TUNIS EL MANAR
NATIONAL ENGINEERING SCHOOL OF TUNIS
FACULTY OF SCIENCES OF TUNIS

Spectral analysis and fast methods for large matrices arising from PDE approximation

Thesis submitted to obtain the grade of

Doctor of Philosophy

Laboratory of Mathematical and Numerical Modelling in Engineering Sciences

Applied Mathematics

Ryma Imene RAHLA

Under the supervision of

Skander BELHAJ and Stefano SERRA-CAPIZZANO

*"MATHEMATICS IS THE LANGUAGE IN
WHICH GOD HAS WRITTEN THE
UNIVERSE"*

Galileo Galilei

I dedicate my Ph.D. thesis to my wonderful supervisor Stefano SERRA-CAPIZZANO

ACKNOWLEDGEMENTS

First and foremost, I would like to thank Almighty **GOD** for providing me the courage and patience to accomplish this work.

I would like to thank my thesis supervisor **Pr. Skander BELHAJ** for guiding me and for his patience, availability, and invaluable assistance during my thesis years.

I am grateful to my co-supervisor **Pr. Stefano SERRA-CAPIZZANO** for sharing his knowledge and experience with me. All my gratitude for your trust and prompt assistance. Finally, during this project, I was acutely aware of his human qualities of listening and comprehension.

I would like to express my heartfelt appreciation to **Pr. Amel BEN ABDA** for the privilege of chairing the jury.

I would like to express my gratitude to **Pr. Carla MANNI** and **Pr. Paris VASSALOS** for agreeing to be the reviewers of my thesis work and for their insightful comments that helped me improve the quality of this manuscript. I would like to thank them for granting me this honour by serving on this jury.

It is also with pleasure that I thank **Pr. Maher MOAKHER** for the honour of reviewing my work as a defense examiner.

My heartfelt gratitude goes to my parents, who have consistently supported me during these hard years of study. Thank you so much for your words of encouragement, love, and spiritual support. GOD protect you and provide you luck, health, and a long life. A big thank you also to my brother, sisters, grandmother, uncle and aunts.

My thoughts also go to my friends. I sincerely appreciate them for the memories we enjoyed together, even if our reunions and meetings are becoming increasingly distant.

Many thanks to all my collaborators, without whom this work would have not been possible.

Finally, I would like to thank everyone who helped me to develop this study, whether directly or indirectly.



LIST OF TABLES

3.1	Minimum and maximum of surfaces s_i , $i = 1, \dots, k^2$. $u = -7.351326809400116e-01$, $v = 2.500707752257475e+00$, $w = 3.053628059289279e+00$, $z = 1.734159144781565e + 00$, $a = 2.576105975943630e - 01$, $b = -2.224247598741574e+00$, $c = 2.896548426609789e+00$, $d = 1.507964473723100e+00$, $e = 1.043008760991811e + 00$, $f = 2.161415745669778e + 00$, $g = 1.627344994559513e+00$, $h = 2.796017461694915e+00$, $i = 7.099999397112930e-01$, $l = 9.550441666912972e - 01$, $m = 2.519557308179014e + 00$	69
3.2	Number of PCG iterations to reach convergence with respect to relative residual less than 1.e-6, Preconditioner $P_n(a)$, $a(x, y) = \exp(x + y)$	79
3.3	Number of PCG iterations to reach convergence with respect to relative relative residual less than 1.e-6 - case $k = 2$	79
3.4	Number of outliers n_{out} (eigenvalues not belonging to $(1 - \varepsilon, 1 + \varepsilon)$ with $\varepsilon = 1.e-1$) and their percentage with respect to the dimension. The second and third columns refer to the Toeplitz case, the fourth and fifth columns to the case of the FEM matrix.	79
3.5	Number of PCG iterations to reach convergence with respect to relative relative residual less than 1.e-6 - case $k = 3$	80
3.6	Number of PCG iterations to reach convergence with respect to relative relative residual less than 1.e-6 - case $k = 4$	80

4.1	Number of iterations needed for the convergence of the two-grid and V-cycle methods for $k = 1, 2, 3$ in one dimension with $a(x) \equiv 1$ and $\text{tol} = 1 \times 10^{-6}$	90
4.2	Number of iterations needed for the convergence of the two-grid and V-cycle methods for $k = 2$ in one dimension with $a(x) \equiv 1$ and $\text{tol} = 1 \times 10^{-2}, 1 \times 10^{-4}$, and 1×10^{-8}	97
4.3	Number of iterations needed for the convergence of the two-grid and V-cycle methods for $k = 3$ in one dimension with $a(x) \equiv 1$ and $\text{tol} = 1 \times 10^{-2}, 1 \times 10^{-4}$, and 1×10^{-8}	98
4.4	Number of iterations needed for the convergence of the two-grid and V-cycle methods for $k = 1, 2, 3$ in dimension $d = 2$ with $a(\mathbf{x}) \equiv 1$	100
4.5	Number of iterations needed for the convergence of the two-grid and V-cycle methods for $k = 2$ in one dimension with $a(x) = e^x$, $a(x) = 10x + 1$, $a(x) = x - 1/2 + 1$, and $\text{tol} = 1 \times 10^{-6}$	100
4.6	Number of iterations needed for the convergence of the two-grid and V-cycle methods for $k = 2$ in two dimensions with $a(x, y) = e^{(x+y)}$, $a(x, y) = 10(x+y) + 1$, $a(x, y) = x - 1/2 + y - 1/2 + 1$, $a(x, y) = 1$ if $x \leq 1/2$ and $y \leq 1/2$, 5000 otherwise, and $\text{tol} = 1 \times 10^{-6}$	101

LIST OF FIGURES

3.1	Friedrics-Keller meshes for \mathbb{P}_k , $k = 1, 2$	57
3.2	Reference element \hat{K} and nodal points for \mathbb{P}_k , $k = 1, \dots, 4$	58
3.3	Nodal points reordering in \mathbb{P}_2 and \mathbb{P}_3 cases.	63
3.4	Ordered equispaced samplings of $\lambda_j(a(x, y)\mathbf{f}_{\mathbb{P}_k}(\boldsymbol{\theta}))$, $j = 1, \dots, k^2$ (green dots) and ordered eigenvalues $\lambda_l(A_n(a, \Omega, \mathbb{P}_k))$ with $a(x, y) \equiv 1$	81
3.5	Ordered equispaced samplings of $\lambda_j(a(x, y)\mathbf{f}_{\mathbb{P}_k}(\boldsymbol{\theta}))$, $j = 1, \dots, k^2$ (green dots) and ordered eigenvalues $\lambda_l(A_n(a, \Omega, \mathbb{P}_k))$ with $a(x, y) = e^{x+y}$	82
3.6	Ordered equispaced samplings of $\lambda_j(a(x, y)\mathbf{f}_{\mathbb{P}_k}(\boldsymbol{\theta}))$, $j = 1, \dots, k^2$ (green dots) and ordered eigenvalues $\lambda_l(A_n(a, \Omega, \mathbb{P}_k))$ with $a(x, y) = 1 + 2\sqrt{x} + y$	83
3.7	Ordered equispaced samplings of $\lambda_j(a(x, y)\mathbf{f}_{\mathbb{P}_k}(\boldsymbol{\theta}))$, $j = 1, \dots, k^2$ (green dots) and ordered eigenvalues $\lambda_l(A_n(a, \Omega, \mathbb{P}_k))$ with $a(x, y) = 1$ if $y \geq x$ and $a(x, y) = 2$ otherwise.	84
4.1	Construction of the \mathbb{Q}_2 prolongation operator: basis functions on the reference element.	91
4.2	Check of conditions for \mathbb{Q}_2 prolongation: (left) the plot of the eigenvalues of $\mathbf{p}(\vartheta)^*\mathbf{p}(\vartheta) + \mathbf{p}(\vartheta + \pi)^*\mathbf{p}(\vartheta + \pi)$ for $\vartheta \in [0, 2\pi]$; and (right) the plot of the eigenvalues of $R(\vartheta)$ for $\vartheta \in [0, 2\pi]$	94
4.3	Construction of the \mathbb{Q}_3 prolongation operator: basis functions on the reference element.	99

4.4 Check of conditions for \mathbb{Q}_3 prolongation: **(left)** the plot of the eigenvalues of $p(\vartheta)^H p(\vartheta) + p(\vartheta + \pi)^H p(\vartheta + \pi)$ for $\vartheta \in [0, 2\pi]$; and **(right)** the plot of the eigenvalues of $R(\vartheta)$ for $\vartheta \in [0, 2\pi]$ 99

CONTENTS

Introduction	13
1 Notations, definitions and preliminaries	21
1.1 General notations	21
1.1.1 Multi-index notation	24
1.2 Matrix norms	25
1.2.1 The norms induced by vector norms	26
1.2.2 Frobenius norm	26
1.2.3 The Schatten norms	26
1.2.4 The Euclidean norm weighted by a matrix	27
1.3 L^p spaces	28
1.4 Iterative Methods	29
1.4.1 Preconditioning	31
1.4.2 Multigrid Methods	33
2 Spectral properties of matrix-sequences described by a function	39
2.1 Asymptotic distribution of matrix-sequences	39
2.2 Zero-Distributed matrix-sequences	43
2.3 Toeplitz and Circulant matrices	44
2.3.1 Scalar Toeplitz matrices	44
2.3.2 Scalar Circulant matrices	46
2.3.3 Multilevel block-Toeplitz matrices	47

2.3.4	Multilevel block Circulant matrices	49
2.4	Generalized Locally Toeplitz (GLT) sequences	50
3	Spectral analysis of \mathbb{P}_k Finite Element Matrices in the case of Friedrichs-Keller triangulations via GLT Technology	53
3.1	Finite Element approximation	54
3.2	A Few remarks on the monodimensional case: $\mathbb{Q}_k \equiv \mathbb{P}_k, d = 1$. . .	55
3.3	Two dimensional case: $\mathbb{P}_k, d = 2$ - symbol definition	56
3.3.1	Case $k = 1$	59
3.3.2	Case $k = 2$	60
3.3.3	Case $k = 3$	64
3.4	Symbol spectral analysis	68
3.4.1	Extremal eigenvalues and conditioning	74
3.5	The case of variable coefficients and non-Cartesian domains	75
3.6	Preconditioning and complexity issues	77
4	Multigrid for \mathbb{Q}_k Finite Element Matrices Using a (Block) Toeplitz Symbol Approach	85
4.1	Optimality of two-grid method in the case of Toeplitz matrices . . .	86
4.2	Structure of the Matrices and Spectral Analysis	87
4.3	Multigrid Strategy Definition, Symbol Analysis, and Numerics . . .	87
4.3.1	\mathbb{Q}_1 Case	88
4.3.2	\mathbb{Q}_2 Case	90
4.3.3	\mathbb{Q}_3 Case	94
	Conclusion and Perspectives	103
	Bibliography	104

INTRODUCTION

Mathematical modelling occurs in several areas: chemistry, economy, physics, engineering and many other fields. It consists in presenting mathematically a real phenomenon such that the theoretical or numerical analysis of this mathematical presentation gives answers, insights, and direction relevant to the original application.

When modelling complex systems, such as elastic deformation, wave propagation, heat transport, etc., Partial Differential Equations (PDEs) are frequently encountered, and in general, the analytical solution of these PDEs seldom has a closed form expression. Thus, it is critical to use appropriate numerical approaches to estimate the solution \mathbf{x} of the PDE.

The principle behind numerical approximations is to convert the PDE, from its continuous form, to a discrete version, by introducing a mesh depending on a parameter n , and gradually refined when n increases. Thus, the initial infinite-dimensional PDE problem is reduced to a finite-dimensional problem whose solution \mathbf{x}_n converges to \mathbf{x} , when n tends to ∞ . Thus, by considering a linear approximation of the linear PDE of the form

$$\mathcal{A}\mathbf{x} = \mathbf{b},$$

(where \mathcal{A} indicates the linear differential operator), and by refining progressively the mesh, we obtain a sequence of linear systems of the form

$$\{A_n\mathbf{x}_n = \mathbf{b}_n\}_n.$$

These linear systems are in general of large dimensions, as the dimension of the problem depends on the number of discretisation points, and therefore, increasing the size of the system is essential to attain more precision. Thus, the study of appropriate techniques frequently focuses on analysing their behaviour as the system size grows. As a result, it is essential to analyse not only the single system $A_n \mathbf{x}_n = \mathbf{b}_n$ but also the entire sequence of linear systems $\{A_n \mathbf{x}_n = \mathbf{b}_n\}_n$ that depends on n .

The matrices arising from the approximation of PDEs with constant coefficient when using local methods such that Finite Elements, Finite Differences, etc., are frequently of type Toeplitz in the monodimensional case and multilevel block Toeplitz in multidimensional case. Nevertheless, the approximation of PDEs with a non-constant coefficient, gives rise to matrix-sequences belonging to the Generalized Locally Toeplitz (GLT) class.

For the resolution of a large ill-conditioned system, direct methods are usually unstable [15] and require high computational time. Moreover, these methods do not take fully into consideration the structure or sparsity of the matrix in order to minimize the number of algebraic operations or optimize the storage space.

On the other hand, iterative methods such as multigrid and preconditioned Krylov methods are much more favourable: they are less sensitive to numerical instability caused by the ill-conditioning and more adapted to problems of specific structure since they use the spectral information of the given matrix.

The spectrum of the matrix has a major effect on the convergence of the related system. Regarding the structured matrix-sequences, the asymptotic distribution of the spectrum of the discretized problem is described by a function called "symbol", that is, for all continuous functions with bounded support $F \in C_c(\mathbb{C})$, the spectrum of A_n has a spectral distribution as the symbol $\mathbf{f} : D \subset \mathbb{R}^t \rightarrow \mathbb{C}^{r \times r}$ in the sense of the eigenvalues:

$$\lim_{n \rightarrow \infty} \frac{1}{d_n} \sum_{i=1}^{d_n} F(\lambda_i(A_n)) = \frac{1}{\mu_t(D)} \int_D \frac{\sum_{i=1}^r F(\lambda_i(\mathbf{f}(\mathbf{x})))}{r} d\mathbf{x}, \quad (1)$$

where D is a measurable subset with $0 < \mu_t(D) < \infty$, and $\lambda_i(A_n), \lambda_j(\mathbf{f}(\mathbf{x}))$, $i = 1, \dots, d_n, j = 1, \dots, s$, represent the eigenvalues of A_n and the eigenvalues of \mathbf{f} , respectively. The interpretation of the relation (1) is as follows: as $d_n \rightarrow \infty$, the spectrum of A_n is approximated by evaluating of the eigenvalues of the symbol

$\lambda_i(\mathbf{f}(\mathbf{x}))$ over an equispaced grid on D .

The analysis of the symbol gives a precise information regarding the asymptotic behaviour of the spectrum of A_n . For instance when the matrix A_n is Hermitian, the symbol often provides an effective estimation of the spectral condition number A_n for sufficiently large n .

The objective of this thesis is to illustrate some concrete examples in order to show the role of the symbol in analysing the spectrum of the matrix and in performing an efficient method to solve the problem arising from PDE approximation. We deal with a class of elliptic partial differential equations with Dirichlet boundary conditions, where the operator is $\operatorname{div}(-a(\mathbf{x})\nabla\cdot)$, see (3.1), (4.1). In Chapter 3, we will investigate the features of the symbol, extracted from the matrices arising in the classical \mathbb{P}_k Finite Elements Approximation, while in Chapter 4, we will develop a multigrid method for the matrices resulting in the case of the \mathbb{Q}_k Finite Elements Approximation.

In the first part [58], we discuss the spectral analysis of matrix sequences resulting from the \mathbb{P}_k Lagrangian Finite Element approximation of the elliptic problem (3.1) where the operator is $\operatorname{div}(-a(\mathbf{x})\nabla\cdot)$, and a being continuous and positive on $\overline{\Omega}$.

Our theoretical analysis focuses on the stiffness matrix-sequences $\{A_n\}_n$ related to \mathbb{P}_k Finite Element approximations on uniform structured meshes [19, 35, 57, 63], such as Friedrichs-Keller triangulations, in which context the powerful spectral tools derived from the Toeplitz theory [12, 69, 38, 39, 71] greatly facilitate the required spectral analysis.

We provide a detailed study in the case where $a(\mathbf{x}) \equiv 1$. Then we sketch the general setting by considering a Riemann integrable diffusion coefficient a and/or a domain Ω not necessarily of Cartesian structure. We recall that the same type of analysis of the linear Finite Elements in two dimensions is already considered in [6, 55] for the same equation considered in our study, while coupled partial differential equations (PDEs) with stable pairs of Finite Element Approximations in two dimensions are considered in [30]. It is worth noticing the systematic work in [40], where the case of tensor rectangular Finite Element Approximations $\mathbb{Q}_{\mathbf{k}}$ of any degree $\mathbf{k} = (k_1, \dots, k_d)$ and of any dimensionality $d \geq 1$ is studied.

Following the pattern indicated in [40], we start a systematic approach for the Finite Element Approximations \mathbb{P}_k for $k \geq 2$ and for $d = 2$. The analysis for $d = 1$

is contained in [40], trivially because $\mathbb{Q}_k \equiv \mathbb{P}_k$ for every $k \geq 1$, while for $d = 2$, and even more for $d \geq 3$, the situation is greatly complicated by the fact that we do not encounter a tensor structure. Nevertheless, the spectral picture is quite similar and the obtained information in terms of spectral symbol is sufficient for deducing a quite accurate analysis concerning the distribution and the extremal behaviour of the eigenvalues of the resulting matrix-sequences.

More in details, regarding the resulting stiffness matrices, we will consider the following items, from the perspective of (block) multilevel Toeplitz operators [12, 75] and (block) Generalized Locally Toeplitz (GLT) sequences [69, 71]:

- spectral distribution in the Weyl sense,
- spectral clustering,

with a concise analysis of the extremal eigenvalues, conditioning, spectral localization, and where the ultimate objective is:

- the analysis and the design of fast iterative solvers for the associated linear systems.

We recall that the spectral distribution and the clustering results are essential components in the design and in the convergence analysis of specialised multigrid methods and preconditioned Krylov solvers [62], such as preconditioned conjugate gradient (PCG); see [71, Subsection 3.7] and [1, 5, 25, 26, 28, 34, 54] for more information. In fact, the knowledge of the spectral distribution is the key for explaining the superlinear convergence history of PCG, thus improving the classical bounds; see [5] and references therein. Most of our study is devoted to the identification of the spectral symbol using the GLT technology, and hence to the first item.

Numerous studies have investigated the spectral analysis of the matrices arising from PDE approximations, but with different approximation techniques. We mention, for instance, the case of the stiffness/collocation matrices coming from the \mathbf{k} -degree B-spline Isogeometric Analysis (IgA) approximation of maximal smoothness [20] of (3.1); see [27, 37]. The same kind of analysis in the case of $\mathbb{Q}_{\mathbf{k}}$ Finite Elements approximating again (3.1) is discussed in [40]. A review comparing the latter two approaches with a language tailored for engineers can be found in [44].

In the IgA case, the (spectral) symbol $f_{\text{IgA}_{\mathbf{k}}}$ describing the spectral distribution is a scalar-valued d -variate function defined over $[-\pi, \pi]^d$, and hence the eigenvalues

of the IgA discretization matrices are approximated by a uniform sampling of $f_{\text{IgA}_{\mathbf{k}}}$ over $[-\pi, \pi]^d$. In this context, the surprising behaviour is that, when all the spline degrees k increase, $f_{\text{IgA}_{\mathbf{k}}}(\boldsymbol{\theta})$ collapses exponentially to zero at all points $\boldsymbol{\theta} = (\theta_1, \dots, \theta_d)$ with some component $\theta_j = \pi$. According to the interpretation based on the theory of Toeplitz matrices and matrix algebras, this phenomenon implies that the IgA matrices are ill-conditioned, not only in the low frequencies (as expected), but also in the high frequencies, as in the approximation of integral operators [31]. Through the explicit use of this spectral information, it was possible to develop ad hoc iterative solvers with an optimal convergence rate, substantially independent of \mathbf{k} and d ; see [25, 26, 28].

In the $\mathbb{Q}_{\mathbf{k}}$ Lagrangian setting, we are still able to identify the spectral distribution, as for the IgA case. The related symbol $\mathbf{f}_{\mathbb{Q}_{\mathbf{k}}}$ is d -variate and defined on $[-\pi, \pi]^d$, but the surprise is that $\mathbf{f}_{\mathbb{Q}_{\mathbf{k}}}$ is a $N(\mathbf{k}) \times N(\mathbf{k})$ Hermitian matrix-valued function, with $\mathbf{k} = (k_1, \dots, k_d)$ vector of the partial degrees in the different directions, $N(\mathbf{k}) = \prod_{j=1}^d k_j$ (a similar situation is encountered when dealing with discontinuous Galerkin methods [7, 29]). No specific pathologies regarding $f_{\mathbb{Q}_{\mathbf{k}}}$ are observed for large \mathbf{k} at the points $\boldsymbol{\theta}$ such that $\theta_j = \pi$ for some j , implying that the source of ill-conditioning, with respect to the fineness parameters, is only in the low frequencies. However, exactly as in our \mathbb{P}_k setting, where the scalar k represents the global polynomial degree, we observe a serious dimensionality problem, since for moderate k and d , the quantity $N(k, d) = k^d$ is very large.

More specifically, the problem is that the spectrum of the $\mathbb{Q}_{\mathbf{k}}$ ($\mathbf{k} = (k_1, \dots, k_d)$, $d \geq 1$) Lagrangian Finite Element stiffness matrices is split into $N(\mathbf{k}) = \prod_{j=1}^d k_j$ subsets, or branches in the engineering terminology [21, 51, 52, 59], of approximately the same cardinality and the i -th branch is approximately a uniform sampling of the scalar-valued function $\lambda_i(\mathbf{f}_{\mathbb{Q}_{\mathbf{k}}})$, $i = 1, \dots, N(\mathbf{k})$. The exponential scattering (in \mathbf{k} and d) of the eigenvalue functions $\lambda_i(\mathbf{f}_{\mathbb{Q}_{\mathbf{k}}})$ provides an explanation of the difficulties encountered by the solvers in the literature, already for moderate \mathbf{k} and d . Indeed, it is relatively easy to design a mesh-independent solver, but the dependency on \mathbf{k} and d is generally bad.

At this point, it is worthwhile stressing that a cardinality of the branches equal to $N(\mathbf{k})$ is expected in the tensor setting $\mathbb{Q}_{\mathbf{k}}$, while it is somehow a surprise with the current choice of \mathbb{P}_k Finite Elements, where k is a scalar denoting the global degree and $N(k, d) = k^d$. Indeed, we have verified this formula only for $d = 2$ and

$k = 2, 3, 4$, and hence, a deeper analysis of this phenomenon will be the subject of future investigations.

In the second part of the thesis [33], a multigrid method is developed for the resolution of the problem coming from \mathbb{Q}_k Finite Element Approximation of the same elliptic problem considered previously, see (4.1). By defining the prolongation operator using the inclusion property between the coarser and the finer grid, we provide a study of the relevant analytical features of all the involved spectral symbols, both of the stiffness matrices $\mathbf{f}_{\mathbb{Q}_k}$ and of the projection operators $\mathbf{p}_{\mathbb{Q}_k}$, $k = 1, 2, 3$. While the two-grid and V-cycle show optimal or quasi-optimal convergence rate, with respect to all the relevant parameters (size, dimensionality, polynomial degree k , and diffusion coefficient), the theoretical prescriptions are only partly satisfied. In fact, with reference to the brief study in Section 4.1, our choices are in agreement with the mathematical conditions set in items **(A)** and **(B)**, while Condition **(C)** is violated. Here, by quasi-optimal convergence rate, we mean that the convergence speed does not depend on the size (optimality with respect to this parameter) and it mildly depends on the other relevant parameters such as dimensionality, polynomial degree k , and diffusion coefficient. By looking at the mathematical derivations in [24], we observe that the latter condition indeed is a technical one. In reality, we believe that Condition **(C)** is not essential and the commutation request can be substituted by a less restrictive one, possibly following the considerations in Remark 4.3.1.

Now, we provide a concise summary of the Thesis content.

- In **Chapter 1**: we provide the notations, the necessary definitions, and some known results that lay the groundwork for the succeeding chapters. The final section of this chapter reviews the principles of iterative methods, with specific emphasis on preconditioning and multigrid methods.
- In **Chapter 2**: we introduce the fundamental tools for spectral analysis of matrix-sequences, by discussing distribution in terms of eigenvalues and singular values, clustering, essential range, spectral attraction, and by offering helpful characterizations of zero-distributed sequences. Then, we will explore Toeplitz and Circulant matrices and their spectral properties in both the scalar and block settings. Finally, we will investigate Generalized Locally Toeplitz sequences.

- In **Chapter 3:** we consider a class of elliptic partial differential equations with Dirichlet boundary conditions and where the operator is $\operatorname{div}(-a(\mathbf{x})\nabla\cdot)$, with a continuous and positive over $\overline{\Omega}$, Ω being an open and bounded subset of \mathbb{R}^d , $d \geq 1$. For the numerical approximation, we consider the classical \mathbb{P}_k Finite Elements, in the case of Friedrichs-Keller triangulations, which results a sequences of matrices of increasing size. The new results concern the spectral analysis of the resulting matrix-sequences in the direction of the global distribution in the Weyl sense, with a concise overview on localization, clustering, extremal eigenvalues, and asymptotic conditioning. We examine in detail the case of constant coefficients on $\Omega = (0, 1)^2$ and provide a quick overview of the more complicated case of variable coefficients and more general domains. Tools are drawn from the Toeplitz technology and from the rather new theory of GLT sequences. Numerical results are included to demonstrate the theoretical findings.
- In **Chapter 4:** Our focus is on multigrid technique for solving linear systems deriving from \mathbb{Q}_k Finite Element approximations of elliptic PDEs with Dirichlet boundary conditions, where the operator is $\operatorname{div}(-a(\mathbf{x})\nabla\cdot)$, with a continuous and positive over $\overline{\Omega} = [0, 1]^2$. While the analysis is performed in one dimension, the numerics are carried out also in higher dimension, showing an optimal behaviour in terms of the dependency on the matrix size and a substantial robustness with respect to the dimensionality d and to the polynomial degree k .

A final chapter with conclusions, open problems, and perspectives ends the current PhD Thesis.

CHAPTER 1

NOTATIONS, DEFINITIONS AND PRELIMINARIES

The goal of the current chapter relies in laying a groundwork for the succeeding chapters by providing the notations, the definitions, and some known results, that will be used throughout the whole thesis.

1.1 General notations

- The space of real (resp. complex) $n \times m$ matrices is indicated by $\mathbb{R}^{m \times n}$ (resp. $\mathbb{C}^{m \times n}$).
- $\#S$ denotes the cardinality of the set S .
- Let $p \in [1, \infty]$, the p -norm of the vector \mathbf{x} is denoted by $\|\mathbf{x}\|_p$ and defined as:

$$\|\mathbf{x}\|_p = \begin{cases} (\sum_{i=1}^n |x_i|^p)^{1/p}, & \text{if } p \in [1, \infty), \\ \max_{i=1, \dots, n} |x_i|, & \text{if } p = \infty. \end{cases}$$

- If $A \in \mathbb{C}^{m \times n}$, we denote by A^T the transpose of A and by A^* the conjugate transpose of A .
- If $A \in \mathbb{C}^{m \times n}$, we denote by A^\dagger the Moore-Penrose pseudoinverse of A ($A^\dagger = A^{-1}$ whenever A is invertible).

- The identity matrix (resp. the zero matrix) of order m is denoted by I_m (resp. O_m).
- Let $A \in \mathbb{C}^{n \times n}$, the singular values and the eigenvalues of A are denoted by $\sigma_1(A), \dots, \sigma_n(A)$ and $\lambda_1(A), \dots, \lambda_n(A)$, respectively.
- Given $A \in \mathbb{C}^{n \times n}$, $\Lambda(A) = \{\lambda_1(A), \dots, \lambda_n(A)\}$ denotes the spectrum of A and $\rho(A) = \max_{\lambda \in \Lambda(A)} |\lambda|$ is the spectral radius of A .
- A matrix $A \in \mathbb{C}^{n \times n}$ is said Hermitian if $A = A^*$.
- A matrix $A \in \mathbb{C}^{n \times n}$ is said Hermitian Positive Semi-Definite if A is Hermitian and all its eigenvalues are positive. Furthermore A is Hermitian Positive Definite if it is Hermitian and all its eigenvalues are nonnegative. Notice that there exist other equivalent characterisations, like that using the Rayleigh quotient.
- If $A \in \mathbb{C}^{n \times n}$ is Hermitian (which implies that its eigenvalues are real), λ_{max} and λ_{min} denote the maximal and minimal eigenvalue of A , respectively.
- A matrix $A \in \mathbb{C}^{n \times n}$ is said unitary if $A^*A = AA^* = I_n$.
- The matrix $A \in \mathbb{C}^{n \times n}$ is normal if and only if $A^*A = AA^*$.
- Given $A, B \in \mathbb{C}^{n \times n}$, if A, B are Hermitian, the symbol $A > B$ (resp. $A \geq B$) is used to indicate that $A - B$ is Hermitian Positive Definite (resp. Hermitian Positive Semi-Definite).
- Given $A \in \mathbb{C}^{n \times n}$, $A^{1/2}$ is the square root of A , if A is Hermitian Positive Semi-Definite matrix.
- Given a matrix norm $\|\cdot\|$, the condition number of an invertible matrix $A \in \mathbb{C}^{n \times n}$ is defined by:

$$\kappa(A) = \|A\| \|A^{-1}\|.$$

- If $A, B \in \mathbb{C}^{n \times n}$, $A \sim B$ indicates that the matrix A is similar to the matrix B .

- The tensor (Kronecker) product of two matrices $A \in \mathbb{C}^{n_1 \times m_1}$ and $B \in \mathbb{C}^{n_2 \times m_2}$ (with $n_1, n_2, m_1, m_2 \in \mathbb{N}^*$) is defined as

$$A \otimes B = \begin{bmatrix} a_{11}B & a_{12}B & \cdots & a_{1n_2}B \\ a_{21}B & a_{22}B & \cdots & a_{2n_2}B \\ \vdots & \vdots & \ddots & \vdots \\ a_{n_1 1}B & a_{n_1 2}B & \cdots & a_{n_1 n_2}B \end{bmatrix} \in \mathbb{C}^{n_1 n_2 \times m_1 m_2}.$$

- Let $\mathbf{y} = [y_j]_{j=1}^n \in \mathbb{C}^n$, $M = \text{diag}(\mathbf{y})$ is the diagonal matrix whose entries are y_1, y_2, \dots, y_n , i.e., $M_{jj} = y_j$, for $j = 1, \dots, n$.
- μ_t is used to indicate the Lebesgue measure in \mathbb{R}^t , $t \geq 1$.
- We denote by $C_c(\mathbb{R})$ (resp. $C_c(\mathbb{C})$) the space of continuous complex-valued functions with bounded support defined on \mathbb{R} (resp. \mathbb{C}).
- Given two positive sequences $\{x_n\}_n$ and $\{y_n\}_n$
 - The notation $x_n = o(y_n)$ means that $x_n/y_n \rightarrow 0$ as $n \rightarrow \infty$.
 - The notation $x_n = O(y_n)$ is used to indicate that there exists $C > 0$ such that $x_n \leq C y_n$, $\forall n \geq 0$.
- For $z \in \mathbb{C}$ and $\epsilon > 0$, let $B(z, \epsilon)$ the disk with centre z and radius ϵ ,

$$B(z, \epsilon) := \{w \in \mathbb{C} : |w - z| < \epsilon\}.$$

For $S \subseteq \mathbb{C}$ and $\epsilon > 0$, we denote by $B(S, \epsilon)$ the ϵ -expansion of S , defined as $B(S, \epsilon) := \bigcup_{z \in S} B(z, \epsilon)$.

- \hat{i} is the imaginary unit, $\hat{i}^2 = -1$.
- Given two real valued functions h_1, h_2 defined on a domain D , the notation $(h_1 \sim h_2)$ means that there exist two constants $C_1, C_2 \in \mathbb{R}^+$ such that

$$\forall x \in D, \quad C_1 h_1(x) \leq h_2(x) \leq C_2 h_1(x).$$

- Let $f : D \subseteq \mathbb{R}^d \rightarrow \mathbb{C}$. We say that the function f has a zero of order s at x_0 if $f(x) \sim \|x - x_0\|^s$ at least locally. If $D \subseteq \mathbb{R}$ and f is smooth enough, then the general definition is reduced to the following relations

$$\begin{aligned} f^{(j)}(x_0) &= 0, \text{ for } j < s, \\ f^{(s)}(x_0) &\neq 0, \end{aligned}$$

where $f^{(j)}(x_0)$ is the j -th derivative of $f(x)$ at x_0 .

1.1.1 Multi-index notation

- A vector \mathbf{j} of the form $\mathbf{j} = (j_1, j_2, \dots, j_t) \in \mathbb{Z}^t$ is called a multi-index.
- For all $\mathbf{n} \in \mathbb{N}_+^t$, the multi-dimensional length is $N(\mathbf{n}) = \prod_{i=1}^t n_i$.
- $\mathbf{0}, \mathbf{e}, \mathbf{2}, \dots$ denote respectively the vectors $(0, \dots, 0), (1, \dots, 1), (2, \dots, 2), \dots$
- $\mathbf{n} \rightarrow \infty$ has the meaning that $\min_{1 \leq j \leq t} n_j \rightarrow \infty$.
- Given $\mathbf{m}, \mathbf{n} \in \mathbb{Z}^t$,

1. $\mathbf{m} \leq \mathbf{n} \Leftrightarrow m_r \leq n_r, \forall r = 1, \dots, t$.

2. $\mathbf{k} = \mathbf{m}, \dots, \mathbf{n}$ means that the multi-index \mathbf{k} varies from \mathbf{m} to \mathbf{n} following the lexicographical way.

For example, if $t = 2$ the ordering as follows:

$$\begin{aligned} & (m_1, m_2), (m_1, m_2 + 1), \dots, (m_1, n_2), (m_1 + 1, m_2), \\ & (m_1 + 1, m_2 + 1), \dots, (m_1 + 1, n_2), \dots, (n_1, m_2), (n_1, m_2 + 1), \dots, (n_1, n_2). \end{aligned} \tag{1.1}$$

3. If $\mathbf{m} \leq \mathbf{n}$, $\sum_{\mathbf{k}=\mathbf{m}}^{\mathbf{n}}$ (resp. $\prod_{\mathbf{k}=\mathbf{m}}^{\mathbf{n}}$) is used to indicate the summation (resp. product) over all the multi-indices \mathbf{k} in the range $\mathbf{m}, \dots, \mathbf{n}$.

- If $\mathbf{n} \in \mathbb{Z}^t$, $\mathbf{x} = [x_i]_{i=\mathbf{e}}^{\mathbf{n}}$ is a vector of size $N(\mathbf{n})$ and it is given by

$$\mathbf{X} = \begin{bmatrix} x_{(1,1,\dots,1,1)} \\ x_{(1,1,\dots,1,2)} \\ \vdots \\ x_{(1,1,\dots,1,n_t)} \\ \hline x_{(1,1,\dots,2,1)} \\ x_{(1,1,\dots,2,2)} \\ \vdots \\ x_{(1,1,\dots,2,n_t)} \\ \hline \vdots \\ \vdots \\ \hline x_{(n_1,n_2,\dots,1)} \\ x_{(n_1,n_2,\dots,2)} \\ \vdots \\ x_{(n_1,n_2,\dots,n_t)} \end{bmatrix}.$$

- Given $\mathbf{n} \in \mathbb{Z}^t$, $\mathbf{X} = [x_{ij}]_{i,j=\mathbf{e}}^{\mathbf{n}}$ is the $N(\mathbf{n}) \times N(\mathbf{n})$ matrix.

For instance in the case $t = 2$ the matrix $\mathbf{X} = [x_{ij}]_{i,j=\mathbf{e}}^{\mathbf{n}}$ is given by:

$$\begin{bmatrix} x_{(1,1),(1,1)} & x_{(1,1),(1,2)} & \cdots & x_{(1,1),(1,n_2)} & x_{(1,1),(2,1)} & \cdots & x_{(1,1),(2,n_2)} & \cdots & x_{(1,1),(n_1,1)} & \cdots & x_{(1,1),(n_1,n_2)} \\ x_{(1,2),(1,1)} & x_{(1,2),(1,2)} & \cdots & x_{(1,2),(1,n_2)} & x_{(1,2),(2,1)} & \cdots & x_{(1,2),(2,n_2)} & \cdots & x_{(1,2),(n_1,1)} & \cdots & x_{(1,2),(n_1,n_2)} \\ \vdots & \vdots & & \vdots & \vdots & & \vdots & \cdots & \vdots & \cdots & \vdots \\ \vdots & \vdots & & \vdots & \vdots & & \vdots & \cdots & \vdots & \cdots & \vdots \\ \hline x_{(1,n_2),(1,1)} & x_{(1,n_2),(1,2)} & \cdots & x_{(1,n_2),(1,n_2)} & x_{(1,n_2),(2,1)} & \cdots & x_{(1,n_2),(2,n_2)} & \cdots & x_{(1,n_2),(n_1,1)} & \cdots & x_{(1,n_2),(n_1,n_2)} \\ \hline x_{(2,1),(1,1)} & x_{(2,1),(1,2)} & \cdots & x_{(2,1),(1,n_2)} & x_{(2,1),(2,1)} & \cdots & x_{(2,1),(2,n_2)} & \cdots & x_{(2,1),(n_1,1)} & \cdots & x_{(2,1),(n_1,n_2)} \\ \vdots & \vdots & & \vdots & \vdots & & \vdots & \cdots & \vdots & \cdots & \vdots \\ \hline x_{(2,n_2),(1,1)} & x_{(2,n_2),(1,2)} & \cdots & x_{(2,n_2),(1,n_2)} & x_{(2,n_2),(2,1)} & \cdots & x_{(2,n_2),(2,n_2)} & \cdots & x_{(2,n_2),(n_1,1)} & \cdots & x_{(2,n_2),(n_1,n_2)} \\ \vdots & \vdots & & \vdots & \vdots & & \vdots & \cdots & \vdots & \cdots & \vdots \\ \vdots & \vdots & & \vdots & \vdots & & \vdots & \cdots & \vdots & \cdots & \vdots \\ \vdots & \vdots & & \vdots & \vdots & & \vdots & \cdots & \vdots & \cdots & \vdots \\ \hline x_{(n_1,1),(1,1)} & x_{(n_1,1),(1,2)} & \cdots & x_{(n_1,1),(1,n_2)} & x_{(n_1,1),(2,1)} & \cdots & x_{(n_1,1),(2,n_2)} & \cdots & x_{(n_1,1),(n_1,1)} & \cdots & x_{(n_1,1),(n_1,n_2)} \\ \vdots & \vdots & & \vdots & \vdots & & \vdots & \cdots & \vdots & \cdots & \vdots \\ \hline x_{(n_1,n_2),(1,1)} & x_{(n_1,n_2),(1,2)} & \cdots & x_{(n_1,n_2),(1,n_2)} & x_{(n_1,n_2),(2,1)} & \cdots & x_{(n_1,n_2),(2,n_2)} & \cdots & x_{(n_1,n_2),(n_1,1)} & \cdots & x_{(n_1,n_2),(n_1,n_2)} \end{bmatrix}.$$

1.2 Matrix norms

Given $A, B \in \mathbb{C}^{n \times n}$, a matrix norm is an application $\|\cdot\| : \mathbb{C}^{n \times n} \rightarrow \mathbb{R}^+$ satisfying

- $\|A\| = 0 \Leftrightarrow A = 0$;
- $\|\lambda A\| = |\lambda| \|A\|, \forall \lambda \in \mathbb{C}$;
- $\|A + B\| \leq \|A\| + \|B\|$;

There exists various type of matrix-norm:

• 1.2.1 The norms induced by vector norms

For $p \in [1, \infty]$, the p -norm of the matrix A is defined by

$$\|A\|_p = \sup_{u \in \mathbb{C}^n, \|u\|_p=1} \|Au\|_p = \sup_{u \in \mathbb{C}^n, u \neq 0} \frac{\|Au\|_p}{\|u\|_p}.$$

For $p = 1, 2, \infty$, the norm $\|A\|_p$ is presented as follows [46]:

$$\|A\|_1 = \max_{j=1, \dots, n} \sum_{i=1}^n |a_{ij}|,$$

$$\|A\|_2 = \sqrt{\rho(A^*A)} = \sigma_{max} \text{ (spectral norm) },$$

$$\|A\|_\infty = \max_{i=1, \dots, n} \sum_{j=1}^n |a_{ij}|.$$

• 1.2.2 Frobenius norm

$$\|A\|_F = (\text{tr}(A^*A))^{1/2} = \left(\sum_{i=1}^n \sum_{j=1}^n |a_{ij}|^2 \right)^{1/2} = \sqrt{\sigma_1^2(A) + \dots + \sigma_n^2(A)}.$$

• 1.2.3 The Schatten norms

Given $1 \leq p \leq \infty$, $\|A\|_p$ is the Schatten p -norm of A , i.e., the p -norm of the vector $\sigma(A) = (\sigma_1(A), \dots, \sigma_n(A))$.

The Schatten ∞ -norm $\|A\|_\infty$ is the largest singular value of A and coincides with the spectral norm

$$\|A\|_\infty = \sigma_{max} = \|A\|_2.$$

The Schatten 1-norm $\|A\|_1$ is the sum of the singular values of A and is often referred to as the trace-norm of A

$$\|A\|_1 = \sum_{i=1}^n \sigma_i(A).$$

The Schatten 2-norm $\|A\|_2$ coincides with the Frobenius norm of A

$$\|A\|_2 = \|A\|_F.$$

For more details on Schatten p -norms, see [8].

• 1.2.4 The Euclidean norm weighted by a matrix

If $A \in \mathbb{C}^{n \times n}$ is an Hermitian Positive Definite matrix, then the Euclidean norm of a matrix weighted by A is defined by

$$\|B\|_A = \max_{\|x\|_A=1} \|Bx\|_A \quad (1.2)$$

where $\|x\|_A = \|A^{\frac{1}{2}}x\|_2$ is called the energy norm.

It is easy to verify $\|B\|_A = \|A^{\frac{1}{2}}BA^{-\frac{1}{2}}\|_2$. In fact,

$$\|B\|_A = \max_{\|x\|_A=1} \|Bx\|_A = \max_{\|A^{\frac{1}{2}}x\|_2=1} \|A^{\frac{1}{2}}Bx\|_2 = \max_{\|y\|_2=1} \|A^{\frac{1}{2}}BA^{-\frac{1}{2}}y\|_2 = \|A^{\frac{1}{2}}BA^{-\frac{1}{2}}\|_2 \quad (1.3)$$

where $y = A^{\frac{1}{2}}x$.

Here, we report some useful properties on the matrix norms that are often utilised, (see [46]).

1. The induced norms are sub-multiplicative, i.e $\forall A, B \in \mathbb{C}^{n \times n}$,
 $\|AB\|_p \leq \|A\|_p \|B\|_p$.
2. The induced norms satisfy $\rho(A) \leq \|A\|_p, \forall A \in \mathbb{C}^{n \times n}$.
3. The Schatten p -norms are unitarily invariants, i.e $\|UAV\|_p = \|A\|_p$,
 $\forall A \in \mathbb{C}^{n \times n}$ and $\forall U, V \in \mathbb{C}^{n \times n}$ unitary matrices.
4. The estimation of the spectral norm can be deduced by the following relation

$$\|A\|_2 \leq \sqrt{\|A\|_1 \|A\|_\infty}, \forall A \in \mathbb{C}^{n \times n}.$$

5. $\max_{1 \leq i, j \leq n} |a_{ij}| \leq \|A\|_2 \leq n \max_{1 \leq i, j \leq n} |a_{ij}|$.
6. If $B \in \mathbb{C}^{n-1 \times n-1}$ is submatrix of $A \in \mathbb{C}^{n \times n}$ then $\|B\|_p \leq \|A\|_p$.
7. The Frobenius norm is unitarily invariant, that is, $\forall A \in \mathbb{C}^{n \times n}, \forall U, V \in \mathbb{C}^{n \times n}$ unitary matrices, $\|UAV\|_F = \|A\|_F$. The same is true for every Schatten norm.
8. The Frobenius norm is equivalent to the spectral norm and the following inequalities hold

$$\|A\|_2 \leq \|A\|_F \leq \sqrt{n} \|A\|_2.$$

9. All the norms acting on finite dimensional spaces are topologically equivalent.

1.3 L^p spaces

Let $D \subseteq \mathbb{R}^t$ a measurable set, for $p \geq 1$ we define

- The space $L^p(D) = \left\{ f : D \rightarrow \mathbb{C} : f \text{ measurable, such that } \int_D |f| < \infty \right\}$.
- The space of all measurable functions essentially bounded is denoted by:

$$L^\infty(D) = \left\{ f : D \rightarrow \mathbb{C} : f \text{ measurable, such that } \text{ess sup}_D |f| < \infty \right\}.$$

- If $f \in L^p(D)$, the L^p -norm of the function f is denoted by $\|f\|_p$ and defined as:

$$\begin{aligned} \|f\|_p &= (\int_D |f|^p)^{1/p}, \text{ if } p \in [1, \infty), \\ \|f\|_\infty &= \text{ess sup}_D |f|, \text{ if } p = \infty. \end{aligned}$$

Let \mathbf{f} be a matrix-valued function $\mathbf{f} : D \subseteq \mathbb{R}^t \rightarrow \mathbb{C}^{r \times r}$, for $p \in [1, \infty)$ we set

$$L^p(D, r) = \left\{ \mathbf{f} : D \rightarrow \mathbb{C}^{r \times r} \text{ such that } \mathbf{f} \in L^p(D) \right\}.$$

- A matrix-valued function \mathbf{f} is said to be measurable (resp. continuous, Riemann-integrable, in $L^p(D)$, etc.) if its components $f_{\alpha\beta} : D \rightarrow \mathbb{C}$, $\alpha, \beta = 1, \dots, r$, are measurable (resp. continuous, Riemann-integrable, in $L^p(D)$, etc.).

- If $\mathbf{f}_m, \mathbf{f} : D \subseteq \mathbb{R}^t \rightarrow \mathbb{C}^{r \times r}$ are measurable matrix-valued functions, we say that \mathbf{f}_m converges to \mathbf{f} in measure (resp., almost everywhere, in $L^p(D)$, etc.) if $(\mathbf{f}_m)_{\alpha\beta}$ converges to $\mathbf{f}_{\alpha\beta}$ in measure (resp., almost everywhere, in $L^p(D)$, etc.) for all $\alpha, \beta = 1, \dots, r$.
- If $\mathbf{f} \in L^p(D, r)$, we define

$$\begin{aligned} \|\mathbf{f}\|_p &= \left(\int_D \|\mathbf{f}(\boldsymbol{\theta})\|_p^p \right)^{1/p}, & \text{if } p \in [1, \infty), \\ \|\mathbf{f}\|_\infty &= \text{ess sup}_{\boldsymbol{\theta} \in D} \|\mathbf{f}(\boldsymbol{\theta})\|_\infty, & \text{if } p = \infty. \end{aligned}$$

- If $1 \leq p, q \leq \infty$ such that $\frac{1}{p} + \frac{1}{q} = 1$ and $\mathbf{f} \in L^p(D, r)$, $\mathbf{g} \in L^q(D, r)$ then the inequality of Holder holds for p -schatten norm

$$\|\mathbf{f}\mathbf{g}\|_1 \leq \|\mathbf{f}\|_p \|\mathbf{g}\|_q.$$

- When \mathbf{f} is a matrix-valued function, $\sigma_i(\mathbf{f}(\boldsymbol{\theta}))$ (resp. $\lambda_i(\mathbf{f}(\boldsymbol{\theta}))$), $i = 1, \dots, r$ is used to indicate the evaluation of singular value (resp. the eigenvalue) functions at the point $\boldsymbol{\theta} \in D$.

1.4 Iterative Methods

Now, in this part, we will start by providing a brief description of the two major types of approaches for solving a linear system. We will next focus on the iterative approach, discussing preconditioning for Toeplitz structures. The Multigrid method is finally introduced.

Suppose we have the following linear system

$$A\mathbf{x} = \mathbf{b}, \tag{1.4}$$

where $\mathbf{b} \in \mathbb{C}^n$ and $A \in \mathbb{C}^{n \times n}$ is invertible, thus the system admits only one solution.

Numerical techniques for solving the linear system (1.4) break down into two major classes:

1. **Direct methods:** they consist in converting a generic linear system through a finite number of operations into a linear system with a specific structure that simplifies its resolution (for instance Gauss elimination method, LU and Cholesky factorization etc...)

2. **Iterative methods:** they consist in building a sequence of vectors $\{\mathbf{x}^{(k)}\}_k$ converging to exact solution $\bar{\mathbf{x}} = A^{-1}b$ such that $\lim_{k \rightarrow \infty} \mathbf{x}^{(k)} = \bar{\mathbf{x}}$. These types of methods are effective for sparse matrices because they retain the sparsity of the matrix, and hence they are highly favored for large problems, as they demand less computer's memory. They are also more suitable for solving ill-conditioned problems since they allow a better control of the error.

Definition 1.4.1. *An iterative method for solving the linear system (1.4) has the form*

$$\mathbf{x}^{(k)} = Q\mathbf{x}^{(k-1)} + q \quad k = 1, 2, \dots, \quad \text{and } \mathbf{x}^{(0)} \text{ is an initial vector} \quad (1.5)$$

where $Q \in \mathbb{C}^{n \times n}$ is called the iteration matrix and $q \in \mathbb{C}^n$ is a fixed vector. The method (1.5) is called stationary iterative method, where the word "stationary" highlights the fact that the matrix of iteration Q is fixed a priori.

A method as in (1.5) is obtained by decomposing the matrix A in the form $A = M - N$, where $M \in \mathbb{C}^{n \times n}$ is an invertible matrix. We can then rewrite the system (1.4) in the form $\mathbf{x} = M^{-1}(N\mathbf{x} + b)$, setting $Q = M^{-1}N$ and $q = M^{-1}b$ we obtain (1.5).

Definition 1.4.2. *The method (1.5) is said to be consistent with (1.4) if the solution $\bar{\mathbf{x}}$ of (1.4) is a fixed point, i.e., $\bar{\mathbf{x}} = Q\bar{\mathbf{x}} + q$.*

Definition 1.4.3. *We say that the method (1.5) is convergent if for every initial choice $\mathbf{x}^{(0)} \in \mathbb{C}^{n \times n}$, the sequence $\{\mathbf{x}^{(n)}\}_{n \in \mathbb{N}}$ converges to $\bar{\mathbf{x}}$ ($\lim_{k \rightarrow \infty} \|\bar{\mathbf{x}} - \mathbf{x}^{(k)}\| = 0$).*

The next theorem establishes the link between the convergence of the method (1.5) and the iteration matrix Q

Theorem 1.4.4. [18] *Let $Q \in \mathbb{C}^{n \times n}$, then the following propositions are equivalent:*

- The method (1.5) is convergent for any choice of $b \in \mathbb{C}^n$ and $\mathbf{x}^{(0)}$;
- $\rho(Q) < 1$;

- There exists p such that $\|Q\|_p < 1$.

Now, we provide the definition of the optimality for the iterative methods, which is useful for evaluating the efficiency and the performance of the method.

Definition 1.4.5 (Optimality). *An iterative method is said to be optimal for a class of a sequence of linear systems $\{A_n \mathbf{x}_n = \mathbf{b}_n\}_n$ if*

1. *the number of iterations is bounded by a constant and independent from the size of the matrix A_n ,*
2. *each iteration has a cost proportional to the matrix-vector product with matrix A_n .*

1.4.1 Preconditioning

The basic principle behind the preconditioning process is to replace the ill-conditioned system

$$A_n \mathbf{x} = \mathbf{b} \tag{1.6}$$

where $A_n \in \mathbb{C}^{d_n \times d_n}$, $\mathbf{x}, \mathbf{b} \in \mathbb{C}^{d_n}$ ($\kappa(A_n) \rightarrow \infty$ when $n \rightarrow \infty$) by an analogous system $\tilde{A}_n \mathbf{x} = \tilde{\mathbf{b}}$ for which the new system converges faster than the original system (the number of iterations required for the convergence is reduced).

A common strategy is to consider a Hermitian Positive Definite matrix $P \in \mathbb{C}^{d_n \times d_n}$ such that

$$P_n^{-1} A_n \mathbf{x} = P_n^{-1} \mathbf{b}. \tag{1.7}$$

Since the convergence of the iterative method depends a lot on the spectral properties of the associated matrix, P_n should be chosen in such a way, the matrix $P_n^{-1} A_n$ is better conditioned and its spectrum is clustered around one. Consequently, the matrix P_n should be determined in accordance with the following conditions:

1. The construction of the preconditioner demands at most the cost of $A_n \mathbf{x}$;
2. The solution of $P_n \mathbf{x} = \mathbf{y}$ has at most the cost of $A_n \mathbf{x}$ product;

3. P_n has the same spectral properties as A_n , i.e; the spectrum of $P_n^{-1}A_n - I_n$ is strongly clustered around zero or the condition number of $P_n^{-1}A_n$ is bounded by c , i.e $\exists c > 0, \kappa(P_n^{-1}A_n) < c, \forall n$.

There are two extreme cases: $P_n = I_n$ satisfies the requirements 1.,2. but not 3., in which case convergence is not accelerated; when $P_n = A_n$ satisfies the first and the third requirements, but it fails to meet the second: in this case the convergence is immediate but not beneficial, due to the difficulty of the problem. Creating a preconditioner that is efficient should help to strike a good compromise between the three requirements of creating a matrix P_n similar to A_n , at least spectrally, but less computationally expensive to invert.

Preconditioners for Toeplitz matrices

Because there is so much information on preconditioners for structured matrices in the literature, we will only mention a few results in the case of Toeplitz matrices, which have been explored by many authors, see for instance [16, 56, 67], (for more information regarding Toeplitz matrices, see Section 2.3).

- **Strang’s preconditioner:** In 1986 G.Strang [74] introduced the first Circulant preconditioner (for more information concerning Circulant matrices, see Section 2.3) given by

$$S = \begin{bmatrix} a_0 & a_1 & \cdots & a_{\lfloor \frac{n}{2} \rfloor} & a_{\lfloor \frac{n-1}{2} \rfloor} & \cdots & a_2 & a_1 \\ a_1 & a_0 & a_1 & \cdots & a_{\lfloor \frac{n}{2} \rfloor} & a_{\lfloor \frac{n-1}{2} \rfloor} & \cdots & a_2 \\ \vdots & a_1 & a_0 & a_1 & \cdots & \ddots & \ddots & \vdots \\ a_{\lfloor \frac{n}{2} \rfloor} & \ddots & \ddots & \ddots & \ddots & \ddots & \ddots & a_{\lfloor \frac{n-1}{2} \rfloor} \\ a_{\lfloor \frac{n-1}{2} \rfloor} & a_{\lfloor \frac{n}{2} \rfloor} & \ddots & \ddots & \ddots & \ddots & \ddots & a_{\lfloor \frac{n}{2} \rfloor} \\ \vdots & \ddots & a_{\lfloor \frac{n}{2} \rfloor} & \cdots & \ddots & a_0 & a_1 & \vdots \\ a_2 & \cdots & a_{\lfloor \frac{n-1}{2} \rfloor} & a_{\lfloor \frac{n}{2} \rfloor} & \cdots & a_1 & a_0 & a_1 \\ a_1 & a_2 & \cdots & a_{\lfloor \frac{n-1}{2} \rfloor} & a_{\lfloor \frac{n}{2} \rfloor} & \cdots & a_1 & a_0 \end{bmatrix}$$

where the coefficients a_j are the coefficients of the Toeplitz matrix $T_n(a) = [a_{i-j}]_{i,j=1,\dots,n}$. The matrix S has interesting properties given

by $S = \arg \min_{C:\text{Circulant}} \|C - T_n(a)\|_1$ and $S = \arg \min_{C:\text{Circulant}} \|C - T_n(a)\|_\infty$.

Under some conditions on the generating function a the PCG method with the Strang preconditioner converges superlinearly, see [16, 32, 68].

- **T.Chan’s preconditioner:** Chan’s preconditioner is given by

$$\hat{C} = \arg \min_{C:\text{Circulant}} \|C - T_n(a)\|_F$$

and the entries of the matrix are given by

$$c_j = \begin{cases} \frac{(n-j)a_j + ja_{j-n}}{n}, & 0 \leq j < n \\ c_{n+j}, & 0 < -j < n \end{cases}.$$

The optimality of the PCG with $P_n = \hat{C}$ is ensured when the generating function a is positive continuous function, see [17, 67, 68].

1.4.2 Multigrid Methods

The classical iterative methods produce a poor approximation of the solution when $\kappa(A_n)$ diverges as $n \rightarrow \infty$. The slow convergence is caused by the space generated by the eigenvectors of A_n associated to eigenvalues that are close to zero, resulting in global slowdown of the method. This impediment can be addressed by using either preconditioning in Krylov algorithms or Multigrid methods. The latter methods are extremely effective for dealing with quite ill-conditioned linear systems, under the condition of having a partial knowledges of the ill-conditioned subspaces. The principle of Multigrid, when applied to differential problems, is to speed up the convergence of a basic iterative approach, which in general reduces effectively the oscillatory modes of the error (short-wavelength errors are eliminated), and solves the problem in a coarse-grid (where the resolution of the problem is cheaper, and the smooth mode of the error appears more oscillatory). The coarse problem contains also both short and long-wavelength errors. Additionally, a combination of relaxation and coarser grids can be used to overcome the problem. Then the procedure is continued until a grid is found where the cost is much cheaper compared to the first one (the finer one). For a detailed study of Multigrid methods, we recommend [14, 48, 60]. In this section, we concentrate on the Algebraic Multigrid method by presenting Two-Grid Method and the V-cycle method.

Consider the linear system $A_n \mathbf{x} = \mathbf{b}$ where $A_n \in \mathbb{C}^{n \times n}$ and $\mathbf{x}, \mathbf{b} \in \mathbb{C}^n$ and let $\mathbf{x}^{(k)}$ an approximation to $\bar{\mathbf{x}}$. There are two important measures

- The algebraic error

$$\mathbf{e}^{(k)} = \bar{\mathbf{x}} - \mathbf{x}^{(k)},$$

- The residual

$$\mathbf{r}^{(k)} = \mathbf{b} - A_n \mathbf{x}^{(k)},$$

however, since the algebraic error is not available whenever the exact solution $\bar{\mathbf{x}}$ is unknown, we use the residual which compute how much the approximation fails to solve the original problem $A_n \mathbf{x} = \mathbf{b}$. By uniqueness of the solution $\mathbf{r}^{(k)} = \mathbf{0}_n \iff \mathbf{e}^{(k)} = \mathbf{0}_n$.

Since $A_n \bar{\mathbf{x}} = \mathbf{b}$ and by using the definitions of the residual and the algebraic error we obtain the following residual equation

$$A_n \mathbf{e}^{(k)} = \mathbf{r}^{(k)}.$$

In fact $\mathbf{r}^{(k)} = \mathbf{b} - A_n \mathbf{x}^{(k)} = A_n \bar{\mathbf{x}} - A_n \mathbf{x}^{(k)} = A_n \mathbf{e}^{(k)}$.

When \mathbf{b} of the original system is substituted by $\mathbf{r}^{(k)}$, the solution $\mathbf{e}^{(k)}$ of the residual equation satisfies the same set of equations as the unknown \mathbf{x} .

We now have a handle on how the residual equation will be put to use: after obtaining the approximation $\mathbf{x}^{(k)}$ by some iterative method, we compute the residual $\mathbf{r}^{(k)} = \mathbf{b} - A_n \mathbf{x}^{(k)}$, solve the residual equation and lastly apply the residual correction to improve the approximation $\mathbf{x}^{(k+1)} = \mathbf{x}^{(k)} + \mathbf{e}^{(k)}$.

The residual equation $A_n \mathbf{e}^{(k)} = \mathbf{r}^{(k)}$ is not simpler to solve than the original problem; however, here we know that the exact solution 'the error' is smooth if $x^{(k)}$ is obtained by an iterative method, contrary to the original problem, we do not know anything about the behaviour of the exact solution. Therefore instead of solving the residual equation in the fine grid, we project it into the coarse grid where the problem will be solved; then, by re-projecting the solution found on the coarse grid into the fine grid, we obtain a new approximate solution that is considerably closer to $\bar{\mathbf{x}}$ than $\mathbf{x}^{(k)}$ was, this procedure called Coarse Grid Correction (CGC).

Algebraic Two-Grid Method (TGM)

We start by taking into consideration the generic linear system $A_n \mathbf{x}_n = \mathbf{b}_n$ with large dimension n , where $A_n \in \mathbb{C}^{n \times n}$ is a Hermitian Positive Definite matrix and $\mathbf{x}_n, \mathbf{b}_n \in \mathbb{C}^n$. Let $n_0 = n > n_1 > \dots > n_s > \dots > n_{s_{\min}}$ and let $P_s^{s+1} \in \mathbb{C}^{n_{s+1} \times n_s}$ be a full-rank matrix for any s . At last, let us denote by \mathcal{V}_s a class of stationary iterative methods for given linear systems of dimension n_s .

In accordance with [48], the algebraic two-grid Method (TGM) can be easily seen a stationary iterative method whose generic steps are reported below.

$$\mathbf{x}_s^{\text{out}} = \mathcal{TGM}(s, \mathbf{x}_s^{\text{in}}, \mathbf{b}_s)$$

$$\mathbf{x}_s^{\text{pre}} = \mathcal{V}_{s,\text{pre}}^{\nu_{\text{pre}}}(\mathbf{x}_s^{\text{in}}, \mathbf{b}_s)$$

Pre-smoothing iterations

$$\begin{aligned} \mathbf{r}_s &= \mathbf{b}_s - A_s \mathbf{x}_s^{\text{pre}} \\ \mathbf{r}_{s+1} &= (P_{n_s}^{n_{s+1}})^*_{n_s} \mathbf{r}_s \\ A_{s+1} &= (P_{n_s}^{n_{s+1}})^* A_s P_{n_s}^{n_{s+1}} \\ \text{Solve } A_{s+1} \mathbf{y}_{s+1} &= \mathbf{r}_{s+1} \\ \hat{\mathbf{x}}_s &= \mathbf{x}_s^{\text{pre}} + P_{n_s}^{n_{s+1}} \mathbf{y}_{s+1} \end{aligned}$$

Exact Coarse Grid Correction (CGC)

$$\mathbf{x}_s^{\text{out}} = \mathcal{V}_{s,\text{post}}^{\nu_{\text{post}}}(\hat{\mathbf{x}}_s, \mathbf{b}_s)$$

Post-smoothing iterations

where we refer to the dimension n_s by means of its subscript s .

In the first and last steps, a *pre-smoothing iteration* and a *post-smoothing iteration* are applied ν_{pre} times and ν_{post} times, respectively, in accordance with the considered stationary iterative method in the class \mathcal{V}_s . Furthermore, the intermediate steps define the *exact coarse grid correction operator*, which is depending on the considered projector operator P_s^{s+1} . The resulting iteration matrix of the TGM is then defined as

$$TGM_s = V_{s,\text{post}}^{\nu_{\text{post}}} CGC_s V_{s,\text{pre}}^{\nu_{\text{pre}}}, \quad (1.8)$$

$$CGC_s = I^{(s)} - P_{n_s}^{n_{s+1}} A_{s+1}^{-1} (P_{n_s}^{n_{s+1}})^* A_s \quad A_{s+1} = (P_{n_s}^{n_{s+1}})^* A_s P_{n_s}^{n_{s+1}}, \quad (1.9)$$

where $V_{s,\text{pre}}$ and $V_{s,\text{post}}$ represent the pre-smoothing and post-smoothing iteration matrices, respectively, and $I^{(s)}$ is the identity matrix at the s th level. The following theorem allows us to estimate an upper bound on the TGM's speed of convergence.

Theorem 1.4.6. [60] *Let $A \in \mathbb{C}^{n \times n}$ be a Hermitian Positive Definite matrix, $P_m^n \in \mathbb{C}^{n \times m}$ a full-rank matrix with $n > m$ and $V_{n,\text{post}}$ a post-smoothing iteration matrix. If we assume*

- (i) $\exists \alpha_{\text{post}} > 0 : \|V_{n,\text{post}}\mathbf{x}_n\|_{A_n}^2 \leq \|\mathbf{x}_n\|_{A_n}^2 - \alpha_{\text{post}}\|\mathbf{x}_n\|_{A_n}^2, \forall \mathbf{x} \in \mathbb{C}^n,$ (smoothing property)
- (ii) $\exists \beta > 0 : \min_{\mathbf{y} \in \mathbb{C}^{n \times n}} \|\mathbf{x}_n - P_m^n \mathbf{y}\|_2^2 \leq \beta \|\mathbf{x}_n\|_{A_n}^2, \forall \mathbf{x} \in \mathbb{C}^n,$ (approximation property)

Then $\beta > \alpha_{\text{post}}$ and

$$\|TGM\|_{A_n} \leq \sqrt{1 - \frac{\alpha_{\text{post}}}{\beta}}.$$

The fact that α_{post} and β are independent of n means that, if the hypotheses (i), (ii), are satisfied, then the TGM is not just convergent, but also optimal.

V-cycle method

By employing a recursive procedure, the TGM leads to a Multi-Grid Method (MGM): indeed, the standard V-cycle can be expressed in the following way:

$$\mathbf{x}_s^{\text{out}} = \mathcal{MGM}(s, \mathbf{x}_s^{\text{in}}, \mathbf{b}_s)$$

if $s \leq s_{\min}$ then

Solve $A_s \mathbf{x}_s^{\text{out}} = \mathbf{b}_s$	Exact solution
--	----------------

else

$\mathbf{x}_s^{\text{pre}} = \mathcal{V}_{s,\text{pre}}^{\nu}(\mathbf{x}_s^{\text{in}}, \mathbf{b}_s)$	Pre-smoothing iterations
--	--------------------------

$\begin{aligned} \mathbf{r}_s &= \mathbf{b}_s - A_s \mathbf{x}_s^{\text{pre}} \\ \mathbf{r}_{s+1} &= (P_{m_s}^{m_{s+1}})^* \mathbf{r}_s \\ \mathbf{y}_{s+1} &= \mathcal{MGM}(s+1, \mathbf{0}_{s+1}, \mathbf{r}_{s+1}) \\ \hat{\mathbf{x}}_s &= \mathbf{x}_s^{\text{pre}} + P_{m_s}^{m_{s+1}} \mathbf{y}_{s+1} \end{aligned}$	Coarse Grid Correction
--	------------------------

$\mathbf{x}_s^{\text{out}} = \mathcal{V}_{s,\text{post}}^{\nu}(\hat{\mathbf{x}}_s, \mathbf{b}_s)$	Post-smoothing iterations
---	---------------------------

From a computational viewpoint, it is more efficient that the matrices $A_{s+1} = P_s^{s+1} A_s (P_s^{s+1})^*$ are computed in the so-called *setup phase* for reducing the related costs.

According to the previous setting, the global iteration matrix of the MGM is recursively defined as

$$MGM_{s_{\min}} = O \in \mathbb{C}^{s_{\min} \times s_{\min}},$$

$$MGM_s = V_{s,\text{post}}^{\nu} \left[I^{(s)} - P_{m_s}^{m_{s+1}} \left(I^{(s+1)} - MGM_{s+1} \right) A_{s+1}^{-1} (P_{m_s}^{m_{s+1}})^* A_s \right] V_{s,\text{pre}}^{\nu},$$

$$s = s_{\min} - 1, \dots, 0.$$

CHAPTER 2

SPECTRAL PROPERTIES OF MATRIX-SEQUENCES DESCRIBED BY A FUNCTION

In this chapter, we begin by introducing the basic tools for spectral analysis of matrix-sequences, by presenting the notion of distribution both in the sense of the eigenvalues and singular values, clustering, essential range and spectral attraction and by providing useful characterizations of zero-distributed sequences. Then we will go through Toeplitz and Circulant matrices and their spectral characteristics both in the scalar and the block setting. Finally, we will explore the $*$ -algebra of Generalized Locally Toeplitz matrix sequences.

2.1 Asymptotic distribution of matrix-sequences

Definition 2.1.1 (Matrix-sequence distributed as complex-valued function). *Let $\{A_n\}_n$ be a sequence of matrices, with A_n of size d_n , with $d_k < d_{k+1}$ for every $k \in \mathbb{N}$ and let $f : D \subset \mathbb{R}^t \rightarrow \mathbb{C}$ be a measurable function defined on a set D with $0 < \mu_t(D) < \infty$.*

- *We say that $\{A_n\}_n$ has a (asymptotic) singular value distribution described*

by f , and we write $\{A_n\}_n \sim_\sigma f$, if

$$\lim_{n \rightarrow \infty} \frac{1}{d_n} \sum_{i=1}^{d_n} F(\sigma_i(A_n)) = \frac{1}{\mu_t(D)} \int_D F(|f(\mathbf{x})|) d\mathbf{x}, \quad \forall F \in C_c(\mathbb{R}). \quad (2.1)$$

- We say that $\{A_n\}_n$ has a (asymptotic) spectral (or eigenvalue) distribution described by f , and we write $\{A_n\}_n \sim_\lambda f$, if

$$\lim_{n \rightarrow \infty} \frac{1}{d_n} \sum_{i=1}^{d_n} F(\lambda_i(A_n)) = \frac{1}{\mu_t(D)} \int_D F(f(\mathbf{x})) d\mathbf{x}, \quad \forall F \in C_c(\mathbb{C}). \quad (2.2)$$

If $\{A_n\}_n$ has both a singular value and an eigenvalue distribution described by f , then we write $\{A_n\}_n \sim_{\sigma,\lambda} f$.

Whenever we write a relation such as $\{A_n\}_n \sim_\lambda f$, it is understood that f is as in Definition 2.1.1; that is, f is a measurable function defined on a subset D of some \mathbb{R}^t with $0 < \mu_t(D) < \infty$ and taking values in \mathbb{C} .

Definition 2.1.2 (Matrix-sequence distributed as matrix-valued function). Let $\{A_n\}_n$ be a sequence of matrices, with A_n of size d_n , and let $\mathbf{f} : D \subset \mathbb{R}^t \rightarrow \mathbb{C}^{r \times r}$ be a measurable function defined on a set D with $0 < \mu_t(D) < \infty$.

- We say that $\{A_n\}_n$ has a (asymptotic) singular value distribution described by \mathbf{f} , and we write $\{A_n\}_n \sim_\sigma \mathbf{f}$, if

$$\lim_{n \rightarrow \infty} \frac{1}{d_n} \sum_{i=1}^{d_n} F(\sigma_i(A_n)) = \frac{1}{\mu_t(D)} \int_D \frac{\sum_{i=1}^r F(\sigma_i(\mathbf{f}(\mathbf{x})))}{r} d\mathbf{x}, \quad \forall F \in C_c(\mathbb{R}). \quad (2.3)$$

- We say that $\{A_n\}_n$ has a (asymptotic) spectral (or eigenvalue) distribution described by \mathbf{f} , and we write $\{A_n\}_n \sim_\lambda \mathbf{f}$, if

$$\lim_{n \rightarrow \infty} \frac{1}{d_n} \sum_{i=1}^{d_n} F(\lambda_i(A_n)) = \frac{1}{\mu_t(D)} \int_D \frac{\sum_{i=1}^r F(\lambda_i(\mathbf{f}(\mathbf{x})))}{r} d\mathbf{x}, \quad \forall F \in C_c(\mathbb{C}). \quad (2.4)$$

If $\{A_n\}_n$ has both a singular value and an eigenvalue distribution described by \mathbf{f} , we write $\{A_n\}_n \sim_{\sigma,\lambda} \mathbf{f}$.

We note that Definition 2.1.2 is well-posed because the functions

$$\mathbf{x} \mapsto \sum_{i=1}^r F(\sigma_i(\mathbf{f}(\mathbf{x}))) \quad \text{and} \quad \mathbf{x} \mapsto \sum_{i=1}^r F(\lambda_i(\mathbf{f}(\mathbf{x})))$$

are measurable.

The informal meaning behind the spectral distribution (2.4) is the following: if \mathbf{f} is continuous, then a suitable ordering of the eigenvalues $\{\lambda_j(A_n)\}_{j=1,\dots,d_n}$, assigned in correspondence with an equispaced grid on D , reconstructs approximately the r surfaces $\mathbf{x} \mapsto \lambda_i(\mathbf{f}(\mathbf{x}))$, $i = 1, \dots, r$.

For instance, if $t = 1$, $d_n = nr$, and $D = [a, b]$, then the eigenvalues of A_n are approximately equal to $\lambda_i(\mathbf{f}(a + j(b - a)/n))$, $j = 1, \dots, n$, $i = 1, \dots, r$; if $t = 2$, $d_n = n^2r$, and $D = [a_1, b_1] \times [a_2, b_2]$, then the eigenvalues of A_n are approximately equal to $\lambda_i(\mathbf{f}(a_1 + j_1(b_1 - a_1)/n, a_2 + j_2(b_2 - a_2)/n))$, $j_1, j_2 = 1, \dots, n$, $i = 1, \dots, r$ (and so on for $t \geq 3$). This type of information is useful in engineering applications [44], e.g. for the computation of the relevant vibrations, and in the analysis of the (asymptotic) convergence speed of iterative solvers for large linear systems or for improving the convergence rate by e.g. the design of appropriate preconditioners [5, 6].

The next theorem gives useful tools for computing the spectral distribution of sequences formed by Hermitian matrices. For the related proof, we refer the reader to [54, Theorem 4.3].

Theorem 2.1.3. *Let $\{A_n\}_n$ be a sequence of matrices, with A_n Hermitian of size d_n , and let $\{P_n\}_n$ be a sequence such that $P_n \in \mathbb{C}^{d_n \times \delta_n}$, $P_n^* P_n = I_{\delta_n}$, $\delta_n \leq d_n$ and $\delta_n/d_n \rightarrow 1$ as $n \rightarrow \infty$. Then, $\{A_n\}_n \sim_{\sigma, \lambda} \mathbf{f}$ if and only if $\{P_n^* A_n P_n\}_n \sim_{\sigma, \lambda} \mathbf{f}$.*

Definition 2.1.4 (Clustering of a matrix sequence). *Given $\{A_n\}_n$ a sequence of matrices of increasing size d_n and let $S \subseteq \mathbb{C}$ be a non-empty closed subset of \mathbb{C} .*

- $\{A_n\}_n$ is strongly clustered at S in the sense of the eigenvalues if, every $\epsilon > 0$ there exists a constant $q_\epsilon(n, S)$ independent from n such that the number of eigenvalues of A_n outside $B(S, \epsilon)$ is bounded by q_ϵ . In symbols,

$$q_\epsilon(n, S) := \#\{j \in \{1, \dots, d_n\} : \lambda_j(A_n) \notin B(S, \epsilon)\} = O(1), \quad \text{as } n \rightarrow \infty.$$

- $\{A_n\}_n$ is weakly clustered at S if, for all $\epsilon > 0$,

$$q_\epsilon(n, S) = o(d_n), \quad \text{as } n \rightarrow \infty.$$

If $\{A_n\}_n$ is strongly or weakly clustered at S and S is not connected, then the connected components of S are called sub-clusters.

Definition 2.1.5 (Essential range of complex-valued function). Let $f : D \subseteq \mathbb{R}^t \rightarrow \mathbb{C}$ be a measurable function, with D a measurable set of finite measure. The set $\mathcal{ER}(f) := \{z \in \mathbb{C} : \mu_t(\{f \in B(z, \epsilon)\}) > 0 \text{ for all } \epsilon > 0\}$, is the essential range of f where $\{f \in B(z, \epsilon)\} := \{x \in D : f(x) \in B(z, \epsilon)\}$.

$\mathcal{ER}(f)$ is always closed; moreover, if f is continuous and D is contained in the closure of its interior, then $\mathcal{ER}(f)$ coincides with the closure of the image of f .

Definition 2.1.6 (Essential range of matrix-valued function). Let $\mathbf{f} : D \subseteq \mathbb{R}^t \rightarrow \mathbb{C}^{r \times r}$ be a measurable function, with D a measurable set of finite measure, the essential range of \mathbf{f} is defined as the union of the essential ranges of the eigenvalue functions $\lambda_i(\mathbf{f})$, $i = 1, \dots, r$: $\mathcal{ER}(\mathbf{f}) := \bigcup_{i=1}^r \mathcal{ER}(\lambda_i(\mathbf{f}))$.

Theorem 2.1.7. If $\{A_n\}_n \sim_\lambda \mathbf{f}$ (with $\{A_n\}_n$, \mathbf{f} as in Definition 2.1.2), then, by [45, Theorem 4.2], $\{A_n\}_n$ is weakly clustered at the essential range of \mathbf{f} , defined as the union of the essential ranges of the eigenvalue functions $\lambda_i(\mathbf{f})$, $i = 1, \dots, r$: $\mathcal{ER}(\mathbf{f}) := \bigcup_{i=1}^s \mathcal{ER}(\lambda_i(\mathbf{f}))$.

Definition 2.1.8 (Spectral attraction). Let $\{A_n\}_n$ be a sequence of matrices of size d_n tending to infinity, let $z \in \mathbb{C}$ and let $\lambda_1, \lambda_2, \dots, \lambda_{d_n}$ the eigenvalues of A_n ordered according to their distance from z , i.e.

$$|\lambda_1 - z| \leq |\lambda_2 - z| \leq \dots \leq |\lambda_{d_n} - z|,$$

We say that z strongly attracts the spectrum $\Lambda(A_n)$ with infinite order if, for each fixed k ,

$$\lim_{n \rightarrow \infty} |\lambda_k - z| = 0.$$

Theorem 2.1.9. [45, Theorem 4.2] If $\{A_n\}_n \sim_\lambda \mathbf{f}$ (with $\{A_n\}_n$, \mathbf{f} as in Definition 2.1.2), then each point $z \in \mathcal{ER}(\mathbf{f})$ strongly attracts $\Lambda(A_n)$ with infinite order.

Now, we provide a classical theorem that is the Gershgorin's theorem; see [8] which provide the spectral localization of a matrix.

Theorem 2.1.10. Let $A \in \mathbb{C}^{n \times n}$, we define the Gershgorin disk as

$$B(a_{jj}, z_j) = \{z \in \mathbb{C} : |a_{jj} - z| \leq z_j\}, \text{ where } z_j = \sum_{k \neq j} |a_{jk}|.$$

Then

$$\Lambda(A) \subset \cup_{j=1}^n B(a_{jj}, z_j).$$

The next result is known as Cauchy's interlacing theorem for Hermitian matrices, which is useful to get information about the eigenvalues of a Hermitian matrix if we know those of any principal submatrix. We refer to [8, Corollary III.1.5] and [53] for the proof.

Theorem 2.1.11. *Let $A \in \mathbb{C}^{n \times n}$ be a Hermitian matrix and let $B \in \mathbb{C}^{m \times m}$ its principal submatrix. Let $\lambda_1 \leq \lambda_2 \leq \dots \leq \lambda_n$ and $\mu_1 \leq \mu_2 \leq \dots \leq \mu_m$ be the eigenvalues of A and B respectively arranged in non-decreasing order, then*

$$\lambda_k \leq \mu_k \leq \lambda_{k+n-m}, \text{ for } k = 1, \dots, m.$$

Moreover, if $m = n - 1$,

$$\lambda_1 \leq \mu_1 \leq \lambda_2 \leq \mu_2 \leq \dots \leq \mu_{n-1} \leq \lambda_n.$$

To end this section, we give a useful result for computing the spectral distribution of a sequence of perturbed Hermitian matrices of the form $\{A_n + B_n\}_n$, for more details, see [41, Theorem 3.3].

Theorem 2.1.12. *Let $\{A_n\}, \{B_n\}$ be a sequence of matrices of increasing size d_n , if we assume that the following conditions are satisfied.*

- *Each A_n is Hermitian and $\{A_n\} \sim_\lambda \mathbf{f}$, where $\mathbf{f} : D \subseteq \mathbb{R}^t \rightarrow \mathbb{C}^{r \times r}$.*
- *There exists a constant $C > 0$, for all n , $\|A_n\|, \|B_n\| \leq C$.*
- *$\|B_n\|_1 = o(d_n)$.*

Then $\{C_n\} \sim_\lambda \mathbf{f}$ with $C_n = A_n + B_n$, and $\lambda_i(\mathbf{f}) \in \overline{\cup_n \Lambda(A_n)} \subseteq [-C, C]$ almost everywhere, for $i = 1, \dots, r$.

2.2 Zero-Distributed matrix-sequences

A sequence of matrices $\{Z_n\}_n$ such that $\{Z_n\}_n \sim_\sigma 0$ is referred to as a zero-distributed sequence. Note that, for any $r \geq 1$, $\{Z_n\}_n \sim_\sigma 0$ is equivalent to $\{Z_n\}_n \sim_\sigma O_r$. Proposition 2.2.1 provides an important characterization of zero-distributed sequences, together with a useful sufficient condition for detecting such sequences. Throughout this paper we use the natural convention $1/\infty = 0$.

Proposition 2.2.1. *Let $\{Z_n\}_n$ be a sequence of matrices, with Z_n of size d_n with $d_k < d_{k+1}$, $\forall k \in \mathbb{N}$. Then*

- $\{Z_n\}_n$ is zero-distributed if and only if $Z_n = R_n + N_n$ with $\text{rank}(R_n)/d_n \rightarrow 0$ and $\|N_n\|_2 \rightarrow 0$ as $n \rightarrow \infty$.
- $\{Z_n\}_n$ is zero-distributed if there exists $p \in [1, \infty]$ such that $\|Z_n\|_p/(d_n)^{1/p} \rightarrow 0$ as $n \rightarrow \infty$.

2.3 Toeplitz and Circulant matrices

Toeplitz matrices are a significant and current topic, which has been used for well over a century, introduced in Toeplitz's initial works [76] and have been the subject of numerous works [11, 12, 47]. These types of matrices arise in several applications such as the discretization of systems of constant coefficient-differential equations [71], Markov chains [10], in the reconstruction of signals and images with missing data [22, 50], Riccati equations [9].

In this part, we describe Toeplitz and Circulant matrices, giving both their description and some of their features. Subsections 2.3.1, 2.3.2 describe the case of the scalar setting, while Subsections 2.3.3, 2.3.4 focus on the most general setting where Toeplitz and Circulant matrices are extended to a Multilevel Block form.

2.3.1 Scalar Toeplitz matrices

Any matrix $A_n \in \mathbb{C}^{n \times n}$ having the form

$$A_n = [a_{i-j}]_{i,j=1}^n = \begin{bmatrix} a_0 & a_{-1} & a_{-2} & \dots & \dots & a_{-(n-1)} \\ a_1 & \ddots & \ddots & \ddots & & \vdots \\ a_2 & \ddots & \ddots & \ddots & \ddots & \vdots \\ \vdots & \ddots & \ddots & \ddots & \ddots & a_{-2} \\ \vdots & & \ddots & \ddots & \ddots & a_{-1} \\ a_{n-1} & \dots & \dots & a_2 & a_1 & a_0 \end{bmatrix},$$

i.e., whose elements are constant along each diagonal, is called Toeplitz. This matrix is completely characterized by the elements of the first row and column $[a_{n-1}, \dots, a_2, a_1, a_0, a_{-1}, a_{-2}, \dots, a_{-(n-1)}]$.

The entries of A_n can be generated from the Fourier coefficients of a 2π -periodic function $f \in L^1([-\pi, \pi])$

$$a_k = \frac{1}{2\pi} \int_{-\pi}^{\pi} f(\theta) e^{-ik\theta} d\theta, \quad k \in \mathbb{Z},$$

where f is called the generating function, and it is given by Fourier series

$$f(\theta) = \sum_{k=-\infty}^{\infty} a_k e^{ik\theta}.$$

In this case A_n is the Toeplitz matrix associated with f , expressed through the Toeplitz operator, i.e., $A_n = T_n(f)$.

It follows that the properties of the matrix $T_n(f)$ and its eigenvalues can be defined from the properties of the generating function f , see [38, 66]. The most relevant features are listed below:

1. If f is real-valued almost everywhere ($f(\theta) = \overline{f(\theta)}$), then $T_n(f)$ is Hermitian ($a_{-k} = \overline{a_k}$, $k \in \mathbb{Z}$) for all n .
2. If f is even ($f(\theta) = f(-\theta)$), then $T_n(f)$ is (complex) symmetric ($a_k = a_{-k}$, $k \in \mathbb{Z}$) for all n .
3. If f is positive almost everywhere ($f \geq 0$), then $T_n(f)$ is Hermitian Positive Semi-Definite ($T_n(f) \geq 0$) for all n .
4. Let $f \in L^1([-\pi, \pi])$ real-valued almost everywhere, and let $m_f = \text{ess inf}_{\theta \in [-\pi, \pi]} f(\theta)$, $M_f = \text{ess sup}_{\theta \in [-\pi, \pi]} f(\theta)$.
 - If $m_f = M_f$, then $T_n(f) = m_f I_n$ and $\Lambda(T_n(f)) = \{m_f\}$.
 - If $m_f < M_f$, then $\Lambda(T_n(f)) \subset (m_f, M_f)$.
5. Let $\lambda_1(T_n(f)) \leq \lambda_2(T_n(f)) \leq \dots \leq \lambda_n(T_n(f))$ be the eigenvalues of $T_n(f)$ ordered in non-decreasing order. Then for all n fixed, for each $s \geq 1$ independent of n , we have

$$\lim_{n \rightarrow \infty} \lambda_s(T_n(f)) = m_f, \quad \lim_{n \rightarrow \infty} \lambda_{n-s+1}(T_n(f)) = M_f.$$

6. Let $f \in L^1([-\pi, \pi])$ be real-valued almost everywhere, and let $m_f = \text{ess inf}_{\theta \in [-\pi, \pi]} f(\theta)$, $M_f = \text{ess sup}_{\theta \in [-\pi, \pi]} f(\theta)$. Assume that $f(\theta) - m_f$ has a finite number of zeros of order $\alpha_1, \alpha_2, \dots, \alpha_k > 0$ and assume that $M_f - f(\theta)$ has a finite number of zeros of order $\beta_1, \beta_2, \dots, \beta_q > 0$, then

- For each fixed j with respect to n

$$\lambda_j(T_n(f)) - m_f \sim \frac{1}{n^\alpha}, \quad \text{with } \alpha = \max_{1 \leq s \leq k} \alpha_s.$$

- For each fixed j with respect to n

$$M_f - \lambda_j(T_n(f)) \sim \frac{1}{n^\beta}, \quad \text{with } \beta = \max_{1 \leq s \leq q} \beta_s.$$

2.3.2 Scalar Circulant matrices

Now, we provide a particular case of Toeplitz matrices which have the following form

$$A_n = [a_{(i-j) \bmod n}]_{i,j=1}^n = \begin{bmatrix} a_0 & a_{n-1} & a_{n-2} & \cdots & \cdots & a_1 \\ a_1 & \ddots & \ddots & \ddots & & \vdots \\ a_2 & \ddots & \ddots & \ddots & \ddots & \vdots \\ \vdots & \ddots & \ddots & \ddots & \ddots & a_{n-2} \\ \vdots & & \ddots & \ddots & \ddots & a_{n-1} \\ a_{n-1} & \cdots & \cdots & a_2 & a_1 & a_0 \end{bmatrix}.$$

This kind of matrix is called a Circulant matrix and it can be written as the following expression

$$A_n = \sum_{s=0}^{n-1} a_s Z_n^{(s)}, \quad (2.5)$$

where $Z_n^{(s)} = \begin{cases} 1 & \text{if } (i-j) \bmod n = s, \\ 0 & \text{otherwise,} \end{cases}$ and $Z_n^{(s)} = Z_n^{s \bmod n}$ for every $s \in \mathbb{Z}$.

The Circulant matrices are diagonalizable by the unitary Fourier matrix F_n given by

$$F_n = \left[\frac{1}{\sqrt{n}} e^{-i \frac{2\pi ij}{n}} \right]_{i,j=1}^n.$$

Therefore, the algebra of Circulant matrices is defined as

$$\mathcal{C}_n = \left\{ A_n \in \mathbb{C}^{n \times n} \mid A_n = F_n D_n F_n^*, \quad D_n = \text{diag}_{j=0, \dots, n-1} f\left(\frac{2\pi j}{n}\right) \right\},$$

where $f(x) = p \circ e^{\hat{i}x}$, $p \in \mathcal{P}_{n-1}$ (\mathcal{P}_n denote the space of polynomials of degree less or equal to n), and $p(z) = \sum_{s=0}^{n-1} a_s z^s$, that is the spectrum of every Circulant is uniquely determined by its first column.

2.3.3 Multilevel block-Toeplitz matrices

This subsection is devoted to the concept of multilevel block-Toeplitz matrices, these matrices have the same structure as the scalar Toeplitz matrices, but this time the entries a_k are matrices instead of scalars.

A matrix $\mathbf{A}_n \in \mathbb{C}^{rn \times rn}$ of the following structure

$$\mathbf{A}_n = [A_{i-j}]_{i,j=1}^n = \begin{bmatrix} A_0 & A_{-1} & A_{-2} & \dots & \dots & A_{-(n-1)} \\ A_1 & \ddots & \ddots & \ddots & & \vdots \\ A_2 & \ddots & \ddots & \ddots & \ddots & \vdots \\ \vdots & \ddots & \ddots & \ddots & \ddots & A_{-2} \\ \vdots & & \ddots & \ddots & \ddots & A_{-1} \\ A_{n-1} & \dots & \dots & A_2 & A_1 & A_0 \end{bmatrix}$$

is a block-Toeplitz matrix, where $A_k \in \mathbb{C}^{r \times r}$, $k \in \mathbb{Z}$.

Notice that the unilevel block Toeplitz matrix \mathbf{A}_n can be written as

$$\mathbf{A}_n = \sum_{k=-(n-1)}^{n-1} J_n^{(k)} \otimes A_k, \quad (2.6)$$

where $J_m^{(l)}$ is the matrix of order m whose (i, j) entry equals 1 if $i - j = l$ and zero otherwise.

Definition 2.3.1. *The Fourier coefficients of a matrix-valued function $\mathbf{f} \in L^1([-\pi, \pi], r)$ are given by*

$$\hat{f}_k := \frac{1}{2\pi} \int_{(-\pi, \pi)} \mathbf{f}(\theta) e^{-ik\theta} d\theta \in \mathbb{C}^{r \times r}, \quad k \in \mathbb{Z},$$

where the integrals are computed componentwise. Then, we define the block-Toeplitz matrix $T_n(\mathbf{f})$ associated with \mathbf{f} as the $rn \times rn$ matrix given by

$$T_n(\mathbf{f}) = \sum_{|k| < n} J_n^{(k)} \otimes \hat{f}_k,$$

with $J_n^{(k)}$ is the matrix as defined in (2.6). The set $\{T_n(\mathbf{f})\}_n$ is called the family of block-Toeplitz matrices generated by \mathbf{f} .

The next definition is an extension of the definition of the Toeplitz matrix in a more general case, when the entries elements are generated by a t -variate matrix-valued function, and the resulting matrix is multilevel block Toeplitz matrix.

Definition 2.3.2. Given $\mathbf{n} \in \mathbb{N}^t$, a matrix of the form

$$[A_{\mathbf{i}-\mathbf{j}}]_{\mathbf{i},\mathbf{j}=\mathbf{e}}^{\mathbf{n}} \in \mathbb{C}^{N(\mathbf{n})r \times N(\mathbf{n})r}$$

with blocks $A_{\mathbf{k}} \in \mathbb{C}^{r \times r}$, $\mathbf{k} = -(\mathbf{n}-\mathbf{e}), \dots, \mathbf{n}-\mathbf{e}$, is called a multilevel block Toeplitz matrix, or, more precisely, a t -level r -block Toeplitz matrix.

Given a matrix-valued function $\mathbf{f} \in L^1([-\pi, \pi]^t, r)$, we denote its Fourier coefficients by

$$\hat{\mathbf{f}}_{\mathbf{k}} = \frac{1}{(2\pi)^t} \int_{[-\pi, \pi]^t} \mathbf{f}(\boldsymbol{\theta}) e^{-i(\mathbf{k}, \boldsymbol{\theta})} d\boldsymbol{\theta} \in \mathbb{C}^{r \times r}, \quad \mathbf{k} \in \mathbb{Z}^t, \quad (2.7)$$

where the integrals are computed componentwise and $(\mathbf{k}, \boldsymbol{\theta}) = k_1\theta_1 + \dots + k_t\theta_t$. For every $\mathbf{n} \in \mathbb{N}^t$, the \mathbf{n} -th Toeplitz matrix associated with \mathbf{f} is defined as

$$T_{\mathbf{n}}(\mathbf{f}) := [\hat{\mathbf{f}}_{\mathbf{i}-\mathbf{j}}]_{\mathbf{i},\mathbf{j}=\mathbf{e}}^{\mathbf{n}} \quad (2.8)$$

or, equivalently, as

$$T_{\mathbf{n}}(\mathbf{f}) = \sum_{|j_1| < n_1} \dots \sum_{|j_t| < n_t} [J_{n_1}^{(j_1)} \otimes \dots \otimes J_{n_t}^{(j_t)}] \otimes \hat{\mathbf{f}}_{(j_1, \dots, j_t)}. \quad (2.9)$$

Analogously to the scalar Toeplitz matrix case, some properties of the matrix $T_{\mathbf{n}}(\mathbf{f})$ and its eigenvalues can be extracted from the properties of \mathbf{f} as follows, see [3, 4, 36, 39]

1. If the matrix $\mathbf{f} \in L^1([-\pi, \pi]^t, r)$ is Hermitian ($\mathbf{f}(\boldsymbol{\theta}) = \mathbf{f}^*(\boldsymbol{\theta})$) almost everywhere, then all the matrices $T_{\mathbf{n}}(\mathbf{f})$ are Hermitian.
2. If the matrix $\mathbf{f} \in L^1([-\pi, \pi]^t, r)$ is Hermitian Positive Semi-Definite ($\mathbf{f}(\boldsymbol{\theta}) \geq 0$) almost everywhere, then all the matrices $T_{\mathbf{n}}(\mathbf{f})$ are Hermitian Positive Semi-Definite.
3. Let $\mathbf{f} \in L^1([-\pi, \pi]^t, r)$ be a Hermitian matrix and let $\mathbf{m}_{\mathbf{f}} = \operatorname{ess\,inf}_{\boldsymbol{\theta} \in [-\pi, \pi]^t} \lambda_{\min}(\mathbf{f}(\boldsymbol{\theta}))$, $\mathbf{M}_{\mathbf{f}} = \operatorname{ess\,sup}_{\boldsymbol{\theta} \in [-\pi, \pi]^t} \lambda_{\max}(\mathbf{f}(\boldsymbol{\theta}))$ then
 - If $\mathbf{m}_{\mathbf{f}} = \mathbf{M}_{\mathbf{f}}$ then $T_{\mathbf{n}}(\mathbf{f}) = \mathbf{m}_{\mathbf{f}} I_{N(\mathbf{n})r}$ and $\Lambda(T_{\mathbf{n}}(\mathbf{f})) = \{\mathbf{m}_{\mathbf{f}}\}$.
 - If $\mathbf{m}_{\mathbf{f}} < \operatorname{ess\,sup}_{\boldsymbol{\theta} \in [-\pi, \pi]^t} \lambda_{\min}(\mathbf{f}(\boldsymbol{\theta})) \leq \mathbf{M}_{\mathbf{f}}$ then $\Lambda(\mathbf{f}) \subset (\mathbf{m}_{\mathbf{f}}, \mathbf{M}_{\mathbf{f}}]$.
 - If $\mathbf{m}_{\mathbf{f}} \leq \operatorname{ess\,inf}_{\boldsymbol{\theta} \in [-\pi, \pi]^t} \lambda_{\max}(\mathbf{f}(\boldsymbol{\theta})) < \mathbf{M}_{\mathbf{f}}$ then $\Lambda(\mathbf{f}) \subset [\mathbf{m}_{\mathbf{f}}, \mathbf{M}_{\mathbf{f}})$.

4. Let $\lambda_1(T_{\mathbf{n}}(\mathbf{f})) \leq \lambda_2(T_{\mathbf{n}}(\mathbf{f})) \leq \dots \leq \lambda_{N(\mathbf{n})r}(T_{\mathbf{n}}(\mathbf{f}))$ be the eigenvalues of $T_{\mathbf{n}}(\mathbf{f})$ ordered in non-decreasing order. Then for each fixed $s \geq 1$, independent of \mathbf{n} , we have

$$\lim_{\mathbf{n} \rightarrow \infty} \lambda_s(T_{\mathbf{n}}(\mathbf{f})) = \mathbf{m}_{\mathbf{f}}, \quad \lim_{\mathbf{n} \rightarrow \infty} \lambda_{N(\mathbf{n})r-s+1}(T_{\mathbf{n}}(\mathbf{f})) = \mathbf{M}_{\mathbf{f}}.$$

5. Let $\mathbf{f} \in L^1([-\pi, \pi]^t, r)$ be a Hermitian matrix-valued and let $\mathbf{m}_{\mathbf{f}} = \operatorname{ess\,inf}_{\boldsymbol{\theta} \in ([-\pi, \pi]^t)^t} \lambda_{\min}(\mathbf{f}(\boldsymbol{\theta}))$, $\mathbf{M}_{\mathbf{f}} = \operatorname{ess\,sup}_{\boldsymbol{\theta} \in ([-\pi, \pi]^t)^t} \lambda_{\max}(\mathbf{f}(\boldsymbol{\theta}))$. Assume that $\lambda_{\min}(\mathbf{f}(\boldsymbol{\theta})) - \mathbf{m}_{\mathbf{f}}$ has a finite number of zeros of order $\alpha_1, \alpha_2, \dots, \alpha_k > 0$, then

- For each fixed j with respect to \mathbf{n} and assuming that $n_1 \sim n_2 \sim \dots \sim n_t$

$$\lambda_j(T_{\mathbf{n}}(\mathbf{f})) - \mathbf{m}_{\mathbf{f}} \sim \frac{1}{[N(\mathbf{n})]^{\alpha/t}}, \quad \text{with } \alpha = \max_{1 \leq s \leq k} \alpha_s.$$

Remark 2.3.3. From Item 2 we conclude that if $\mathbf{f}_1, \mathbf{f}_2 \in L^1([-\pi, \pi]^t, r)$ and $\mathbf{f}_1(\boldsymbol{\theta}) \geq \mathbf{f}_2(\boldsymbol{\theta})$ almost everywhere, then $T_n(\mathbf{f}_1) \geq T_n(\mathbf{f}_2)$.

2.3.4 Multilevel block Circulant matrices

If $A_{\mathbf{k}} \in \mathbb{C}^{r \times r}$ then, the matrix having the following form

$$\mathbf{A} = \left[A_{(\mathbf{i}-\mathbf{j}) \bmod \mathbf{n}} \right]_{\mathbf{i}, \mathbf{j}=\mathbf{e}}^{\mathbf{n}} \in \mathbb{C}^{rN(\mathbf{n}) \times rN(\mathbf{n})}$$

is called multilevel Circulant matrix, where $Z_n^{(j)}$ is defined as in (2.5).

The \mathbf{n} -th Circulant matrix associated with $\mathbf{f} : [-\pi, \pi]^t \rightarrow \mathbb{C}^{r \times r}$ is defined as

$$\mathcal{C}_{\mathbf{n}}(\mathbf{f}) = \sum_{|j_1| < n_1} \dots \sum_{|j_t| < n_t} [Z_{n_1}^{(j_1)} \otimes \dots \otimes Z_{n_t}^{(j_t)}] \otimes \hat{\mathbf{f}}_{(j_1, \dots, j_t)}.$$

Theorem 2.3.4. [36] The Circulant matrix \mathbf{A} can be decomposed as follows

$$\mathbf{A} = (F_{\mathbf{n}} \otimes I_r) \operatorname{diag}_{\mathbf{j}=0, \dots, \mathbf{n}-1} \mathbf{g}_{\mathbf{n}} \left(\frac{2\pi \mathbf{j}}{\mathbf{n}} \right) (F_{\mathbf{n}} \otimes I_r)^*$$

where

$$\mathbf{g}_{\mathbf{n}}(\boldsymbol{\theta}) = \sum_{|k_1| < n_1} \sum_{|k_2| < n_2} \dots \sum_{|k_t| < n_t} \hat{\mathbf{f}}_{\mathbf{k}} e^{i(\mathbf{k}, \boldsymbol{\theta})} \quad \text{and} \quad F_{\mathbf{n}} = \frac{1}{\sqrt{N(\mathbf{n})}} \left(e^{i(\mathbf{k}, \frac{2\pi \mathbf{j}}{\mathbf{n}})} \right)_{\mathbf{j}, \mathbf{k}=0}^{\mathbf{n}-\mathbf{e}}.$$

2.4 Generalized Locally Toeplitz (GLT) sequences

A GLT sequences [3, 4, 38, 39] is a specific sequence of matrices of size d_n tending to infinity associated with a Lebesgue-measurable complex-valued function κ which is defined on $[0, 1]^t \times [-\pi, \pi]^t$, $t \geq 1$, where $[0, 1]^t$ and $[-\pi, \pi]^t$ represent the domains of physical variable and Fourier variable, respectively. In this section, we will give a brief overview on the multilevel form of GLT sequences class [42, 43] (or r -block GLT sequences class, $r \geq 1$) where the associated function is measurable matrix-valued function $\kappa : [0, 1]^t \times [-\pi, \pi]^t \rightarrow \mathbb{C}^{r \times r}$, $t \geq 1$. We use the notation $\{A_{\mathbf{n}}\}_{\mathbf{n}} \sim_{\text{GLT}} \kappa$ to indicate that $\{A_{\mathbf{n}}\}_{\mathbf{n}}$ is a GLT sequences with symbol κ . The symbol of a GLT sequences is unique in the sense that if $\{A_{\mathbf{n}}\}_{\mathbf{n}} \sim_{\text{GLT}} \kappa$ and $\{A_{\mathbf{n}}\}_{\mathbf{n}} \sim_{\text{GLT}} \varsigma$ then $\kappa = \varsigma$ almost everywhere in $[0, 1]^t \times [-\pi, \pi]^t$.

• **Block Diagonal Sampling Matrices.** For $n \in \mathbb{N}$, $t = 1$, and $a : [0, 1] \rightarrow \mathbb{C}^{r \times r}$, we define the block diagonal sampling matrix $D_n(a)$ as the block diagonal matrix

$$D_n(a) = \text{diag}_{i=1, \dots, n} a\left(\frac{i}{n}\right) = \begin{bmatrix} a\left(\frac{1}{n}\right) & & & \\ & a\left(\frac{2}{n}\right) & & \\ & & \ddots & \\ & & & a(1) \end{bmatrix} \in \mathbb{C}^{rn \times rn}.$$

For a general dimensionality $t \geq 2$, we consider $a : [0, 1]^t \rightarrow \mathbb{C}^{r \times r}$, $\mathbf{n} = (n_1, \dots, n_t)$ and we define the block multilevel diagonal sampling matrix $D_{\mathbf{n}}(a)$ as the block diagonal matrix

$$D_{\mathbf{n}}(a) = \text{diag}_{\mathbf{i}=\mathbf{e}, \dots, \mathbf{n}} a\left(\frac{\mathbf{i}}{\mathbf{n}}\right) \in \mathbb{C}^{rN(\mathbf{n}) \times rN(\mathbf{n})},$$

where the multi-index \mathbf{i}/\mathbf{n} has to be intended as $(i_1/n_1, \dots, i_t/n_t)$ and the ordering is the lexicographical one as in the work by E. Tyrtyshnikov, (see for instance [77]).

The main properties of r -block GLT sequences proved in [42, 43] are listed below: they represent a complete characterization of GLT sequences, equivalent to the full constructive definition.

GLT 1. If $\{A_{\mathbf{n}}\}_{\mathbf{n}} \sim_{\text{GLT}} \kappa$ then $\{A_{\mathbf{n}}\}_{\mathbf{n}} \sim_{\sigma} \kappa$. If moreover each $A_{\mathbf{n}}$ is Hermitian then $\{A_{\mathbf{n}}\}_{\mathbf{n}} \sim_{\lambda} \kappa$.

GLT 2. We have:

- $\{T_{\mathbf{n}}(\mathbf{f})\}_{\mathbf{n}} \sim_{\text{GLT}} \kappa(\mathbf{x}, \boldsymbol{\theta}) = \mathbf{f}(\boldsymbol{\theta})$ if $\mathbf{f} : [-\pi, \pi]^t \rightarrow \mathbb{C}^{r \times r}$ is in $L^1([-\pi, \pi]^t)$;

- $\{D_n(a)\}_n \sim_{\text{GLT}} \kappa(\mathbf{x}, \boldsymbol{\theta}) = a(\mathbf{x})$ if $a : [0, 1]^t \rightarrow \mathbb{C}^{r \times r}$ is Riemann-integrable;
- $\{Z_n\}_n \sim_{\text{GLT}} \kappa(\mathbf{x}, \boldsymbol{\theta}) = O_r$ if and only if $\{Z_n\}_n \sim_{\sigma} 0$.

GLT 3. If $\{A_n\}_n \sim_{\text{GLT}} \kappa$ and $\{B_n\}_n \sim_{\text{GLT}} \varsigma$ then:

- $\{A_n^*\}_n \sim_{\text{GLT}} \kappa^*$;
- $\{\alpha A_n + \beta B_n\}_n \sim_{\text{GLT}} \alpha \kappa + \beta \varsigma$ for all $\alpha, \beta \in \mathbb{C}$;
- $\{A_n B_n\}_n \sim_{\text{GLT}} \kappa \varsigma$;
- $\{A_n^\dagger\}_n \sim_{\text{GLT}} \kappa^{-1}$ provided that κ is invertible almost everywhere.

GLT 4. $\{A_n\}_n \sim_{\text{GLT}} \kappa$ if and only if there exist r -block GLT sequences $\{B_{n,m}\}_n \sim_{\text{GLT}} \kappa_m$ such that $\{B_{n,m}\}_n \xrightarrow{\text{a.c.s.}} \{A_n\}_n$ and $\kappa_m \rightarrow \kappa$ in measure, where the a.c.s. convergence is studied in [38].

CHAPTER 3

SPECTRAL ANALYSIS OF \mathbb{P}_K FINITE ELEMENT MATRICES IN THE CASE OF FRIEDRICHS-KELLER TRIANGULATIONS VIA GLT TECHNOLOGY

The current chapter deals with the spectral analysis of matrix-sequences arising from the \mathbb{P}_k Lagrangian Finite Element approximation of the elliptic problem.

$$\begin{cases} \operatorname{div}(-a(\mathbf{x})\nabla u) = f, & \mathbf{x} \in \Omega \subseteq \mathbb{R}^d, \\ u|_{\partial\Omega} = 0, \end{cases} \quad (3.1)$$

with Ω bounded connected subset of \mathbb{R}^d , $d \geq 1$, having smooth boundaries for $d \geq 2$, and a being continuous and positive on $\overline{\Omega}$ and $f \in L^2(\Omega)$. For the numerical approximation we consider the classical \mathbb{P}_k Finite Elements, where k is a scalar indicating the global polynomial degree, in the case of Friedrichs-Keller triangulations, leading, as usual, to sequences of matrices of increasing size. The new results concern the spectral analysis of the resulting matrix-sequences in the direction of the global distribution in the Weyl sense, with a concise overview on

localization, clustering, extremal eigenvalues, and asymptotic conditioning. We study in detail the case of constant coefficients on $\Omega = (0, 1)^2$ and we give a brief account in the more involved case of variable coefficients and more general domains. Tools are drawn from the Toeplitz technology and from the rather new theory of GLT sequences, (see [3, 4, 38, 39] and references therein). Numerical results are shown for providing a practical evidence of the theoretical findings.

3.1 Finite Element approximation

Problem (3.1) can be formulated in variational form as follows:

$$\text{find } u \in H_0^1(\Omega) \text{ such that } \int_{\Omega} (a \nabla u \cdot \nabla \varphi) = \int_{\Omega} f \varphi \quad \text{for all } \varphi \in H_0^1(\Omega), \quad (3.2)$$

where $H_0^1(\Omega)$ is the space of square integrable functions vanishing on $\partial\Omega$, with square integrable weak derivatives. We assume that $\Omega \subseteq \mathbb{R}^2$ is a bounded connected set with smooth boundaries (in practice in our numerical tests Ω will be a polygonal domain). Furthermore, we make the following hypotheses on the coefficients:

$$a \in C(\overline{\Omega}), \text{ with } a(\mathbf{x}) \geq a_0 > 0, \text{ and } f \in L^2(\Omega), \quad (3.3)$$

so that existence and uniqueness for problem (3.2) are guaranteed. Hereafter, we consider \mathbb{P}_k Lagrangian Finite Element approximation of problem (3.2). To this end, let $\mathcal{T}_h = \{K\}$ be a usual Finite Element partition of $\overline{\Omega}$ into triangles, with $h_K = \text{diam}(K)$ and $h = \max_K h_K$, and let $V_h \subset H_0^1(\Omega)$ be the space of \mathbb{P}_k Lagrangian Finite Element, i.e.

$$V_h = \{ \varphi_h : \overline{\Omega} \rightarrow \mathbb{R} \text{ s.t. } \varphi_h \text{ is continuous, } \varphi_h|_K \text{ is a polynomial of degree less or equal to } k, \text{ and } \varphi_h|_{\partial\Omega} = 0 \}.$$

The Finite Element approximation of problem (3.2) reads as follows:

$$\text{find } u_h \in V_h \text{ such that } \int_{\Omega} (a \nabla u_h \cdot \nabla \varphi_h) = \int_{\Omega} f \varphi_h \quad \text{for all } \varphi_h \in V_h. \quad (3.4)$$

For each internal node i of the mesh \mathcal{T}_h , meaning both vertices and additional nodal values associated to the \mathbb{P}_k approximation, let $\varphi_i \in V_h$ be such that $\varphi_i(\text{node } i) = 1$, and $\varphi_i(\text{node } j) = 0$ if $i \neq j$. Then, the collection of all φ_i 's is a basis for V_h and

we denote by $n(h)$ its dimension. Then, we write u_h as $u_h = \sum_{j=1}^{n(h)} u_j \varphi_j$ and the variational equation (3.4) becomes an algebraic linear system:

$$\sum_{j=1}^{n(h)} \left(\int_{\Omega} a \nabla \varphi_j \cdot \nabla \varphi_i \right) u_j = \int_{\Omega} f \varphi_i, \quad i = 1, \dots, n(h). \quad (3.5)$$

Our aim is to analyse the spectral properties of the matrix-sequences $\{A_n(a, \Omega, \mathbb{P}_k)\}_n$ arising in the quoted linear systems (3.5), both from the theoretical and numerical point of view.

3.2 A Few remarks on the monodimensional case:

$$\mathbb{Q}_k \equiv \mathbb{P}_k, \quad d = 1$$

We report some results derived in [40] for the Lagrangian Finite Elements $\mathbb{Q}_k \equiv \mathbb{P}_k$, $d = 1$. Let us consider the Lagrange polynomials L_0, \dots, L_k associated with the reference knots $t_j = j/k$, $j = 0, \dots, k$:

$$L_i(t) = \prod_{\substack{j=0 \\ j \neq i}}^k \frac{t - t_j}{t_i - t_j} = \prod_{\substack{j=0 \\ j \neq i}}^k \frac{kt - j}{i - j}, \quad i = 0, \dots, k, \quad (3.6)$$

$$L_i(t_j) = \delta_{ij}, \quad i, j = 0, \dots, k,$$

and let the symbol $\langle \cdot, \cdot \rangle$ denote the scalar product in $L^2([0, 1])$, i.e., $\langle \varphi, \psi \rangle := \int_0^1 \varphi \psi$. In the case $a(x) \equiv 1$ and $\Omega = (0, 1)$ the \mathbb{Q}_k matrix $A_n(a, \Omega, \mathbb{Q}_k)$ equals the matrix $K_n^{(k)}$ in Theorem 3.2.1.

Theorem 3.2.1. *Let $k, n \geq 1$. Then*

$$K_n^{(k)} = \begin{bmatrix} K_0 & K_1^T & & & \\ K_1 & \ddots & \ddots & & \\ & \ddots & \ddots & K_1^T & \\ & & & K_1 & K_0 \end{bmatrix}_- \quad (3.7)$$

where the subscript ‘ $-$ ’ means that the last row and column of the matrix in square

brackets are deleted, while K_0, K_1 are $k \times k$ blocks given by

$$\begin{aligned}
 K_0 &= \left[\begin{array}{ccc|c} \langle L'_1, L'_1 \rangle & \cdots & \langle L'_{k-1}, L'_1 \rangle & \langle L'_k, L'_1 \rangle \\ \vdots & & \vdots & \vdots \\ \langle L'_1, L'_{k-1} \rangle & \cdots & \langle L'_{k-1}, L'_{k-1} \rangle & \langle L'_k, L'_{k-1} \rangle \\ \hline \langle L'_1, L'_k \rangle & \cdots & \langle L'_{k-1}, L'_k \rangle & \langle L'_k, L'_k \rangle + \langle L'_0, L'_0 \rangle \end{array} \right], \\
 K_1 &= \left[\begin{array}{ccc|c} 0 & 0 & \cdots & 0 \\ 0 & 0 & \cdots & 0 \\ \vdots & \vdots & & \vdots \\ 0 & 0 & \cdots & 0 \end{array} \begin{array}{c} \langle L'_0, L'_1 \rangle \\ \langle L'_0, L'_2 \rangle \\ \vdots \\ \langle L'_0, L'_k \rangle \end{array} \right],
 \end{aligned} \tag{3.8}$$

with L_0, \dots, L_k being the Lagrange polynomials in (3.6). In particular, $K_n^{(k)}$ is the $(nk-1) \times (nk-1)$ leading principal submatrix of the block Toeplitz matrices $T_n(\mathbf{f}_k)$ and $\mathbf{f}_k : [-\pi, \pi] \rightarrow \mathbb{C}^{k \times k}$ is an Hermitian matrix-valued function given by

$$\mathbf{f}_k(\theta) := K_0 + K_1 e^{i\theta} + K_1^T e^{-i\theta}. \tag{3.9}$$

An interesting property of the Hermitian matrix-valued functions $\mathbf{f}_k(\theta)$ defined in (3.9) is reported in the theorem below. From the point of view of the spectral distribution, the message is that, independently of the parameter k , the spectral symbol is of the same character as $2 - 2 \cos(\theta)$ which is the symbol of the basic linear Finite Elements and the most standard Finite Differences approximation.

Theorem 3.2.2. *Let $k \geq 1$, then*

$$\det(\mathbf{f}_k(\theta)) = d_k(2 - 2 \cos(\theta)), \tag{3.10}$$

where $d_k = \det([\langle L'_j, L'_i \rangle]_{i,j=1}^k) = \det([\langle L'_j, L'_i \rangle]_{i,j=1}^{k-1}) > 0$ (with $d_1 = 1$ being the determinant of the empty matrix by convention) and L_0, \dots, L_k are the Lagrange polynomials (3.6).

3.3 Two dimensional case: \mathbb{P}_k , $d = 2$ - symbol definition

Hereafter we focus on \mathbb{P}_k Lagrangian Finite Elements in the case of Friedrichs-Keller triangulations $\{\mathcal{T}_K\}$ of the domain Ω as reported in Figure 3.3. Nodes,

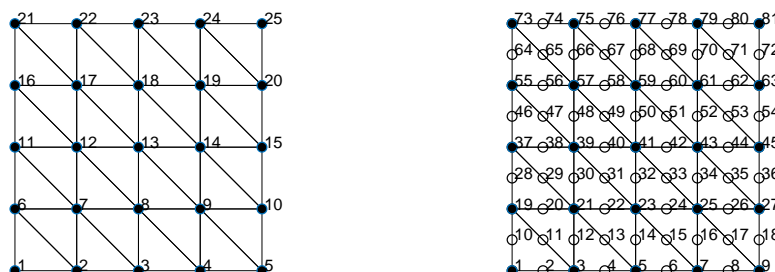


Figure 3.1: Friedrichs-Keller meshes for \mathbb{P}_k , $k = 1, 2$.

that is both vertices and additional nodal values associated to the chosen \mathbb{P}_k approximation, are ordered in standard lexicographical way from left to right, from bottom to top.

The stiffness matrix is built by considering the standard assembling procedure with respect to the reference element \hat{K} in Figure 3.2. Let G be the affine transformation mapping \hat{K} onto a generic $K \in \mathcal{T}_K$ defined as

$$G \left(\begin{bmatrix} \hat{x} \\ \hat{y} \end{bmatrix} \right) = \begin{bmatrix} (e_3)_1 & -(e_2)_1 \\ (e_3)_2 & -(e_2)_2 \end{bmatrix} \begin{bmatrix} \hat{x} \\ \hat{y} \end{bmatrix} + \begin{bmatrix} x^{v_1} \\ y^{v_1} \end{bmatrix},$$

where $e_1 = [x^{v_3} - x^{v_2}, y^{v_3} - y^{v_2}]^T$, $e_2 = [x^{v_1} - x^{v_3}, y^{v_1} - y^{v_3}]^T$, $e_3 = [x^{v_2} - x^{v_1}, y^{v_2} - y^{v_1}]^T$ represent the oriented edge vectors and (x^{v_i}, y^{v_i}) are the coordinates of the i^{th} vertex v_i . Thus,

$$A_K^{El} = \left[\int_K \nabla \varphi_j \cdot \nabla \varphi_i \right]_{i,j}$$

with

$$\int_K \nabla \varphi_j \cdot \nabla \varphi_i = \det(J_G(\hat{x}, \hat{y})) \int_{\hat{K}} [J_{G^{-1}}^T \hat{\nabla} \hat{\varphi}_j(\hat{x}, \hat{y})] \cdot [J_{G^{-1}}^T \hat{\nabla} \hat{\varphi}_i(\hat{x}, \hat{y})] d\hat{x}d\hat{y}, \quad (3.11)$$

where the $\hat{\varphi}_s$'s are the shape functions on \hat{K} , $\det(J_G(\hat{x}, \hat{y})) = 2|K|$ and $J_{G^{-1}}^T$ is the transpose of the Jacobian matrix of the inverse mapping G^{-1} , that is,

$$J_{G^{-1}}^T = \frac{1}{2|K|} \begin{bmatrix} -(e_2)_2 & -(e_3)_2 \\ (e_2)_1 & (e_3)_1 \end{bmatrix}.$$

3.3. Two dimensional case: \mathbb{P}_k , $d = 2$ - symbol definition

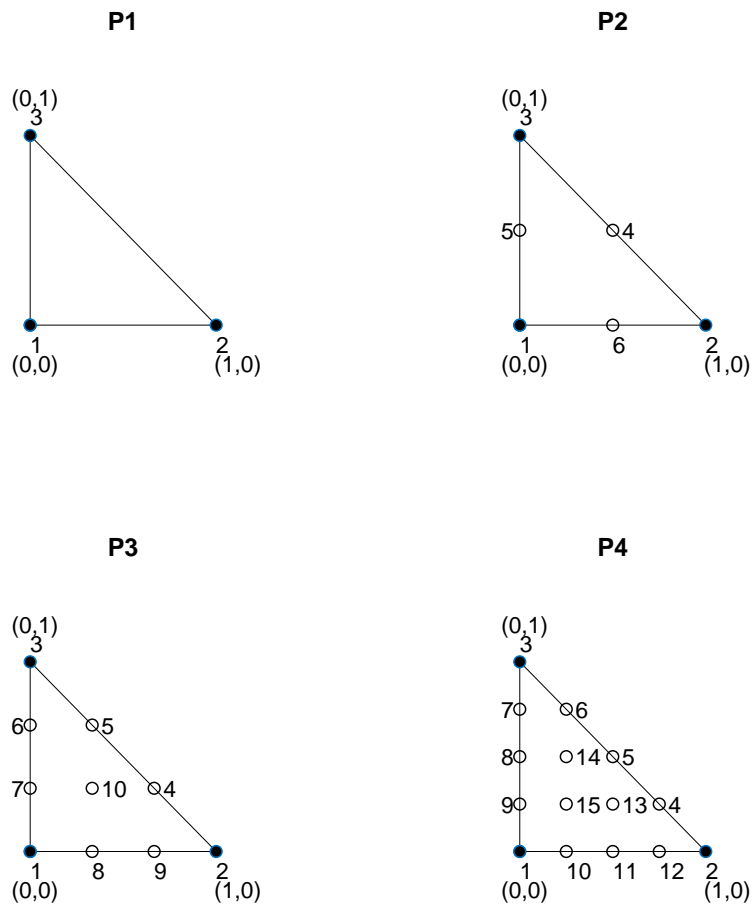


Figure 3.2: Reference element \hat{K} and nodal points for \mathbb{P}_k , $k = 1, \dots, 4$.

In the present section we will preliminarily consider the case $a \equiv 1$ and $\Omega = (0, 1)^2$.

3.3.1 Case $k = 1$

Even if well known, we start by considering the case $k = 1$, that is the one of a linear Lagrangian FE approximation. The shape functions on \hat{K} are defined as

$$\begin{aligned}\hat{\varphi}_1(\hat{x}, \hat{y}) &= -\hat{x} - \hat{y} + 1, \\ \hat{\varphi}_2(\hat{x}, \hat{y}) &= \hat{x}, \\ \hat{\varphi}_3(\hat{x}, \hat{y}) &= \hat{y},\end{aligned}\tag{3.12}$$

so that, according to (3.11), the elemental matrix for a generic triangle of the Friedrichs-Keller triangulation, that is a right-angle triangle of constant edge h , equals

$$A_{K_1}^{El} = \frac{1}{2} \begin{bmatrix} 2 & -1 & -1 \\ -1 & 1 & 0 \\ -1 & 0 & 1 \end{bmatrix} \quad \text{or} \quad A_{K_2}^{El} = \frac{1}{2} \begin{bmatrix} 1 & -1 & 0 \\ -1 & 2 & -1 \\ 0 & -1 & 1 \end{bmatrix},\tag{3.13}$$

for triangles of type 1 (right angle in vertex 1) or type 2 (right angle in vertex 2), respectively.

The stiffness matrix $A_n = A_n(1, \Omega, \mathbb{P}_1)$, that is with $a \equiv 1$, is the twolevel Toeplitz matrix generated by the symbol $f_{\mathbb{P}_1}(\theta_1, \theta_2) = 4 - 2 \cos(\theta_1) - 2 \cos(\theta_2)$. In fact, A_n is block tridiagonal, i.e.

$$A_n = \text{tridiag}(A_1, A_0, A_{-1}),$$

where the triangular blocks are such that $A_0 = \text{tridiag}(a_1^0, a_0^0, a_{-1}^0) = \text{tridiag}(-1, 4, -1)$, $A_1 = A_{-1} = \text{diag}(a_1^1) = -I$, I being the identity matrix. Thus we can easily read the corresponding symbol as follows

$$f_{\mathbb{P}_1}(\theta_1, \theta_2) = f_{A_0}(\theta_1) + f_{A_{-1}}(\theta_1)e^{-i\theta_2} + f_{A_1}(\theta_1)e^{i\theta_2},\tag{3.14}$$

with $f_{A_0}(\theta_1) = a_0^0 + a_{-1}^0 e^{-i\theta_1} + a_1^0 e^{i\theta_1}$ and $f_{A_1}(\theta_1) = f_{A_{-1}}(\theta_1) = a_1^1$.

Clearly, the natural arising question is: which properties are preserved in considering Lagrangian FE of higher order?

3.3.2 Case $k = 2$

Hereafter, we will consider in full detail the case of quadratic Lagrangian FE ($k = 2$), the aim being to introduce a suitable notation making easier the analysis of higher order approximations as well. By referring to the reference element, (see Figure 3.2), we have the following shape functions

$$\begin{aligned}
 \hat{\varphi}_1(\hat{x}, \hat{y}) &= 2\hat{x}^2 + 2\hat{y}^2 + 4\hat{x}\hat{y} - 3\hat{x} - 3\hat{y} + 1, \\
 \hat{\varphi}_2(\hat{x}, \hat{y}) &= \hat{x}(2\hat{x} - 1), \\
 \hat{\varphi}_3(\hat{x}, \hat{y}) &= \hat{y}(2\hat{y} - 1), \\
 \hat{\varphi}_4(\hat{x}, \hat{y}) &= 4\hat{x}\hat{y}, \\
 \hat{\varphi}_5(\hat{x}, \hat{y}) &= -4\hat{y}(\hat{x} + \hat{y} - 1), \\
 \hat{\varphi}_6(\hat{x}, \hat{y}) &= -4\hat{x}(\hat{x} + \hat{y} - 1),
 \end{aligned} \tag{3.15}$$

so that, according to (3.11), the elemental matrix for a generic triangle equals

$$A_{K_1}^{El} = \begin{bmatrix} 1 & \frac{1}{6} & \frac{1}{6} & 0 & -\frac{2}{3} & -\frac{2}{3} \\ \frac{1}{6} & \frac{1}{2} & 0 & 0 & 0 & -\frac{2}{3} \\ \frac{1}{6} & 0 & \frac{1}{2} & 0 & -\frac{2}{3} & 0 \\ 0 & 0 & 0 & \frac{8}{3} & -\frac{4}{3} & -\frac{4}{3} \\ -\frac{2}{3} & 0 & -\frac{2}{3} & -\frac{4}{3} & \frac{8}{3} & 0 \\ -\frac{2}{3} & -\frac{2}{3} & 0 & -\frac{4}{3} & 0 & \frac{8}{3} \end{bmatrix} \tag{3.16}$$

in the case of triangles of type 1, or a suitable permutation in the case of triangles of type 2. in the case of triangles of type 1, or a suitable permutation in the case of triangles of type 2. Despite the use of Lagrangian quadratic approximation, the stiffness matrix $A_n = A_n(1, \Omega, \mathbb{P}_2)$ shows again a block tridiagonal structure $A_n = \text{tridiag}(A_1, A_0, A_{-1})$ as in the linear case, the higher approximation stressing its influence just inside the blocks A_i . We might say that the quoted tridiagonal structure refers once again to triangles' vertices, while the internal structure is stressing the increased number of additional nodal points, that is three in the case at hand. In fact, we observe in each block A_i a 2×2 block structure as follows:

$$A_0 = \begin{bmatrix} B_0^{11} & B_0^{12} \\ (B_0^{12})^T & B_0^{22} \end{bmatrix}, \quad A_{-1} = \begin{bmatrix} 0 & 0 \\ B_{-1}^{21} & B_{-1}^{22} \end{bmatrix}, \quad A_1 = A_{-1}^T, \tag{3.17}$$

where the superscripts i, j in B_l^{ij} denote the position inside the 2×2 block and the subscript l the belonging to the block A_l , so that

$$A_n = \left[\begin{array}{cc|cc|cc|cc} B_0^{11} & B_0^{12} & 0 & 0 & & & & \\ (B_0^{12})^T & B_0^{22} & B_{-1}^{21} & B_{-1}^{22} & & & & \\ \hline 0 & (B_{-1}^{21})^T & B_0^{11} & B_0^{12} & 0 & 0 & & \\ 0 & (B_{-1}^{22})^T & (B_0^{12})^T & B_0^{22} & B_{-1}^{21} & B_{-1}^{22} & & \\ \hline & \ddots & & & \ddots & & & \ddots \\ \hline & & 0 & (B_{-1}^{21})^T & B_0^{11} & B_0^{12} & 0 & \\ & & 0 & (B_{-1}^{22})^T & (B_0^{12})^T & B_0^{22} & B_{-1}^{21} & \\ \hline & & & & 0 & (B_{-1}^{21})^T & B_0^{11} & \end{array} \right]. \quad (3.18)$$

More important, the very same structure depicted in (3.18), including the very same cutting in the lower right corner, appears in every block B_l^{ij} by considering suitable 2×2 matrices as follows

$$B_l^{ij} = \text{tridiag} \left(a_1^{B_l^{ij}}, a_0^{B_l^{ij}}, a_{-1}^{B_l^{ij}} \right), \quad l \in \{-1, 0, 1\}, \quad i, j \in \{1, 2\},$$

where

$$\begin{aligned} a_0^{B_0^{11}} &= \begin{bmatrix} \frac{16}{3} & -\frac{4}{3} \\ -\frac{4}{3} & \frac{16}{3} \end{bmatrix}, & a_{-1}^{B_0^{11}} &= \begin{bmatrix} 0 & 0 \\ -\frac{4}{3} & 0 \end{bmatrix}, & a_1^{B_0^{11}} &= \left(a_{-1}^{B_0^{11}} \right)^T, \\ a_0^{B_0^{22}} &= \begin{bmatrix} \frac{16}{3} & -\frac{4}{3} \\ -\frac{4}{3} & 4 \end{bmatrix}, & a_{-1}^{B_0^{22}} &= \begin{bmatrix} 0 & 0 \\ -\frac{4}{3} & \frac{1}{3} \end{bmatrix}, & a_1^{B_0^{22}} &= \left(a_{-1}^{B_0^{22}} \right)^T, \\ a_0^{B_0^{12}} &= -\frac{4}{3} I_2, & a_{-1}^{B_0^{12}} &= a_1^{B_0^{12}} = O_2, \\ a_0^{B_{-1}^{21}} &= -\frac{4}{3} I_2, & a_{-1}^{B_{-1}^{21}} &= a_1^{B_{-1}^{21}} = O_2, \\ a_0^{B_{-1}^{22}} &= \begin{bmatrix} 0 & 0 \\ 0 & \frac{1}{3} \end{bmatrix}, & a_{-1}^{B_{-1}^{22}} &= a_1^{B_{-1}^{22}} = O_2. \end{aligned}$$

Thus, once again, just by taking into account that we are now facing a matrix-valued symbol, we can easily read the underlying symbol as follows:

$$\mathbf{f}_{\mathbb{P}_2}(\theta_1, \theta_2) = f_{A_0}(\theta_1) + f_{A_{-1}}(\theta_1) e^{-i\theta_2} + f_{A_1}(\theta_1) e^{i\theta_2}, \quad (3.19)$$

with

$$\begin{aligned}
 f_{A_0}(\theta_1) &= \begin{bmatrix} f_{B_0^{11}}(\theta_1) & f_{B_0^{12}}(\theta_1) \\ f_{(B_0^{12})^T}(\theta_1) & f_{B_0^{22}}(\theta_1) \end{bmatrix}, & f_{B_l^{ij}}(\theta_1) &= a_0^{B_l^{ij}} + a_{-1}^{B_l^{ij}} e^{-i\theta_1} + a_1^{B_l^{ij}} e^{i\theta_1}, \\
 & & f_{(B_l^{ij})^T}(\theta_1) &= \overline{f_{B_l^{ij}}(\theta_1)}, \\
 f_{A_{-1}}(\theta_1) &= \begin{bmatrix} 0 & 0 \\ f_{B_{-1}^{21}}(\theta_1) & f_{B_{-1}^{22}}(\theta_1) \end{bmatrix}, & f_{A_1}(\theta_1) &= \begin{bmatrix} 0 & f_{(B_{-1}^{21})^T}(\theta_1) \\ 0 & f_{(B_{-1}^{22})^T}(\theta_1) \end{bmatrix}.
 \end{aligned}$$

To sum up, we have a matrix-valued symbol $\mathbf{f}_{\mathbb{P}_2} : [-\pi, \pi]^2 \rightarrow \mathbb{C}^{4 \times 4}$ with

$$\mathbf{f}_{\mathbb{P}_2}(\theta_1, \theta_2) = \left[\begin{array}{cc|cc} \alpha & -\beta(1 + e^{i\theta_1}) & -\beta(1 + e^{i\theta_2}) & 0 \\ -\beta(1 + e^{-i\theta_1}) & \alpha & 0 & -\beta(1 + e^{i\theta_2}) \\ \hline -\beta(1 + e^{-i\theta_2}) & 0 & \alpha & -\beta(1 + e^{i\theta_1}) \\ 0 & -\beta(1 + e^{-i\theta_2}) & -\beta(1 + e^{-i\theta_1}) & \gamma + \frac{\beta}{2}(\cos(\theta_1) + \cos(\theta_2)) \end{array} \right] \quad (3.20)$$

with $\alpha = \frac{16}{3}$, $\beta = \frac{4}{3}$, and $\gamma = 4$.

Finally, it is worth stressing that the stiffness matrix $A_n(1, \Omega, \mathbb{P}_2)$ is a principal submatrix of a suitable permutation of the Toeplitz matrix $T_n(\mathbf{f}_{\mathbb{P}_2})$ defined according to (2.9). Indeed, the size of the twolevel matrix $A_n = A_n(1, \Omega, \mathbb{P}_2)$ is intrinsically odd both in inner and outer dimensions, (see Theorem 3.2.1 and the explanation after equation (3.7)), while $T_n(\mathbf{f}_{\mathbb{P}_2})$ has even corresponding dimensions: it is enough to cut every last row/column in each inner block, together with the last block with respect rows and columns, in order to obtain A_n from $T_n(\mathbf{f}_{\mathbb{P}_2})$. In other words A_n is a special principal submatrix of $T_n(\mathbf{f}_{\mathbb{P}_2})$ according to the rule given in Theorem 3.2.1. As for the permutation we have just to consider the one defined by ordering nodal values as reported in Figure 3.3, where internal nodal values are grouped four by four. As a consequence the two matrix-sequences $\{T_n(\mathbf{f}_{\mathbb{P}_2})\}_n$ and $\{A_n(1, \Omega, \mathbb{P}_2)\}_n$ share the same spectral distribution, that is, the same spectral symbol $\mathbf{f}_{\mathbb{P}_2}$, by invoking Theorem 2.1.3. The following proposition holds.

Proposition 3.3.1. *The two matrix-sequences $\{T_n(\mathbf{f}_{\mathbb{P}_2})\}_n$ and $\{A_n(1, \Omega, \mathbb{P}_2)\}_n$ are spectrally distributed as $\mathbf{f}_{\mathbb{P}_2}$ in the sense of Definition 2.1.2.*

As an immediate consequence of Proposition 3.3.1 we deduce a corollary regarding the clustering and localization of the spectra of $\{T_n(\mathbf{f}_{\mathbb{P}_2})\}_n$ and $\{A_n(1, \Omega, \mathbb{P}_2)\}_n$.

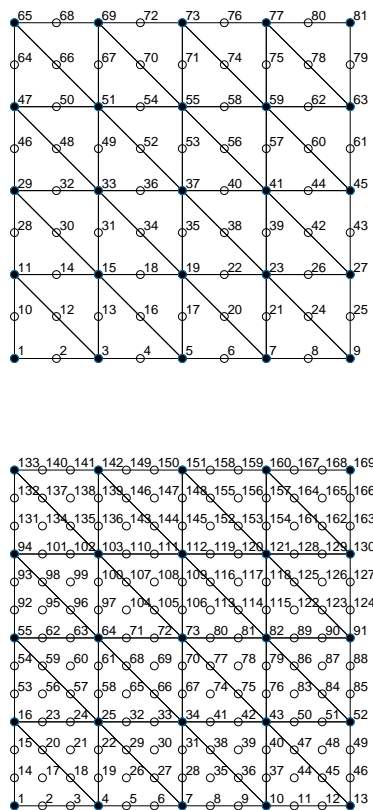


Figure 3.3: Nodal points reordering in \mathbb{P}_2 and \mathbb{P}_3 cases.

Corollary 3.3.2. *The range of $\mathbf{f}_{\mathbb{P}_2}$ is a weak cluster set for the spectra of the two matrix-sequences $\{T_n(\mathbf{f}_{\mathbb{P}_2})\}_n$ and $\{A_n(1, \Omega, \mathbb{P}_2)\}_n$ in the sense of Definition 2.1.4. Furthermore, the convex hull of the range of $\mathbf{f}_{\mathbb{P}_2}$ contains all the eigenvalues of the involved matrices.*

Proof. The proof of the first part is a direct consequence of Proposition 3.3.1, taking into account [45, Theorem 4.2] and observing that in this setting the standard range and the essential range coincide since $\mathbf{f}_{\mathbb{P}_2}$ is continuous, (see the subsection 2.1). For the second part we observe that the result is known for Toeplitz matrices with Hermitian valued symbols [65]: then the localization result for the eigenvalues of $A_n(1, \Omega, \mathbb{P}_2)$ follows, because $A_n(1, \Omega, \mathbb{P}_2)$ is a principal submatrix of $T_n(\mathbf{f}_{\mathbb{P}_2})$ and since all the involved matrices are Hermitian. \square

3.3.3 Case $k = 3$

In the case of cubic Lagrangian FE ($k = 3$), by referring to the reference element, (see Figure 3.2), we have the following shape functions

$$\begin{aligned}
 \hat{\varphi}_1(\hat{x}, \hat{y}) &= -\frac{9}{2}\hat{x}^3 - \frac{27}{2}\hat{x}^2\hat{y} + 9\hat{x}^2 - \frac{27}{2}\hat{x}\hat{y}^2 + 18\hat{x}\hat{y} - \frac{11}{2}\hat{x} - \frac{9}{2}\hat{y}^3 + 9\hat{y}^2 - \frac{11}{2}\hat{y} + 1, \\
 \hat{\varphi}_2(\hat{x}, \hat{y}) &= \frac{\hat{x}}{2}(9\hat{x}^2 - 9\hat{x} + 2), \\
 \hat{\varphi}_3(\hat{x}, \hat{y}) &= \frac{\hat{y}}{2}(9\hat{y}^2 - 9\hat{y} + 2), \\
 \hat{\varphi}_4(\hat{x}, \hat{y}) &= \frac{9}{2}\hat{x}\hat{y}(3\hat{x} - 1), \\
 \hat{\varphi}_5(\hat{x}, \hat{y}) &= \frac{9}{2}\hat{x}\hat{y}(3\hat{y} - 1), \\
 \hat{\varphi}_6(\hat{x}, \hat{y}) &= -\frac{9}{2}\hat{y}(3\hat{y} - 1)(\hat{x} + \hat{y} - 1), \\
 \hat{\varphi}_7(\hat{x}, \hat{y}) &= \frac{9}{2}\hat{y}(3\hat{x}^2 + 6\hat{x}\hat{y} - 5\hat{x} + 3\hat{y}^2 - 5\hat{y} + 2), \\
 \hat{\varphi}_8(\hat{x}, \hat{y}) &= \frac{9}{2}\hat{x}(3\hat{x}^2 + 6\hat{x}\hat{y} - 5\hat{x} + 3\hat{y}^2 - 5\hat{y} + 2), \\
 \hat{\varphi}_9(\hat{x}, \hat{y}) &= -\frac{9}{2}\hat{x}(3\hat{x} - 1)(\hat{x} + \hat{y} - 1), \\
 \hat{\varphi}_{10}(\hat{x}, \hat{y}) &= -27\hat{x}\hat{y}(\hat{x} + \hat{y} - 1),
 \end{aligned}$$

so that, according to (3.11), the elemental matrix for a generic triangle equals

$$A_{K_1}^{El} = \begin{bmatrix}
 \frac{17}{20} & -\frac{7}{80} & -\frac{7}{80} & -\frac{3}{40} & -\frac{3}{40} & \frac{3}{8} & -\frac{51}{80} & -\frac{51}{80} & \frac{3}{8} & 0 \\
 -\frac{7}{80} & \frac{17}{40} & 0 & \frac{3}{80} & \frac{3}{80} & -\frac{3}{80} & -\frac{3}{80} & \frac{27}{80} & -\frac{27}{40} & 0 \\
 -\frac{7}{80} & 0 & \frac{17}{40} & \frac{3}{80} & \frac{3}{80} & -\frac{27}{40} & \frac{27}{80} & -\frac{3}{80} & -\frac{3}{80} & 0 \\
 -\frac{3}{40} & \frac{3}{80} & \frac{3}{80} & \frac{27}{8} & -\frac{27}{40} & \frac{27}{80} & \frac{27}{80} & \frac{27}{80} & -\frac{27}{16} & -\frac{81}{40} \\
 -\frac{3}{40} & \frac{3}{80} & \frac{3}{80} & -\frac{27}{40} & \frac{27}{8} & -\frac{27}{16} & \frac{27}{80} & \frac{27}{80} & \frac{27}{80} & -\frac{81}{40} \\
 \frac{3}{8} & -\frac{3}{80} & -\frac{27}{40} & \frac{27}{80} & -\frac{27}{16} & \frac{27}{8} & -\frac{27}{16} & 0 & 0 & 0 \\
 -\frac{51}{80} & -\frac{3}{80} & \frac{27}{80} & \frac{27}{80} & \frac{27}{80} & -\frac{27}{16} & \frac{27}{8} & 0 & 0 & -\frac{81}{40} \\
 -\frac{51}{80} & \frac{27}{80} & -\frac{3}{80} & \frac{27}{80} & \frac{27}{80} & 0 & 0 & \frac{27}{8} & -\frac{27}{16} & -\frac{81}{40} \\
 \frac{3}{8} & -\frac{27}{40} & -\frac{3}{80} & -\frac{27}{16} & \frac{27}{8} & 0 & 0 & -\frac{27}{16} & \frac{27}{8} & 0 \\
 0 & 0 & 0 & -\frac{81}{40} & -\frac{81}{40} & 0 & -\frac{81}{40} & -\frac{81}{40} & 0 & \frac{81}{10}
 \end{bmatrix} \quad (3.21)$$

in the case of triangles of type 1, or a suitable permutation in the case of triangles of type 2. The stiffness matrix $A_n = A_n(1, \Omega, \mathbb{P}_3)$ shows again a block tridiagonal

structure $A_n = \text{tridiag}(A_1, A_0, A_{-1})$ as in previous cases, the higher approximation stressing its influence just inside the blocks A_i . In fact, we observe in each block A_i a 3×3 block structure as follows:

$$A_0 = \begin{bmatrix} B_0^{11} & B_0^{12} & B_0^{13} \\ (B_0^{12})^T & B_0^{22} & B_0^{23} \\ (B_0^{13})^T & B_0^{23} & B_0^{33} \end{bmatrix}, \quad A_{-1} = \begin{bmatrix} 0 & 0 & 0 \\ 0 & 0 & 0 \\ B_{-1}^{31} & B_{-1}^{32} & B_{-1}^{33} \end{bmatrix}, \quad A_1 = A_{-1}^T. \quad (3.22)$$

More important, the very same structure appears in every block B_l^{ij} by considering suitable 3×3 matrices and indeed we have

$$B_l^{ij} = \text{tridiag} \left(a_1^{B_l^{ij}}, a_0^{B_l^{ij}}, a_{-1}^{B_l^{ij}} \right), \quad l \in \{-1, 0, 1\}, \quad i, j \in \{1, 2, 3\},$$

where

$$\begin{aligned} a_0^{B_0^{11}} &= \begin{bmatrix} \frac{81}{10} & -\frac{81}{40} & 0 \\ -\frac{81}{40} & \frac{27}{4} & -\frac{27}{16} \\ 0 & -\frac{27}{16} & \frac{27}{4} \end{bmatrix}, & a_{-1}^{B_0^{11}} &= \begin{bmatrix} 0 & 0 & 0 \\ 0 & 0 & 0 \\ -\frac{81}{40} & \frac{27}{80} & 0 \end{bmatrix}, & a_1^{B_0^{11}} &= \left(a_{-1}^{B_0^{11}} \right)^T, \\ a_0^{B_0^{22}} &= \begin{bmatrix} \frac{27}{4} & -\frac{81}{40} & \frac{27}{80} \\ -\frac{81}{40} & \frac{81}{10} & -\frac{81}{40} \\ \frac{27}{80} & -\frac{81}{40} & \frac{27}{4} \end{bmatrix}, & a_{-1}^{B_0^{22}} &= \begin{bmatrix} 0 & 0 & 0 \\ 0 & 0 & 0 \\ -\frac{27}{16} & 0 & 0 \end{bmatrix}, & a_1^{B_0^{22}} &= \left(a_{-1}^{B_0^{22}} \right)^T, \\ a_0^{B_0^{33}} &= \begin{bmatrix} \frac{27}{4} & -\frac{27}{8} & \frac{57}{80} \\ -\frac{27}{8} & \frac{27}{4} & -\frac{21}{16} \\ \frac{57}{80} & -\frac{21}{16} & \frac{17}{5} \end{bmatrix}, & a_{-1}^{B_0^{33}} &= \begin{bmatrix} 0 & 0 & 0 \\ 0 & 0 & 0 \\ -\frac{21}{16} & \frac{57}{80} & -\frac{7}{40} \end{bmatrix}, & a_1^{B_0^{33}} &= \left(a_{-1}^{B_0^{33}} \right)^T, \\ a_0^{B_0^{12}} &= \begin{bmatrix} -\frac{81}{40} & 0 & 0 \\ -\frac{27}{20} & -\frac{81}{40} & \frac{27}{80} \\ \frac{27}{80} & 0 & -\frac{27}{8} \end{bmatrix}, & a_{-1}^{B_0^{12}} &= \begin{bmatrix} 0 & 0 & 0 \\ 0 & 0 & 0 \\ \frac{27}{80} & 0 & 0 \end{bmatrix}, & a_1^{B_0^{12}} &= \begin{bmatrix} 0 & 0 & 0 \\ 0 & 0 & \frac{27}{80} \\ 0 & 0 & 0 \end{bmatrix}, \\ a_0^{B_0^{13}} &= \begin{bmatrix} 0 & 0 & 0 \\ \frac{27}{80} & \frac{27}{80} & -\frac{3}{40} \\ 0 & 0 & \frac{57}{80} \end{bmatrix}, & a_{-1}^{B_0^{13}} &= O_3, & a_1^{B_0^{13}} &= \begin{bmatrix} 0 & 0 & 0 \\ 0 & 0 & \frac{3}{40} \\ 0 & 0 & -\frac{3}{80} \end{bmatrix}, \end{aligned}$$

3.3. Two dimensional case: \mathbb{P}_k , $d = 2$ - symbol definition

$$\begin{aligned}
a_0^{B_0^{23}} &= \begin{bmatrix} -\frac{27}{16} & \frac{27}{80} & -\frac{3}{40} \\ 0 & -\frac{81}{40} & 0 \\ 0 & 0 & -\frac{21}{16} \end{bmatrix}, & a_{-1}^{B_0^{23}} &= O_3, & a_1^{B_0^{23}} &= \begin{bmatrix} 0 & 0 & \frac{3}{40} \\ 0 & 0 & 0 \\ 0 & 0 & -\frac{3}{80} \end{bmatrix}, \\
a_0^{B_0^{31}} &= \begin{bmatrix} -\frac{81}{40} & \frac{27}{80} & 0 \\ 0 & -\frac{27}{16} & 0 \\ 0 & \frac{3}{40} & -\frac{21}{16} \end{bmatrix}, & a_{-1}^{B_0^{31}} &= \begin{bmatrix} 0 & 0 & 0 \\ 0 & 0 & 0 \\ 0 & -\frac{3}{40} & 0 \end{bmatrix}, & a_1^{B_0^{31}} &= \begin{bmatrix} 0 & 0 & 0 \\ 0 & 0 & 0 \\ 0 & 0 & -\frac{3}{80} \end{bmatrix}, \\
a_0^{B_0^{32}} &= \begin{bmatrix} \frac{27}{80} & 0 & 0 \\ \frac{27}{80} & 0 & 0 \\ \frac{3}{40} & 0 & \frac{57}{80} \end{bmatrix}, & a_{-1}^{B_0^{32}} &= \begin{bmatrix} 0 & 0 & 0 \\ 0 & 0 & 0 \\ -\frac{3}{40} & 0 & 0 \end{bmatrix}, & a_1^{B_0^{32}} &= \begin{bmatrix} 0 & 0 & 0 \\ 0 & 0 & 0 \\ 0 & 0 & -\frac{3}{80} \end{bmatrix}, \\
a_0^{B_0^{33}} &= \begin{bmatrix} 0 & 0 & 0 \\ 0 & 0 & 0 \\ -\frac{3}{80} & -\frac{3}{80} & -\frac{7}{40} \end{bmatrix}, & a_{-1}^{B_0^{33}} &= O_3, & a_1^{B_0^{33}} &= \begin{bmatrix} 0 & 0 & -\frac{3}{80} \\ 0 & 0 & -\frac{3}{80} \\ 0 & 0 & 0 \end{bmatrix}.
\end{aligned}$$

Thus, once again, just by taking into account that we are now facing a matrix-valued symbol, we can easily read the underlying symbol as follows:

$$\mathbf{f}_{\mathbb{P}_3}(\theta_1, \theta_2) = f_{A_0}(\theta_1) + f_{A_{-1}}(\theta_1)e^{-i\theta_2} + f_{A_1}(\theta_1)e^{i\theta_2}, \quad (3.23)$$

with

$$\begin{aligned}
f_{A_0}(\theta_1) &= \begin{bmatrix} f_{B_0^{11}}(\theta_1) & f_{B_0^{12}}(\theta_1) & f_{B_0^{13}}(\theta_1) \\ f_{(B_0^{12})^T}(\theta_1) & f_{B_0^{22}}(\theta_1) & f_{B_0^{23}}(\theta_1) \\ f_{(B_0^{13})^T}(\theta_1) & f_{(B_0^{23})^T}(\theta_1) & f_{B_0^{33}}(\theta_1) \end{bmatrix}, & f_{B_l^{ij}}(\theta_1) &= a_0^{B_l^{ij}} + a_{-1}^{B_l^{ij}}e^{-i\theta_1} + a_1^{B_l^{ij}}e^{i\theta_1}, \\
& & f_{(B_l^{ij})^T}(\theta_1) &= \overline{f_{B_l^{ij}}(\theta_1)}, \\
f_{A_{-1}}(\theta_1) &= \begin{bmatrix} 0 & 0 & 0 \\ 0 & 0 & 0 \\ f_{B_{-1}^{31}}(\theta_1) & f_{B_{-1}^{32}}(\theta_1) & f_{B_{-1}^{33}}(\theta_1) \end{bmatrix}, & f_{A_1}(\theta_1) &= \begin{bmatrix} 0 & 0 & f_{(B_{-1}^{31})^T}(\theta_1) \\ 0 & 0 & f_{(B_{-1}^{32})^T}(\theta_1) \\ 0 & 0 & f_{(B_{-1}^{33})^T}(\theta_1) \end{bmatrix}.
\end{aligned}$$

To sum up, we find the expression of $\mathbf{f}_{\mathbb{P}_3} : [-\pi, \pi]^2 \longrightarrow \mathbb{C}^{9 \times 9}$ with

$$\mathbf{f}_{\mathbb{P}_3}(\theta_1, \theta_2) = \begin{bmatrix} \alpha & -\frac{\alpha}{4} & -\frac{\alpha}{4}e^{i\theta_1} & -\frac{\alpha}{4} & 0 & 0 & -\frac{\alpha}{4}e^{i\theta_2} & 0 & 0 \\ -\frac{\alpha}{4} & \beta & -\frac{\beta}{4} + \frac{\beta}{20}e^{i\theta_1} & -\frac{\alpha}{4} & -\frac{\beta}{5} & -\frac{\alpha}{4} & \frac{\beta}{20}(1 + e^{i\theta_2}) & \frac{\beta}{20}(1 + e^{i\theta_2}) & \frac{\beta}{20} - \frac{\beta}{4}e^{i\theta_2} & f_{29} \\ -\frac{\alpha}{4}e^{-i\theta_1} & -\frac{\beta}{4} + \frac{\beta}{20}e^{-i\theta_1} & \beta & \frac{\beta}{20}(1 + e^{-i\theta_1}) & 0 & -\frac{\beta}{2} & 0 & 0 & 0 & f_{39} \\ -\frac{\alpha}{4} & 0 & -\frac{\beta}{4} & \frac{\beta}{20}(1 + e^{i\theta_1}) & \beta & -\frac{\alpha}{4} & \frac{\beta}{20} - \frac{\beta}{4}e^{i\theta_1} & -\frac{\beta}{4} + \frac{\beta}{20}e^{i\theta_2} & \frac{\beta}{20}(1 + e^{i\theta_2}) & f_{49} \\ 0 & -\frac{\beta}{4} & 0 & 0 & -\frac{\alpha}{4} & \alpha & -\frac{\alpha}{4} & 0 & -\frac{\alpha}{4} & 0 \\ 0 & \frac{\beta}{20}(1 + e^{-i\theta_1}) & -\frac{\beta}{2} & \frac{\beta}{20} - \frac{\beta}{4}e^{-i\theta_1} & -\frac{\alpha}{4} & \beta & 0 & 0 & 0 & f_{69} \\ -\frac{\alpha}{4}e^{-i\theta_2} & \frac{\beta}{20}(1 + e^{-i\theta_2}) & 0 & -\frac{\beta}{4} + \frac{\beta}{20}e^{-i\theta_2} & 0 & 0 & \beta & -\frac{\beta}{2} & \beta & f_{79} \\ 0 & \frac{\beta}{20} - \frac{\beta}{4}e^{-i\theta_2} & 0 & \frac{\beta}{20}(1 + e^{-i\theta_2}) & -\frac{\alpha}{4} & 0 & -\frac{\beta}{2} & \beta & \beta & f_{89} \\ 0 & \frac{f_{29}}{f_{39}} & \frac{f_{39}}{f_{39}} & \frac{f_{49}}{f_{49}} & 0 & \frac{f_{69}}{f_{69}} & \frac{f_{79}}{f_{79}} & \frac{f_{89}}{f_{89}} & \frac{f_{99}}{f_{99}} & f_{99} \end{bmatrix} \quad (3.24)$$

where

$$\begin{aligned}
 f_{29} &= -\gamma(1 - e^{i\theta_1})(1 - e^{i\theta_2}), & f_{39} &= \delta - \frac{\gamma}{2}e^{i\theta_1} - \varepsilon e^{i\theta_2} - \frac{\gamma}{2}e^{-i\theta_1}e^{i\theta_2}, \\
 f_{49} &= -\gamma(1 - e^{i\theta_1})(1 - e^{i\theta_2}), & f_{69} &= -\varepsilon - \frac{\gamma}{2}e^{i\theta_1} + \delta e^{i\theta_2} - \frac{\gamma}{2}e^{-i\theta_1}e^{i\theta_2}, \\
 f_{79} &= \delta - \varepsilon e^{i\theta_1} - \frac{\gamma}{2}e^{i\theta_1}e^{-i\theta_2} - \frac{\gamma}{2}e^{i\theta_2}, & f_{89} &= -\varepsilon + \delta e^{i\theta_1} - \frac{\gamma}{2}e^{i\theta_1}e^{-i\theta_2} - \frac{\gamma}{2}e^{i\theta_2}, \\
 f_{99} &= \zeta - 2\eta(\cos(\theta_1) + \cos(\theta_2)),
 \end{aligned}$$

and $\alpha = 81/10$, $\beta = 27/4$, $\gamma = 3/40$, $\delta = 57/80$, $\varepsilon = 21/16$, $\zeta = 17/5$, $\eta = 7/40$.

Finally, the stiffness matrix $A_n = A_n(1, \Omega, \mathbb{P}_3)$ is a principal submatrix of a suitable permutation of the Toeplitz matrix $T_n(\mathbf{f}_{\mathbb{P}_3})$. In order to obtain the stiffness matrix A_n from $T_n(\mathbf{f}_{\mathbb{P}_3})$ it is enough to group internal nodal values nine by nine. Again by referring to Theorem 2.1.3, the following proposition holds.

Proposition 3.3.3. *The two matrix-sequences $\{T_n(\mathbf{f}_{\mathbb{P}_3})\}_n$ and $\{A_n(1, \Omega, \mathbb{P}_3)\}_n$ are spectrally distributed as $\mathbf{f}_{\mathbb{P}_3}$ in the sense of Definition 2.1.2.*

As an immediate consequence of Proposition 3.3.3 we deduce a corollary regarding the clustering and localization of the spectra of $\{T_n(\mathbf{f}_{\mathbb{P}_3})\}_n$ and $\{A_n(1, \Omega, \mathbb{P}_3)\}_n$ as well.

Corollary 3.3.4. *The range of $\mathbf{f}_{\mathbb{P}_3}$ is a weak cluster set for the spectra of the two matrix-sequences $\{T_n(\mathbf{f}_{\mathbb{P}_3})\}_n$ and $\{A_n(1, \Omega, \mathbb{P}_3)\}_n$ in the sense of Definition 2.1.4. Furthermore, the convex hull of the range of $\mathbf{f}_{\mathbb{P}_3}$ contains all the eigenvalues of the involved matrices.*

Proof. The proof of the first part is a direct consequence of Proposition 3.3.3, taking into account [45, Theorem 4.2] and observing that in this setting the standard range and the essential range coincide since $\mathbf{f}_{\mathbb{P}_3}$ is continuous, (see also the Subsection 2.1). For the second part we observe that the result is known for Toeplitz matrices with Hermitian valued symbols [65]: then the localization result for the eigenvalues of $A_n(1, \Omega, \mathbb{P}_3)$ follows, because $A_n(1, \Omega, \mathbb{P}_3)$ is a principal submatrix of $T_n(\mathbf{f}_{\mathbb{P}_3})$ and since all the involved matrices are Hermitian. The thesis follows with the same reasoning considered in Corollary 3.3.2. \square

3.4 Symbol spectral analysis

We start the spectral analysis of symbols obtained in the previous section from a numerical point of view. As well known, $\mathbf{f}_{\mathbb{P}_1}$ shows a zero of order 2 in $(0, 0)$, while it is positive elsewhere. In the case $k \geq 2$ the symbol is a matrix-valued function, so we consider an equispaced sampling in $[-\pi, \pi]^2$ of the symbol and for each point we evaluate the k^2 eigenvalues, ordering them in non-decreasing way. Thus, k^2 surfaces are defined by s_i , $i = 1, \dots, k^2$ and the i^{th} eigenvalue in a given point of the sampling is given by the evaluation of the surface s_i in such a point. In Table 3.1 the minimal and maximal values of each surface s_i , $i = 1, \dots, k^2$, are reported (for a comparison among the surfaces obtained by using the eigenvalues of the considered matrix-sequence and the corresponding surfaces obtained by properly sampling the symbol of the same matrix-sequence, see the subsequent Figures 3.4-3.7). In the case $k = 2$, it is worth stressing that the chosen sorting of the eigenvalues influences the surfaces definition, the minimal value of the i -th surface being lower of the maximal value of the $(i - 1)$ -th surface: this implies that the union of the ranges of the eigenvalue functions of the symbol produces a connected set which is a cluster for the spectra of the given matrix-sequence. When $k = 3$ the union of the ranges of the first four surfaces is well separated from the union of the remaining five surfaces and hence the cluster is divided into two sub-clusters in the sense of Definition 2.1.4. In the case $k = 4$, the union of the ranges of the first nine surfaces is well separated from the union of the remaining seven surfaces and consequently, as in the case of $k = 3$, the cluster is divided into two sub-clusters.

However, there is a phenomenon which is expected and it is independent of the value of k : only the first surface reaches zero as minimum, while all the other surfaces are strictly positive everywhere.

Now we give a general result regarding the main features of the involved symbols, with the proof in various cases, including both \mathbb{P}_k and \mathbb{Q}_k Finite Element approximations.

Theorem 3.4.1. *Given the symbols $\mathbf{f}_{\mathbb{P}_k}, \mathbf{f}_{\mathbb{Q}_k}$ in dimension $d \geq 1$, the following statements hold true. For every $\mathbf{f} \in \{\mathbf{f}_{\mathbb{P}_k}, \mathbf{f}_{\mathbb{Q}_k}\}$, setting*

$$\lambda_1(\mathbf{f}(\boldsymbol{\theta})) \leq \dots \leq \lambda_{k^d}(\mathbf{f}(\boldsymbol{\theta})),$$

i	$\min(s_i)$	$\operatorname{argmin}(s_i)$	$\max(s_i)$	$\operatorname{argmax}(s_i)$
$k = 1$				
1	0	(0, 0)	8	$(-\pi, -\pi)$
$k = 2$				
1	-2.122988181725368e-17	(0, 0)	2.666666666666667e+00	$(-\pi, -\pi)$
2	2.666666666666667e+00	(0, $-\pi$)	5.333333333333330e+00	(0, 0)
3	5.33333333333325e+00	$(-u, -u)$	7.415403750411773e+00	(0, $-\pi$)
4	5.33333333333333e+00	$(-\pi, -\pi)$	1.066666666666667e+01	(0, 0)
$k = 3$				
1	-2.947870832408496e-16	(0, 0)	1.752299219210445e+00	$(-\pi, -\pi)$
2	1.077001420967619e+00	$(-\pi, 0)$	2.649326100400095e+00	(0, 0)
3	2.024999999999999e+00	$(\pi, -\pi)$	3.374999999999998e+00	(0, 0)
4	2.417725227846304e+00	$(-\pi, -\pi)$	5.473900873539699e+00	(0, 0)
5	6.074999999999998e+00	(0, 0)	8.150826984062711e+00	$(-v, v)$
6	6.075000000000001e+00	(0, 0)	9.450000000000005e+00	$(-\pi, -\pi)$
7	8.100000000000000e+00	$(-\pi, 0)$	1.145177302606021e+01	(0, 0)
8	1.012500000000000e+01	$(-\pi, -\pi)$	1.306461248424784e+01	$(-\pi, 0)$
9	1.215000000000001e+01	(0, 0)	1.542003087979332e+01	$(-\pi, -\pi)$
$k = 4$				
1	8.665811124242140e-15	(0, 0)	1.154132889535501e+00	$(\pi, -\pi)$
2	6.091179158637314e-01	$(-\pi, 0)$	2.028216383055356e+00	$(-\pi, -\pi)$
3	1.183562035003593e+00	$(w, -w)$	2.278229389751864e+00	$(-\pi, 0)$
4	1.228189268889777e+00	$(-\pi, -\pi)$	2.796565325232735e+00	$(z, \pi/10)$
5	2.706589845271391e+00	(0, 0)	3.280192294561743e+00	$(-\pi, -\pi)$
6	3.100532625333826e+00	(0, 0)	4.876190476190478e+00	$(\pi, -\pi)$
7	4.086126343234464e+00	(a, b)	5.001164336911962e+00	$(c, -c)$
8	4.923102258884252e+00	$(d, -d)$	6.507154754218933e+00	(0, $-\pi$)
9	6.351060427971650e+00	(e, e)	7.524544180802064e+00	$(f, -f)$
10	1.124369260315089e+01	$(-\pi, 0)$	1.277464393947364e+01	$(\pi, -\pi)$
11	1.221231815611003e+01	$(-g, g)$	1.319265448651837e+01	(0, $-\pi$)
12	1.312292935024724e+01	(h, h)	1.551857649581396e+01	$(i, -i)$
13	1.403908928314477e+01	$(\pi, -\pi)$	1.715087064330462e+01	$(l, -l)$
14	1.715307867863427e+01	$(l, -l)$	2.041132693707404e+01	$(-\pi, -\pi)$
15	1.987073604165514e+01	(0, 0)	2.261907577519149e+01	(0, π)
16	2.236934933910699e+01	$(m, -m)$	2.492211941947813e+01	(0, 0)

Table 3.1: Minimum and maximum of surfaces s_i , $i = 1, \dots, k^2$. $u = -7.351326809400116e-01$, $v = 2.500707752257475e+00$, $w = 3.053628059289279e+00$, $z = 1.734159144781565e+00$, $a = 2.576105975943630e-01$, $b = -2.224247598741574e+00$, $c = 2.896548426609789e+00$, $d = 1.507964473723100e+00$, $e = 1.043008760991811e+00$, $f = 2.161415745669778e+00$, $g = 1.627344994559513e+00$, $h = 2.796017461694915e+00$, $i = 7.099999397112930e-01$, $l = 9.550441666912972e-01$, $m = 2.519557308179014e+00$.

we obtain

1. $f(\mathbf{0})\mathbf{e} = \mathbf{0}$;

2. there exist constants $C_1, C_2 > 0$ (dependent on \mathbf{f}) such that

$$C_1 \sum_{j=1}^d (2 - 2 \cos(\theta_j)) \leq \lambda_1(\mathbf{f}(\boldsymbol{\theta})) \leq C_2 \sum_{j=1}^d (2 - 2 \cos(\theta_j)); \quad (3.25)$$

3. there exist constants $m, M > 0$ (dependent on \mathbf{f}) such that

$$0 < m \leq \lambda_j(\mathbf{f}(\boldsymbol{\theta})) \leq M, \quad j = 2, \dots, k^d. \quad (3.26)$$

For $\mathbf{f}_{\mathbb{Q}_k}$ the proof is given for every $k, d \geq 1$ (for $d = 1$ we notice again that $\mathbf{f}_{\mathbb{P}_k} \equiv \mathbf{f}_{\mathbb{Q}_k}$). For $\mathbf{f}_{\mathbb{P}_k}$ the proof is given for $d = 2$ and $k = 2, 3$.

Remark 3.4.2. While in the case of \mathbb{Q}_k Finite Elements the analysis of the symbol $\mathbf{f}_{\mathbb{Q}_k}$ given in [40] and in Theorem 3.4.1 is general, for the \mathbb{P}_k Finite Elements in dimension $d > 1$ there is still room for a substantial improvement of the analysis and this will be a target in future researches.

Proof. ■ Case \mathbb{Q}_k Finite Elements: any $k \geq 1, d = 1$.

Claims 2. and 3. have been proved in Theorem 8 and Corollary 1 in [40]. Here, we prove Claim 1.: as first thing we recall that the relation $\mathbf{f}(\mathbf{0})\mathbf{e} = \mathbf{0}$, with \mathbf{e} vector of all ones and $k \geq 1$, is equivalent to say that every row of $\mathbf{f}(\mathbf{0})$ is a vector having rowsum equal to zero. We now show the latter feature. Taking into consideration the notations in Section 3.2, we have

$$(\mathbf{f}(\mathbf{0})\mathbf{e})_s = \sum_{j=1}^k (\mathbf{f}(\mathbf{0}))_{s,j} = \sum_{j=1}^k (K_0 + K_1 + K_1^T)_{s,j}, \quad s = 1, \dots, k.$$

We first observe that the Lagrange polynomial interpolating the constant 1 is exactly equal to 1, by the uniqueness of the interpolant. Therefore $\sum_{j=0}^k L_j = 1$, $(\sum_{j=0}^k L_j)' = \sum_{j=0}^k L_j' = 0$, and hence, for $1 \leq s \leq k - 1$,

$$\begin{aligned} \sum_{j=1}^k (\mathbf{f}(\mathbf{0}))_{s,j} &= \sum_{j=1}^k \langle L_j', L_s' \rangle + \langle L_0', L_s' \rangle \\ &= \left\langle \sum_{j=0}^k L_j', L_s' \right\rangle \\ &= \langle 0, L_s' \rangle = 0. \end{aligned}$$

Finally, for $s = k$ we have

$$\begin{aligned}
 \sum_{j=1}^k (\mathbf{f}(\mathbf{0}))_{k,j} &= \sum_{j=1}^k \langle L'_j, L'_k \rangle + \langle L'_0, L'_0 \rangle + \langle L'_0, L'_k \rangle + \sum_{j=1}^k \langle L'_0, L'_j \rangle \\
 &= \sum_{j=0}^k \langle L'_j, L'_k \rangle + \sum_{j=0}^k \langle L'_0, L'_j \rangle \\
 &= \left\langle \sum_{j=0}^k L'_j, L'_k \right\rangle + \left\langle L'_0, \sum_{j=0}^k L'_j \right\rangle = 0,
 \end{aligned}$$

and consequently we conclude that $\mathbf{f}(\mathbf{0})\mathbf{e} = 0$.

■ Case \mathbb{Q}_k Finite Elements: any $k \geq 1$, any $d \geq 2$. Claim 1. is a direct consequence of the proof for \mathbb{Q}_k Finite Elements, $k \geq 1$, and $d = 1$, given its tensorial structure, (see Formula (5.1) in [40]): in reality it is sufficient to observe that $x \otimes y$ has rowsum equal to zero if and only if either x or y has rowsum equal to zero, with any x, y complex vectors of any size. The case of more than two vectors can be handled by an inductive argument. Furthermore, Claims 2. and 3. are contained in Section 5.1 in [40].

■ Case \mathbb{P}_k Finite Elements: $k = 2, d = 2$. Claim 1. follows by direct check of the zero rowsum property from the expression of the symbol $\mathbf{f}_{\mathbb{P}_k}$ in (3.20), taking into account $\boldsymbol{\theta} = (0, 0)$ and the numerical values of the involved parameters.

Now, since the determinant of a matrix is the product of its eigenvalues and since \mathbf{f} is bounded in infinity norm, in order to prove Claim 2. and 3. with $d = 2$ it is sufficient to show that:

$$\mathbf{A.} \quad \det(\mathbf{f}(\boldsymbol{\theta})) \sim \sum_{j=1}^2 (2 - 2 \cos(\theta_j)), \quad \boldsymbol{\theta} = (\theta_1, \theta_2),$$

$$\mathbf{B.} \quad \text{there exists } C > 0 \text{ such that } \lambda_2(\mathbf{f}(\boldsymbol{\theta})) \geq C > 0,$$

with $\mathbf{f} = \mathbf{f}_{\mathbb{P}_2}$.

We remind that the relation A. means there exist $C_1, C_2 > 0$ such that

$$C_1 \sum_{j=1}^2 (2 - 2 \cos(\theta_j)) \leq \det(\mathbf{f}_{\mathbb{P}_2}(\boldsymbol{\theta})) \leq C_2 \sum_{j=1}^2 (2 - 2 \cos(\theta_j))$$

uniformly in the domain $(\theta_1, \theta_2) \in [-\pi, \pi]^2$.

By direct computation, we find

$$\begin{aligned} \det(\mathbf{f}_{\mathbb{P}_2}(\boldsymbol{\theta})) &= C' (-2 \cos(\theta_1) - 2 \cos(\theta_2) - \cos(\theta_1) \cos(\theta_2) + 5) \\ &= C' \left(\sum_{j=1}^2 (2 - 2 \cos(\theta_j)) + (1 - \cos(\theta_1) \cos(\theta_2)) \right) \\ &\geq C' \left(\sum_{j=1}^2 (2 - 2 \cos(\theta_j)) \right) \end{aligned}$$

with $C' = 4096/81$, being $-1 \leq \cos(\theta_1) \cos(\theta_2) \leq 1$ for all $(\theta_1, \theta_2) \in [-\pi, \pi]^2$. Thus, $C_1 = C'$.

Furthermore, for $c = 1/2$ it holds $1 - \cos(\theta_1) \cos(\theta_2) \leq c \left(\sum_{j=1}^2 (2 - 2 \cos(\theta_j)) \right)$ for all $(\theta_1, \theta_2) \in [-\pi, \pi]^2$. Thus, $C_2 = 3C'/2$.

Finally, let $\lambda_1 \leq \lambda_2 \leq \lambda_3 \leq \lambda_4$ be the eigenvalues of the Hermitian matrix $\mathbf{f}_{\mathbb{P}_2}(\boldsymbol{\theta})$ and let $\mu_1 \leq \mu_2 \leq \mu_3$ be the eigenvalues of the principal submatrix $\mathbf{g}(\boldsymbol{\theta})$ chosen as $\mathbf{g}(\boldsymbol{\theta}) = (\mathbf{f}_{\mathbb{P}_2}(\boldsymbol{\theta}))_{i,j=2}^4$.

Since the approximation matrices of problem (3.1) are all Hermitian Positive Definite due to

- coerciveness of the continuous problem,
- the use of Galerkin techniques such as the Finite Elements,

it follows that the symbol

$$\mathbf{f}_{\mathbb{P}_2}(\boldsymbol{\theta})$$

of the related matrix-sequence has to be Hermitian nonnegative Definite, which means that $\lambda_1 \geq 0$ on the whole definition domain. By contradiction if λ_1 is negative in a set of positive measure then, by the distribution results, (see [3, 4, 38, 39]), many eigenvalues of the approximation matrices would be negative for a matrix size large enough and this is impossible.

By using the interlacing theorem, we have

$$\lambda_1 \leq \mu_1 \leq \lambda_2 \leq \mu_2 \leq \lambda_3 \leq \mu_3 \leq \lambda_4, \quad (3.27)$$

with λ_1 equal to zero at $\boldsymbol{\theta} = \mathbf{0}$ and positive elsewhere. By direct computation of the determinant we find that $\det(\mathbf{g}(\boldsymbol{\theta})) > 0$ and hence, taking into account

that $\mathbf{g}(\boldsymbol{\theta})$ is continuous and Hermitian Positive Definite on the compact square $[-\pi, \pi]^2$, we conclude that all the eigenvalues of $\mathbf{g}(\boldsymbol{\theta})$ are strictly positive and continuous on $[-\pi, \pi]^2$ that is $\mu_j > 0$ for $j = 1, 2, 3$. Thus, using (3.27), we conclude $\lambda_2 \geq \mu_1 \geq \min_{\boldsymbol{\theta} \in [-\pi, \pi]^2} \mu_1 > 0$.

■ Case \mathbb{P}_k Finite Elements: $k = 3, d = 2$. As in the case $k = 2$, Claim 1. follows by direct inspection from the expression of the symbol $\mathbf{f}_{\mathbb{P}_k}$ in (3.24), taking into account $\boldsymbol{\theta} = (0, 0)$ and the numerical values of the involved parameters.

In order to prove Claims 2. and 3. we follow the very same steps as for the case $k = 2$, that is, we prove **A.** and **B.** with $\mathbf{f} = \mathbf{f}_{\mathbb{P}_3}$.

By direct computation we have

$$\begin{aligned} \det(\mathbf{f}_{\mathbb{P}_3}(\boldsymbol{\theta})) &= a(-\cos(\theta_2)\cos^2(\theta_1) - \cos(\theta_1)\cos^2(\theta_2) + 4\cos^2(\theta_1) + 4\cos^2(\theta_2) \\ &\quad - 80\cos(\theta_1)\cos(\theta_2) - 195\cos(\theta_1) - 195\cos(\theta_2) + 464) \end{aligned}$$

where $a = 205891132094649/81920000000$. We write $\det(\mathbf{f}_{\mathbb{P}_3}(\boldsymbol{\theta}))$ in the form

$$\det(\mathbf{f}_{\mathbb{P}_3}(\boldsymbol{\theta})) = a \left(h(\boldsymbol{\theta}) + \frac{195}{2} \sum_{j=1}^2 (2 - 2\cos(\theta_j)) \right)$$

where

$$h(\boldsymbol{\theta}) = -\cos(\theta_2)\cos^2(\theta_1) - \cos(\theta_1)\cos^2(\theta_2) + 4\cos^2(\theta_1) + 4\cos^2(\theta_2) - 80\cos(\theta_1)\cos(\theta_2) + 74.$$

Since $-\cos^2(\theta_k) \leq -\cos(\theta_j)\cos^2(\theta_k)$ and $1 - \cos(\theta_1)\cos(\theta_2) \geq 0$ we obtain

$$\begin{aligned} h(\boldsymbol{\theta}) &\geq 3\cos^2(\theta_1) + 3\cos^2(\theta_2) - 80\cos(\theta_1)\cos(\theta_2) + 74 \\ &\geq 3(\cos(\theta_1) - \cos(\theta_2))^2 - 74\cos(\theta_1)\cos(\theta_2) + 74 \\ &\geq 0, \end{aligned}$$

which implies directly $\det(\mathbf{f}_{\mathbb{P}_3}(\boldsymbol{\theta})) \geq C_1 \sum_{j=1}^2 (2 - 2\cos(\theta_j))$ with $C_1 = \frac{195}{2}a$.

On the other side, taking into account $\cos^2(\theta_j) \leq 1, j = 1, 2$, we deduce

$$\begin{aligned} h(\boldsymbol{\theta}) &= \cos^2(\theta_1)(4 - \cos(\theta_2)) + \cos^2(\theta_2)(4 - \cos(\theta_1)) - 80\cos(\theta_1)\cos(\theta_2) + 74 \\ &\leq 8 - \cos(\theta_1) - \cos(\theta_2) - 80\cos(\theta_1)\cos(\theta_2) + 74 \\ &\leq 2 - \cos(\theta_1) - \cos(\theta_2) + 80(1 - \cos(\theta_1)\cos(\theta_2)) \\ &\leq \frac{81}{2} \sum_{j=1}^2 (2 - 2\cos(\theta_j)). \end{aligned}$$

Owing to the relation $1 - \cos(\theta_1) \cos(\theta_2) \leq \frac{1}{2}(4 - 2 \cos(\theta_1) - 2 \cos(\theta_2))$, as already observed in the case $k = 2$, we find $\det(\mathbf{f}_{\mathbb{P}_3}(\boldsymbol{\theta})) \leq 138a \sum_{j=1}^2 (2 - 2 \cos(\theta_j))$ with $C_2 = 138a$.

Finally, let $\lambda_1 \leq \lambda_2 \leq \dots \leq \lambda_9$ be the eigenvalues of the Hermitian matrix $\mathbf{f}_{\mathbb{P}_3}(\boldsymbol{\theta})$, and let $\mathbf{g}(\boldsymbol{\theta}) = (\mathbf{f}_{\mathbb{P}_3}(\boldsymbol{\theta}))_{i,j=1}^8$ be the principal submatrix and $\mu_1 \leq \dots \leq \mu_8$ its eigenvalues.

Since the approximation matrices of problem (3.1) are all Hermitian Positive Definite due to

- coerciveness of the continuous problem,
- the use of Galerkin techniques such as the Finite Elements,

it follows that the symbol $\mathbf{f}_{\mathbb{P}_3}(\boldsymbol{\theta})$ of the related matrix-sequence has to be Hermitian nonnegative Definite, which means that $\lambda_1 \geq 0$ on the whole definition domain. By contradiction if λ_1 is negative in a set of positive measure then, by the distribution results, (see [38, 39]), many eigenvalues of the approximation matrices would be negative for a matrix size large enough and this is impossible.

By using the interlacing theorem, we have

$$\lambda_1 \leq \mu_1 \leq \lambda_2 \leq \mu_2 \leq \dots \leq \mu_8 \leq \lambda_9, \quad (3.28)$$

with λ_1 equal to zero at $\boldsymbol{\theta} = \mathbf{0}$ and positive elsewhere. By direct computation we find $\det(\mathbf{g}(\boldsymbol{\theta})) = \prod_{j=1}^8 \mu_j > 0$ so that, taking into account that $\mathbf{g}(\boldsymbol{\theta})$ is continuous and Hermitian Positive Definite on the compact square $[-\pi, \pi]^2$, we deduce $\mu_j > 0$ for all $j = 1, \dots, 8$. Consequently, by (3.28), we conclude $\lambda_2 \geq \mu_1 \geq \min_{\boldsymbol{\theta} \in [-\pi, \pi]^2} \mu_1 > 0$. \square

3.4.1 Extremal eigenvalues and conditioning

As already observed, direct consequences of Proposition 3.3.1, Corollary 3.3.2, Proposition 3.3.3, Corollary 3.3.4 are that the sequences of Finite Element matrices are distributed as the symbol \mathbf{f} and that the union of the ranges of the eigenvalue functions of \mathbf{f} represent a cluster for their spectra, while the convex hull of the the union of the ranges of the eigenvalue functions of \mathbf{f} contains all the eigenvalues of the involved matrices.

On the other hand, Theorem 3.4.1 gives information on the analytical properties of \mathbf{f} , which are relevant for giving results on the extreme eigenvalues and the asymptotic conditioning.

Indeed, from Theorem 3.4.1, we know that the minimal eigenvalue function of \mathbf{f} behaves as the symbol of the standard Finite Difference Laplacian, while the other eigenvalue functions are well separated from zero and bounded. Furthermore, thanks to the analysis in [65], the fact that the minimal eigenvalue of \mathbf{f} has a zero of order two implies that

- the minimal eigenvalue goes to zero as $N^{-2/d}$,
- the maximal eigenvalue converges from below to the maximum of the maximal eigenvalue function of \mathbf{f} ,
- and hence the conditioning of the involved matrices grows asymptotically exactly as $N^{2/d}$,

with N being the global matrix size, (see also the argument in Section 5.1 in [40], [66] and the last part of Subsection 2.3.3 of the present thesis).

3.5 The case of variable coefficients and non-Cartesian domains

When the diffusion coefficient $a(\mathbf{x})$ in (3.1) is not constant, the structure of the stiffness matrix is no longer Toeplitz, but somehow the Toeplitz character is hidden in an asymptotic sense and indeed the sequence of matrices $\{A_n(a, \Omega, \mathbb{P}_k)\}_n$ approximating (3.1) can be spectrally treated with the help of the GLT technology with $k = 1, 2, 3$.

Below we report the essentials of the steps for computing the spectral symbol.

Step 1. If $\Omega = (0, 1)^d$, $d \geq 1$, then $\{A_n(a, \Omega, \mathbb{P}_k)\}_n$ can be written as a sequence of principal submatrices of a linear combination of products involving the multilevel block Toeplitz sequence generated by $\mathbf{f}_{\mathbb{P}_k}$, the diagonal sampling sequence of $a(\mathbf{x})I_{N(k,d)}$, and zero distributed sequences. The use of items **GLT 1.–GLT 3.**, combined with Theorem 2.1.3, leads to the conclusion

$$\{A_n(a, \Omega, \mathbb{P}_k)\}_n \sim_{\sigma, \lambda} a(\mathbf{x})f_{\mathbb{P}_k}(\boldsymbol{\theta}), \quad \mathbf{x} \in (0, 1)^d, \quad \boldsymbol{\theta} \in [-\pi, \pi]^d. \quad (3.29)$$

Step 2. If Ω is Peano-Jordan measurable, then without loss of generality, we assume $\Omega \subset \Omega_d = (0, 1)^d$ and $d \geq 2$. Hence $\{A_n(a, \Omega, \mathbb{P}_k)\}_n$ can be seen, up to zero-distributed sequences, as a sequence of principal submatrices of $\{A_n(\hat{a}, \Omega, \mathbb{P}_k)\}_n$, where \hat{a} is equal to a on the domain Ω and it is identically zero in the complement $\Omega_d \setminus \Omega$. In this way we are reduced to **Step 1.** and the use of a reduction argument, (see Section 6 in [69] and Section 3.1.4 in [71]) implies the distribution result

$$\{A_n(a, \Omega, \mathbb{P}_k)\}_n \sim_{\sigma, \lambda} a(\mathbf{x})\mathbf{f}_{\mathbb{P}_k}(\boldsymbol{\theta}), \quad \mathbf{x} \in \Omega, \boldsymbol{\theta} \in [-\pi, \pi]^d. \quad (3.30)$$

The rest of the section is now devoted to show that the predictions in (3.29) and (3.30) are numerically confirmed. Indeed, in the constant coefficient case, we plotted the surface of the different eigenvalue functions $\lambda_j(\mathbf{f}_{\mathbb{P}_k}(\boldsymbol{\theta}))$, $j = 1, \dots, k^2$, $k = 1, 2, 3, 4$, and this was technically possible because the functions are all bivariate as $\boldsymbol{\theta} \in [-\pi, \pi]^2$.

In the variable coefficient case, the visualization is substantially more involved, since the symbol is $a(\mathbf{x})\mathbf{f}_{\mathbb{P}_k}(\boldsymbol{\theta})$ and hence the eigenvalue functions $\lambda_j(a(\mathbf{x})\mathbf{f}_{\mathbb{P}_k}(\boldsymbol{\theta}))$, $j = 1, \dots, k^2$, $k = 1, 2, 3, 4$, are all functions in 4 variables as $\mathbf{x} \in \Omega$, $\boldsymbol{\theta} \in [-\pi, \pi]^2$. Consequently, for visualization purposes, we choose a different technique: for a fixed k and for a fixed matrix size, we make an ordering (nondecreasing) of all the eigenvalues of $A_n(a, \Omega, \mathbb{P}_k)$ and we take the same ordering (nondecreasing) of the values given by an equispaced sampling of all the functions $\lambda_j(a(\mathbf{x})\mathbf{f}_{\mathbb{P}_k}(\boldsymbol{\theta}))$, $j = 1, \dots, k^2$.

As it can be seen from Figures 3.4-3.7, all concerning the case $\Omega = (0, 1)^2$, the match is perfect showing that the distribution result in (3.29) is fully confirmed with $a(x, y) = 1$, $a(x, y) = e^{x+y}$, $a(x, y) = 1 + 2\sqrt{x} + y$, $a(x, y) = 1$ if $y \geq x$ and $a(x, y) = 2$ otherwise.

We have four relevant remarks.

- As a general observation, the graph of the ordered equispaced sampling of $\lambda_j(a(\mathbf{x})\mathbf{f}_{\mathbb{P}_k}(\boldsymbol{\theta}))$, $j = 1, \dots, k^2$, represent a monotone rearrangement, (see [23] for seminal results and [2] for a recent revue) of the different eigenvalue functions and this global rearrangement is a fortiori a univariate monotone function.

- When $a(\mathbf{x}) \equiv 1$, the symbol in (3.29) reduces to $\mathbf{f}_{\mathbb{P}_k}$ and we observe jumps which correspond to the existence of an index l such that

$$\max \lambda_l(\mathbf{f}_{\mathbb{P}_k}(\boldsymbol{\theta})) < \lambda_{l+1}(\mathbf{f}_{\mathbb{P}_k}(\boldsymbol{\theta})),$$

with $1 \leq l \leq k^2 - 1$, $k = 1, 2, 3, 4$. In other words the rearranged function has a few discontinuity points. When $a(\mathbf{x})$ is not constant such a phenomenon disappears, since the range of all eigenvalue functions becomes wider and all the ranges intersect (there is not a range not intersecting at least another range). Furthermore, beside the latter smoothing effect due to $a(\mathbf{x})$, it is worthwhile observing that the regularity of the diffusion coefficient does not affect the qualitative behaviour of the eigenvalue distribution. In fact, the reconstruction given by the symbol of the eigenvalues of $A_n(a, \Omega, \mathbb{P}_k)$ is accurate in all the considered examples and, more specifically, the figures look very similar independently of the fact that the diffusion coefficient is smooth ($a(\mathbf{x}) = e^{x+y}$ in Figure 3.5), or is C^0 but not C^1 ($a(\mathbf{x}) = 1 + 2\sqrt{x} + y$ in Figure 3.6), or is discontinuous ($a(\mathbf{x}) = 1$ if $y \geq x$ and $a(\mathbf{x}) = 2$ otherwise, in Figure 3.7).

- In all Figures 3.5–3.7 the matrix size is quite moderate (of the order of 10^4), showing that the spectral distribution effects, which represent an asymptotic property, can be already visualized for small orders of the considered matrices.
- We did not show any figure regarding the distribution formula (3.30) just because the check has been done and there is no difference with respect to the case of $\Omega = (0, 1)^2$ as in (3.29).

3.6 Preconditioning and complexity issues

Lastly, we consider a few numerical experiments on preconditioning. First of all, the interest in solving the constant coefficient case $a(x, y) \equiv 1$ refers to its use in optimally preconditioning the nonconstant coefficient case whenever a is smooth enough, (see [72, 61] for the case $k = 1$). This is evident from Table 3.2, where we report the number of iterations required by PCG applied to $A_n(a, \Omega, \mathbb{P}_k)$, with $a(x, y) = \exp(x + y)$ in the case of preconditioning with

$P_n(a) = \tilde{D}_n^{1/2}(a)A_n(1, \Omega, \mathbb{P}_k)\tilde{D}_n^{1/2}(a)$ with $\tilde{D}_n(a) = D_n(a)D_n^{-1}(1)$, where $D_n(a)$ is the main diagonal of $A_n(a, \Omega, \mathbb{P}_k)$ and $D_n(1)$ is the main diagonal of $A_n(1, \Omega, \mathbb{P}_k)$.

Therefore, we now focus our attention on the case $a(x, y) \equiv 1$. Taking into account the Toeplitz nature of the matrices at hand, our aim is to preliminarily test a classical preconditioner as the Circulant one, clearly by considering the Strang correction, in order to deal with its singularity. More precisely, we will consider as preconditioner the Circulant matrix generated by the very same function $f_{\mathbb{P}_k}(\boldsymbol{\theta})$ plus the correction h^2ee^T , e being the vector of all ones and h the constant triangle edge. In the even columns of Table 3.3 (case $k = 2$) we report the number of PCG iterations required to solve the system with Toeplitz matrix $T_n(f_{\mathbb{P}_k})$, in the case of no preconditioning ($P_n = I_n$), preconditioning by the incomplete Cholesky factorization, and by the Circulant $C_n(f_{\mathbb{P}_k})$ plus the Strang correction, respectively. To this end, it is worth stressing that we have to consider the dimension of the Toeplitz/Circulant matrix fitting with its natural dimension with respect to the symbol size. Therefore, when instead we want to solve the system with the FEM matrix $A_n(1, \Omega, \mathbb{P}_k)$, principal submatrix of the matrix $T_n(f_{\mathbb{P}_k})$, we need to match its dimension with the one previously considered for the Circulant preconditioner. We obtain that goal just by imposing boundary conditions to $T_n(f_{\mathbb{P}_k})$, but keeping the size unchanged. The related numerical results are reported in odd columns of Table 3.3. In both cases, the number of required iterations increases as the dimension increases. No significant difference in even or odd column is observed in the case of no preconditioning or incomplete Cholesky preconditioning (the results are slightly better in the second case). In the case of the Circulant preconditioning we observe a clear worsening in the effectiveness when the preconditioner is applied not to the Toeplitz matrix, but to its principal submatrix plus boundary conditions, though the iteration growth rate seems smaller than the one observed in the case of incomplete Cholesky preconditioning. Furthermore, as expected from the theory, a weak cluster around 1 is observed, (see Table 3.4).

In Tables 3.5 and 3.6 the same numerical experiments are reported in the case $k = 3$ and $k = 4$. The numerical behavior seems to be substantially of the same type, independently of the parameter k , also in reference to the weak cluster phenomenon observed for $k = 2$ in Table 3.4.

$k = 2$		$k = 3$		$k = 4$	
N	$P_n(a)$	N	$P_n(a)$	N	$P_n(a)$
49	4	121	5	225	5
225	3	529	4	961	5
961	3	2209	4	3969	4
3969	3	9025	4	16129	4
16129	3	36481	4	65025	4

Table 3.2: Number of PCG iterations to reach convergence with respect to relative residual less than 1.e-6, Preconditioner $P_n(a)$, $a(x, y) = \exp(x + y)$.

$k = 2$						
N	$P = I$		$P = IC$		$P = C_S$	
64	26	19	11	10	14	19
256	47	42	18	17	19	30
1024	90	86	32	31	26	42
4096	174	170	56	55	38	59
16384	336	331	98	96	53	87

Table 3.3: Number of PCG iterations to reach convergence with respect to relative residual less than 1.e-6 - case $k = 2$.

$k = 2$					
N	n_{out}	%	n_{out}	%	
64	27	4.2e-1	27	4.2e-1	
256	59	2.3e-1	55	2.1e-1	
1024	123	1.2e-1	111	1.1e-1	
4096	251	6.1e-2	225	5.5e-2	

Table 3.4: Number of outliers n_{out} (eigenvalues not belonging to $(1 - \varepsilon, 1 + \varepsilon)$ with $\varepsilon = 1.e - 1$) and their percentage with respect to the dimension. The second and third columns refer to the Toeplitz case, the fourth and fifth columns to the case of the FEM matrix.

$k = 3$						
N	$P = I$		$P = IC$		$P = C_S$	
144	45	39	16	15	19	30
576	82	78	28	27	26	42
2304	159	155	50	48	36	61
9216	306	301	86	84	49	90

Table 3.5: Number of PCG iterations to reach convergence with respect to relative residual less than 1.e-6 - case $k = 3$.

$k = 4$						
N	$P = I$		$P = IC$		$P = C_S$	
256	74	66	10	10	23	38
1024	134	129	18	17	31	57
4096	261	254	31	30	43	81
16384	502	490	54	51	61	116

Table 3.6: Number of PCG iterations to reach convergence with respect to relative residual less than 1.e-6 - case $k = 4$.

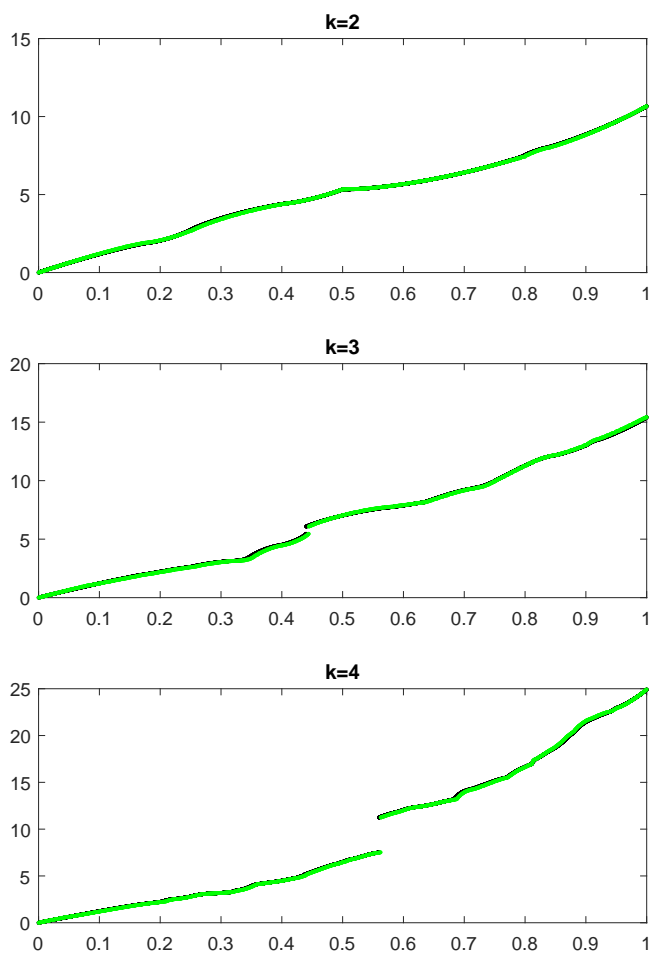


Figure 3.4: Ordered equispaced samplings of $\lambda_j(a(x, y)\mathbf{f}_{\mathbb{P}_k}(\boldsymbol{\theta}))$, $j = 1, \dots, k^2$ (green dots) and ordered eigenvalues $\lambda_l(A_n(a, \Omega, \mathbb{P}_k))$ with $a(x, y) \equiv 1$.

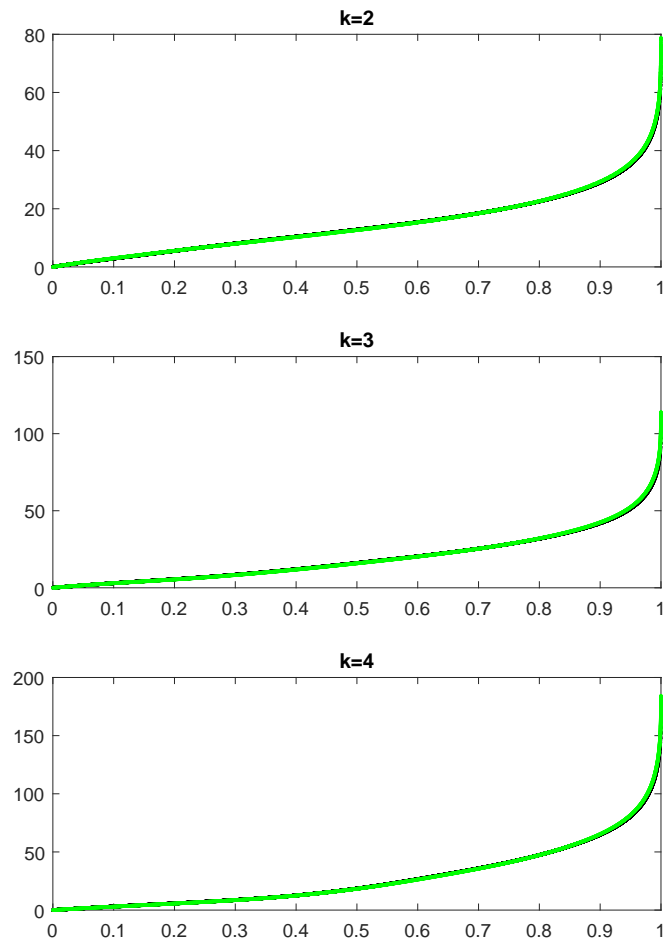


Figure 3.5: Ordered equispaced samplings of $\lambda_j(a(x, y)\mathbf{f}_{\mathbb{P}_k}(\boldsymbol{\theta}))$, $j = 1, \dots, k^2$ (green dots) and ordered eigenvalues $\lambda_l(A_n(a, \Omega, \mathbb{P}_k))$ with $a(x, y) = e^{x+y}$.

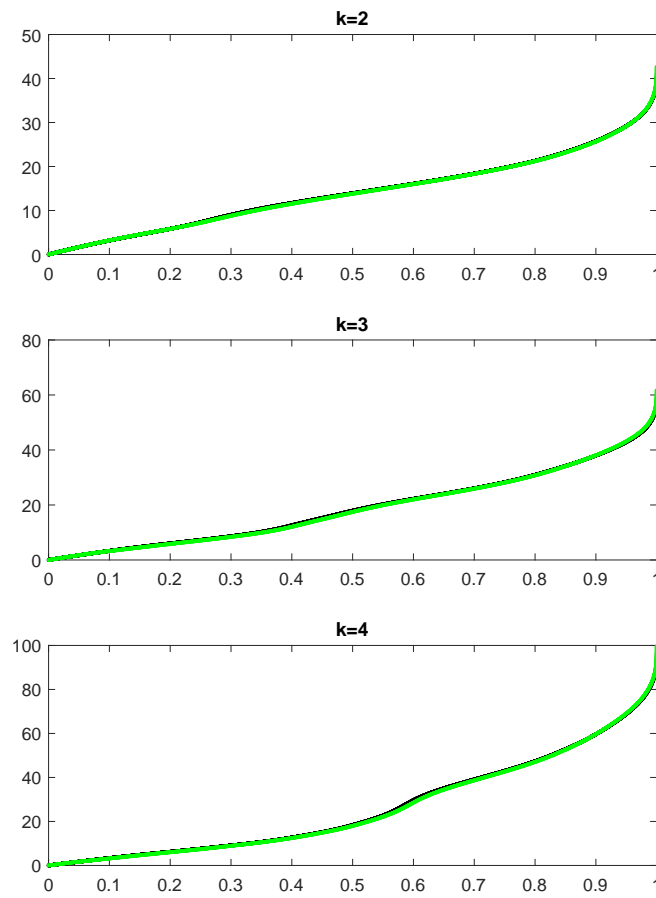


Figure 3.6: Ordered equispaced samplings of $\lambda_j(a(x,y)\mathbf{f}_{\mathbb{P}_k}(\boldsymbol{\theta}))$, $j = 1, \dots, k^2$ (green dots) and ordered eigenvalues $\lambda_l(A_n(a, \Omega, \mathbb{P}_k))$ with $a(x,y) = 1 + 2\sqrt{x} + y$.

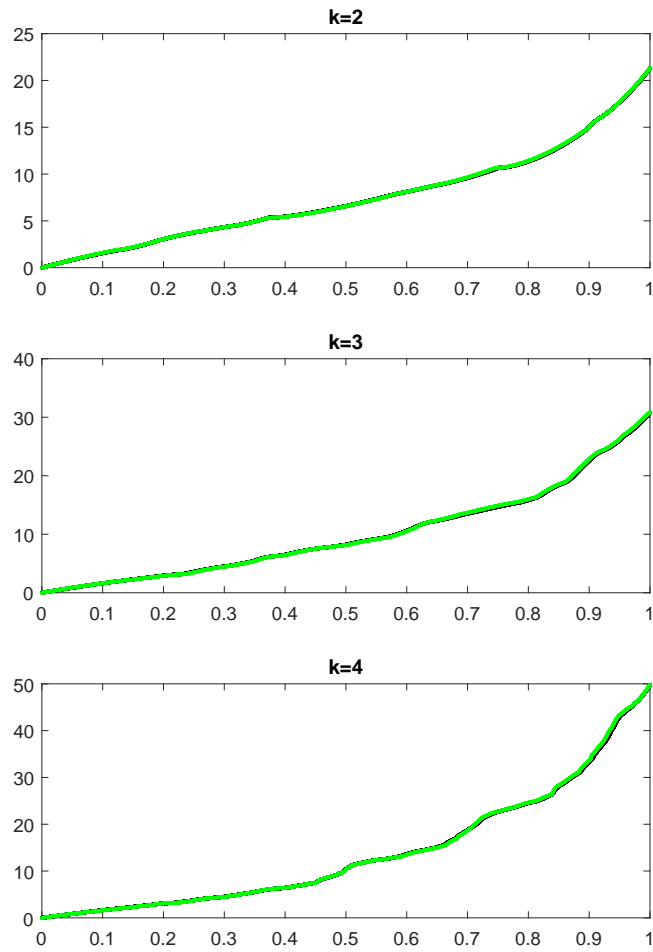


Figure 3.7: Ordered equispaced samplings of $\lambda_j(a(x, y)\mathbf{f}_{\mathbb{P}_k}(\boldsymbol{\theta}))$, $j = 1, \dots, k^2$ (green dots) and ordered eigenvalues $\lambda_l(A_n(a, \Omega, \mathbb{P}_k))$ with $a(x, y) = 1$ if $y \geq x$ and $a(x, y) = 2$ otherwise.

CHAPTER 4

MULTIGRID FOR \mathbb{Q}_K FINITE ELEMENT MATRICES USING A (BLOCK) TOEPLITZ SYMBOL APPROACH

In the present chapter, we consider multigrid strategies for the resolution of linear systems arising from the \mathbb{Q}_k Finite Elements approximation of the elliptic problem

$$\begin{cases} \operatorname{div}(-a(\mathbf{x})\nabla u) = f, & \mathbf{x} \in \Omega \subseteq \mathbb{R}^d, \\ u|_{\partial\Omega} = 0, \end{cases} \quad (4.1)$$

with Ω a bounded subset of \mathbb{R}^d , having smooth boundaries, and with a being continuous and positive on $\bar{\Omega}$. While the analysis is performed in one dimension, the numerics are carried out also in higher dimension $d \geq 2$, showing an optimal behavior in terms of the dependency on the matrix size and a substantial robustness with respect to the dimensionality d and to the polynomial degree k .

4.1 Optimality of two-grid method in the case of Toeplitz matrices

We start the current subsection with a key remark.

Remark 4.1.1. *In the relevant literature, (see for instance, [1]), the convergence analysis of the two-grid method splits into the validation of two separate conditions: the smoothing property and the approximation property. Regarding the latter, with reference to scalar structured matrices [1, 34], the optimality of two-grid methods is given in terms of choosing the proper conditions that the symbol p of a family of projection operators has to fulfill. Indeed, consider $T_n(f)$ with $n = (2^t - 1)$ and f being a nonnegative trigonometric polynomial. Let θ^0 be the unique zero of f . Then, the optimality of the two-grid method applied to $T_n(f)$ is guaranteed if we choose the symbol p of the family of projection operators such that*

$$\begin{aligned} \limsup_{\theta \rightarrow \theta^0} \frac{|p(\eta)|^2}{f(\theta)} < \infty, \quad \eta \in \mathcal{M}(\theta), \\ \sum_{\eta \in \Omega(\theta)} p^2(\eta) > 0, \end{aligned} \tag{4.2}$$

where the sets $\Omega(\theta)$ and $\mathcal{M}(\theta)$ are the following corner and mirror points

$$\Omega(\theta) = \{\eta \in \{\theta, \theta + \pi\}\}, \quad \mathcal{M}(\theta) = \Omega(\theta) \setminus \{\theta\},$$

respectively.

Informally, it means that the optimality of the two-grid method is obtained by choosing the family of projection operators associated to a symbol p such that $|p|^2(\vartheta) + |p|^2(\vartheta + \pi)$ does not have zeros and $|p|^2(\vartheta + \pi)/f(\vartheta)$ is bounded (if we require the optimality of the V-cycle, then the second condition is a bit stronger, see [1]). In a differential context, the previous conditions mean that p has a zero of order at least α at $\vartheta = \pi$, whenever f has a zero at $\theta^0 = 0$ of order 2α .

In our specific block setting, by interpreting the analysis given in [24], all the involved symbols are matrix-valued and the conditions which are sufficient for the two-grid convergence and optimality are the following:

- (A) zero of order 2 at $\vartheta = \pi$ of the proper eigenvalue function of the symbol of the projector for \mathbb{Q}_k , $k = 1, 2, 3$ (mirror point theory [1, 34]);

(B) positive definiteness of $\mathbf{p}\mathbf{p}^*(\vartheta) + \mathbf{p}\mathbf{p}^*(\vartheta + \pi)$; and

(C) commutativity of $\mathbf{p}(\vartheta)$ and $\mathbf{p}(\vartheta + \pi)$.

Our choices are in agreement with the mathematical conditions set in Items (A) and (B), while Condition (C) is not satisfied. The violation of Condition (C) is discussed later, while, in relation to Condition (A), we observe that a stronger condition is met, since the considered order of the zero at $\vartheta = \pi$ is $k + 1$, which is larger than 2 for $k = 2, 3$.

4.2 Structure of the Matrices and Spectral Analysis

Since in the case $d = 1$, $\mathbb{Q}_k \equiv \mathbb{P}_k$, then everything provided in the Section 3.2 remains valid.

4.3 Multigrid Strategy Definition, Symbol Analysis, and Numerics

Let us consider a family of meshes

$$\{\mathcal{T}_{2^s h}\}_{s=0,\dots,\bar{s}} \text{ such that } \mathcal{T}_{2^s h} \subseteq \mathcal{T}_{2^{s-1} h} \subseteq \dots \subseteq \mathcal{T}_{2h} \subseteq \mathcal{T}_h.$$

Clearly, the same inclusion property is inherited by the corresponding Finite Element functional spaces and hence we find $\mathcal{V}_{2^s h} \subseteq \mathcal{V}_{2^{s-1} h} \subseteq \dots \subseteq \mathcal{V}_{2h} \subseteq \mathcal{V}_h$.

Therefore, to formulate a multigrid strategy, it is quite natural to follow a functional approach and to impose the prolongation operator $p_{2h}^h : \mathcal{V}_{2h} \rightarrow \mathcal{V}_h$ to be defined as the identity operator, that is

$$p_{2h}^h v_{2h} = v_{2h} \text{ for all } v_{2h} \in \mathcal{V}_{2h}.$$

Thus, the matrix representing the prolongation operator is formed, column by column, by representing each function of the basis of \mathcal{V}_{2h} as linear combination of the basis of \mathcal{V}_h , the coefficients being the values of the functions φ_i^{2h} on the fine mesh grid points, i.e.,

$$\varphi_i^{2h}(x) = \sum_{x_j \in \mathcal{T}_h} \varphi_i^{2h}(x_j) \varphi_j^h(x). \quad (4.3)$$

In the following subsections, we consider in detail the case of \mathbb{Q}_k Finite Element approximation with $k = 2$ and $k = 3$, the case $k = 1$ being reported in short just for the sake of completeness.

4.3.1 \mathbb{Q}_1 Case

Firstly, let us consider the case of \mathbb{Q}_1 Finite Elements, where, as is well known, the stiffness matrix is the scalar Toeplitz matrix generated by $\mathbf{f}_{\mathbb{Q}_1}(\vartheta) = 2 - 2 \cos(\vartheta)$, and, for the sake of simplicity, let us consider the case of \mathcal{T}_{2h} partitioning with five equispaced points (three internal points) and \mathcal{T}_h partitioning with nine equispaced points (seven internal points) obtained from \mathcal{T}_{2h} by considering the midpoint of each subinterval. In the standard geometric multigrid, the prolongation operator matrix is defined as

$$P_{h \times 2h} = P_3^7 = \begin{bmatrix} \frac{1}{2} & & & & & & & & \\ & 1 & & & & & & & \\ & & \frac{1}{2} & & & & & & \\ & & & \frac{1}{2} & & & & & \\ & & & & 1 & & & & \\ & & & & & \frac{1}{2} & & & \\ & & & & & & \frac{1}{2} & & \\ & & & & & & & 1 & \\ & & & & & & & & \frac{1}{2} \end{bmatrix}. \quad (4.4)$$

Indeed, the basis functions with respect to the reference interval $[0, 1]$ are

$$\begin{aligned} \hat{\varphi}_1(\hat{x}) &= 1 - \hat{x}, \\ \hat{\varphi}_2(\hat{x}) &= \hat{x}, \end{aligned}$$

and, according to Equation (4.3), the φ_i^{2h} coefficients are

$$\hat{\varphi}_2(1/2) = 1/2, \quad \hat{\varphi}_2(1) = 1, \quad \hat{\varphi}_1(1/2) = 1/2,$$

giving the columns of the matrix in Equation (4.4). However, we can think the prolongation matrix above as the product of the Toeplitz matrix generated by the

Table 4.1: Number of iterations needed for the convergence of the two-grid and V-cycle methods for $k = 1, 2, 3$ in one dimension with $a(x) \equiv 1$ and $\text{tol} = 1 \times 10^{-6}$.

# Subintervals	$k = 1$		$k = 2$		$k = 3$	
	TGM	V-Cycle	TGM	V-Cycle	TGM	V-Cycle
8	5	5	7	7	9	9
16	6	7	7	7	9	9
32	7	7	7	7	9	9
64	7	7	7	7	9	9
128	6	7	7	7	9	9
256	6	7	7	7	9	9
512	6	7	7	7	9	9

4.3.2 \mathbb{Q}_2 Case

Let us consider the case of \mathbb{Q}_2 Finite Elements, where we have that the basis functions with respect to the reference interval $[0, 1]$ are

$$\begin{aligned}\hat{\varphi}_1(\hat{x}) &= 2\hat{x}^2 - 3\hat{x} + 1, \\ \hat{\varphi}_2(\hat{x}) &= -4\hat{x}^2 + 4\hat{x}, \\ \hat{\varphi}_3(\hat{x}) &= 2\hat{x}^2 - \hat{x}.\end{aligned}$$

For the sake of simplicity, let us consider the case of \mathcal{T}_{2h} partitioning with five equispaced points (three internal points) and \mathcal{T}_h partitioning with nine equispaced points (seven internal points) obtained from \mathcal{T}_{2h} by considering the midpoint of each subinterval.

Thus, with respect to Equation (4.3), the φ_1^{2h} coefficients are

$$\hat{\varphi}_2(1/4) = 3/4, \quad \hat{\varphi}_2(1/2) = 1, \quad \hat{\varphi}_2(3/4) = 3/4, \quad \hat{\varphi}_2(1) = 0,$$

while the $\hat{\varphi}_2^{2h}$ coefficients are

$$\begin{aligned}\hat{\varphi}_3(1/4) &= -1/8, & \hat{\varphi}_3(1/2) &= 0, & \hat{\varphi}_3(3/4) &= 3/8, & \hat{\varphi}_3(1) &= 1, \\ \hat{\varphi}_1(1/4) &= 3/8, & \hat{\varphi}_1(1/2) &= 0, & \hat{\varphi}_1(3/4) &= -1/8, & \hat{\varphi}_1(1) &= 0,\end{aligned}$$

and so on again as for that first couple of basis functions. Notice also that, to evaluate the coefficients, for the sake of simplicity, we are referring to the basis functions on the reference interval, as depicted in Figure 4.1. As a conclusion, the obtained prolongation matrix is as follows

$$P_{h \times 2h} = P_3^7 = \begin{bmatrix} \frac{3}{4} & -\frac{1}{8} & & & & & & \\ & 1 & 0 & & & & & \\ & \frac{3}{4} & \frac{3}{8} & & & & & \\ 0 & 1 & & & & & & \\ & & \frac{3}{8} & \frac{3}{4} & & & & \\ & & 0 & 1 & & & & \\ & & -\frac{1}{8} & \frac{3}{4} & & & & \end{bmatrix}. \quad (4.6)$$

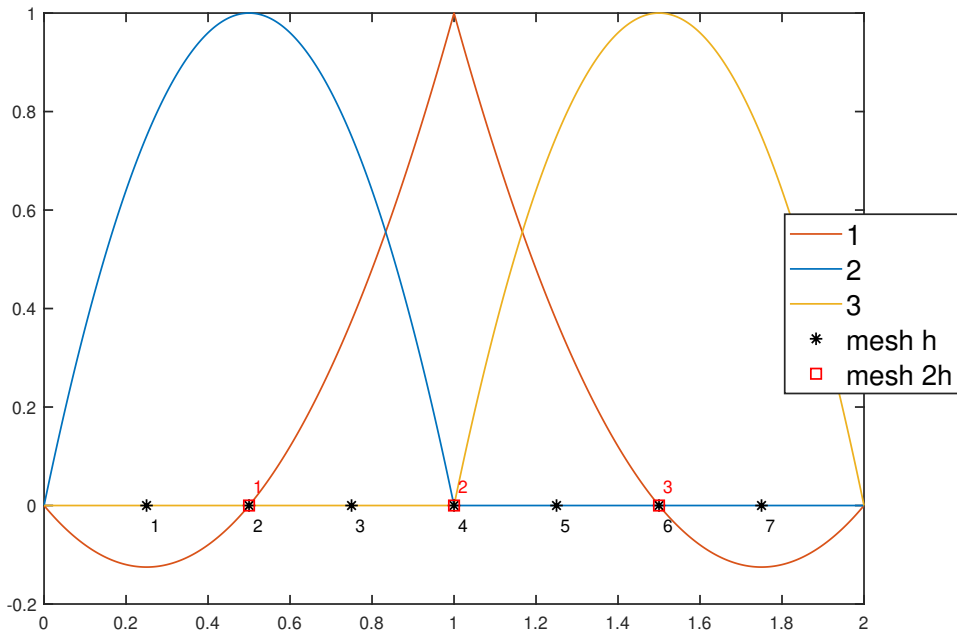


Figure 4.1: Construction of the \mathbb{Q}_2 prolongation operator: basis functions on the reference element.

Hereafter, we are interested in setting such a geometrical multigrid strategy, proposed in [13, 48, 49], in the framework of the more general algebraic multigrid

theory and in particular in the one driven by the matrix symbol analysis. To this end, we represent the prolongation operator quoted above as the product of a Toeplitz matrix generated by a polynomial $\mathbf{p}_{\mathbb{Q}_2}$ and a suitable cutting matrix. We recall that the Finite Element stiffness matrix could be thought as a principal submatrix of a Toeplitz matrix generated by the matrix-valued symbol that, from Equation (3.9), has the compact form

$$\mathbf{f}_{\mathbb{Q}_2}(\vartheta) = \begin{bmatrix} \frac{16}{3} & -\frac{8}{3}(1 + e^{\hat{i}\vartheta}) \\ -\frac{8}{3}(1 + e^{-\hat{i}\vartheta}) & \frac{14}{3} + \frac{1}{3}(e^{\hat{i}\vartheta} + e^{-\hat{i}\vartheta}) \end{bmatrix}. \quad (4.7)$$

Thus, it is quite natural to look for a matrix-valued symbol for the polynomial $\mathbf{p}_{\mathbb{Q}_2}$ as well. In addition, the cutting matrix is also formed through the Kronecker product of the scalar cutting matrix in Equation (4.5) and the identity matrix of order 2, so that

$$P_{m_{s+1}}^{m_s} = (P_{m_s}^{m_{s+1}})^T = A_{m_s}(p_{\mathbb{Q}_2})((K_{m_{s+1} \times m_s})^T \otimes I_2).$$

Taking into account the action of the cutting matrix $(K_{m_{s+1} \times m_s})^T \otimes I_2$, we can easily identify from Equation (4.6) the generating polynomial as

$$\mathbf{p}_{\mathbb{Q}_2}(\vartheta) = K_0 + K_1 e^{\hat{i}\vartheta} + K_{-1} e^{-\hat{i}\vartheta} + K_2 e^{2\hat{i}\vartheta} + K_{-2} e^{-2\hat{i}\vartheta}. \quad (4.8)$$

where

$$K_0 = \begin{bmatrix} \frac{3}{4} & \frac{3}{8} \\ 0 & 1 \end{bmatrix}, \quad K_1 = \begin{bmatrix} 0 & \frac{3}{8} \\ 0 & 0 \end{bmatrix}, \quad K_{-1} = \begin{bmatrix} \frac{3}{4} & -\frac{1}{8} \\ 1 & 0 \end{bmatrix}, \quad K_2 = \begin{bmatrix} 0 & -\frac{1}{8} \\ 0 & 0 \end{bmatrix}, \quad K_{-2} = O_2,$$

that is

$$\mathbf{p}_{\mathbb{Q}_2}(\vartheta) = \begin{bmatrix} \frac{3}{4}(1 + e^{-\hat{i}\vartheta}) & \frac{3}{8}(1 + e^{\hat{i}\vartheta}) - \frac{1}{8}(e^{-\hat{i}\vartheta} + e^{2\hat{i}\vartheta}) \\ e^{-\hat{i}\vartheta} & 1 \end{bmatrix}.$$

A very preliminary analysis, just by computing the determinant of $\mathbf{p}_{\mathbb{Q}_2}(\vartheta)$ shows there is a zero of third order in the mirror point $\vartheta = \pi$, being

$$\det(\mathbf{p}_{\mathbb{Q}_2}(\vartheta)) = \frac{1}{8} e^{-2\hat{i}\vartheta} (e^{\hat{i}\vartheta} + 1)^3.$$

We highlight that our choices are in agreement with the mathematical conditions set in Items **(A)** and **(B)**. Condition **(C)** is violated and we discuss it in Remark 4.3.1. Nevertheless, it is possible to derive the following TGM convergence and optimality sufficient conditions that should be verified by \mathbf{f} and $\mathbf{p} = \mathbf{p}_{\mathbb{Q}_2}$, exploiting the idea in the proof of the main result of [24]:

$$\mathbf{p}(\vartheta)^* \mathbf{p}(\vartheta) + \mathbf{p}(\vartheta + \pi)^* \mathbf{p}(\vartheta + \pi) > O_k \text{ for all } \vartheta \in [0, 2\pi] \quad (4.9)$$

$$R(\vartheta) \leq \gamma I_{2k} \quad (4.10)$$

with

$$R(\vartheta) = \begin{bmatrix} \mathbf{f}(\vartheta) \\ \mathbf{f}(\vartheta + \pi) \end{bmatrix}^{-\frac{1}{2}} \left(I_{2k} - \begin{bmatrix} \mathbf{p}(\vartheta) \\ \mathbf{p}(\vartheta + \pi) \end{bmatrix} q(\vartheta) [\mathbf{p}(\vartheta)^* \mathbf{p}(\vartheta + \pi)^*] \right) \begin{bmatrix} \mathbf{f}(\vartheta) \\ \mathbf{f}(\vartheta + \pi) \end{bmatrix}^{-\frac{1}{2}},$$

where $q(\vartheta) = [\mathbf{p}(\vartheta)^* \mathbf{p}(\vartheta) + \mathbf{p}(\vartheta + \pi)^* \mathbf{p}(\vartheta + \pi)]^{-1}$, $\gamma > 0$ is a constant independent on n . The condition in Equation (4.10) requires the matrix-valued function $R(\vartheta)$ to be uniformly bounded in the spectral norm. These conditions are obtained from the proof of the main convergence result in [24], where, after several numerical derivations, it was concluded that the above conditions are the final requirements needed.

To this end, we have explicitly formed the matrices involved in the conditions in Equations (4.9) and (4.10) and computed their eigenvalues for $\vartheta \in [0, 2\pi]$. The results are reported in Figure 4.2 and are in perfect agreement with the theoretical requirements.

In the second panel of Table 4.1, we report the number of iterations needed for achieving the predefined tolerance 10^{-6} , when increasing the matrix size in the setting of the current subsection. Indeed, we use $A_{m_s}(p_{\mathbb{Q}_2})(K_{m_{s+1} \times m_s})^T$ and its transpose as restriction and prolongation operators and Gauss–Seidel as a smoother. Again, we remind that only one iteration of pre-smoothing and only one iteration of post-smoothing are employed in our numerical setting.

As expected, we observe that the number of iterations needed for the two-grid convergence remains constant, when we increase the matrix size, numerically confirming the optimality of the method.

Moreover, we notice that the V-cycle method is characterised by optimal convergence properties. Although this behaviour is expected from the point of view of differential approximated operators, it is interesting in the setting of algebraic multigrid methods. Indeed, constructing an optimal V-cycle method for matrices in this block setting might require a specific analysis of the spectral properties of the restricted operators, (see [24]).

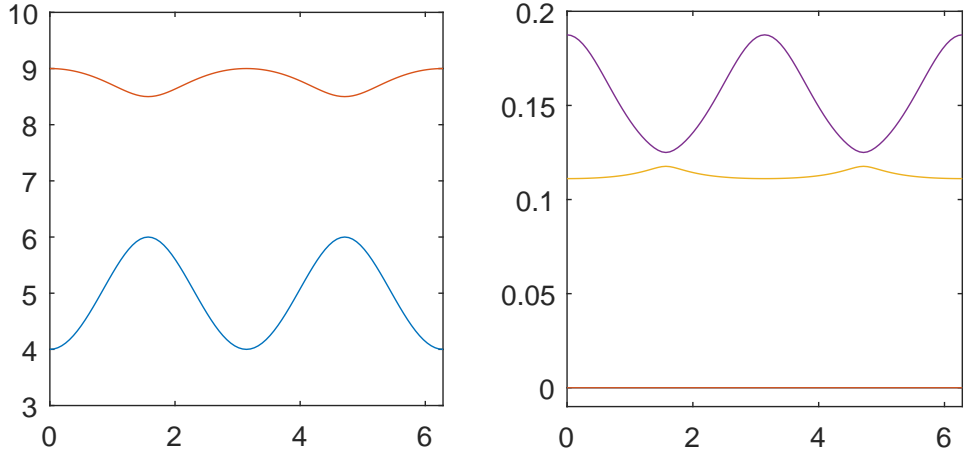


Figure 4.2: Check of conditions for \mathbb{Q}_2 prolongation: **(left)** the plot of the eigenvalues of $\mathbf{p}(\vartheta)^*\mathbf{p}(\vartheta) + \mathbf{p}(\vartheta + \pi)^*\mathbf{p}(\vartheta + \pi)$ for $\vartheta \in [0, 2\pi]$; and **(right)** the plot of the eigenvalues of $R(\vartheta)$ for $\vartheta \in [0, 2\pi]$.

4.3.3 \mathbb{Q}_3 Case

Hereafter, we briefly summarize the case of \mathbb{Q}_3 Finite Elements, following the very same path we already considered in the previous section for \mathbb{P}_2 Finite Elements. The basis functions with respect to the reference interval $[0, 1]$ are

$$\begin{aligned}
 \hat{\varphi}_1(\hat{x}) &= -\frac{9}{2}\hat{x}^3 + 9\hat{x}^2 - \frac{11}{2}\hat{x} + 1, \\
 \hat{\varphi}_2(\hat{x}) &= \frac{27}{2}\hat{x}^3 - \frac{45}{2}\hat{x}^2 + 9\hat{x}, \\
 \hat{\varphi}_3(\hat{x}) &= -\frac{27}{2}\hat{x}^3 + 18\hat{x}^2 - \frac{9}{2}\hat{x}, \\
 \hat{\varphi}_4(\hat{x}) &= \frac{9}{2}\hat{x}^3 - \frac{9}{2}\hat{x}^2 + \hat{x}.
 \end{aligned} \tag{4.11}$$

Therefore, taking into consideration that the stiffness matrix is a principal submatrix of the Toeplitz matrix generated by the matrix-valued function

$$\mathbf{f}_{\mathbb{Q}_3}(\vartheta) = \begin{bmatrix} \frac{54}{5} & -\frac{297}{40} & \frac{27}{20} - \frac{189}{40}e^{\hat{i}\vartheta} \\ -\frac{297}{40} & \frac{54}{5} & -\frac{189}{40} + \frac{27}{20}e^{\hat{i}\vartheta} \\ \frac{27}{20} - \frac{189}{40}e^{-\hat{i}\vartheta} & -\frac{189}{40} + \frac{27}{20}e^{-\hat{i}\vartheta} & \frac{37}{5} - \frac{13}{40}(e^{\hat{i}\vartheta} + e^{-\hat{i}\vartheta}) \end{bmatrix}, \quad (4.13)$$

we are looking for the matrix-valued symbol $\mathbf{p}_{\mathbb{Q}_3}$ as well. By defining

$$P_{m_s+1}^{m_s} = (P_{m_s}^{m_s+1})^T = A_{m_s}(p_{\mathbb{Q}_3})((K_{m_s+1 \times m_s})^T \otimes I_3)$$

it is easy to identify the generating polynomial as

$$\mathbf{p}_{\mathbb{Q}_3}(\vartheta) = K_0 + K_1e^{\hat{i}\vartheta} + K_{-1}e^{-\hat{i}\vartheta} + K_2e^{2\hat{i}\vartheta} + K_{-2}e^{-2\hat{i}\vartheta}, \quad (4.14)$$

where

$$K_0 = \begin{bmatrix} 0 & 1 & 0 \\ -\frac{5}{16} & \frac{15}{16} & \frac{5}{16} \\ 0 & 0 & 1 \end{bmatrix}, \quad K_1 = \begin{bmatrix} 0 & 0 & \frac{5}{16} \\ 0 & 0 & 0 \\ 0 & 0 & -\frac{1}{16} \end{bmatrix}, \quad K_{-1} = \begin{bmatrix} \frac{15}{16} & -\frac{5}{16} & \frac{1}{16} \\ 1 & 0 & 0 \\ \frac{9}{16} & \frac{9}{16} & -\frac{1}{16} \end{bmatrix},$$

$$K_2 = \begin{bmatrix} 0 & 0 & 0 \\ 0 & 0 & \frac{1}{16} \\ 0 & 0 & 0 \end{bmatrix}, \quad K_{-2} = O_3,$$

that is

$$\mathbf{p}_{\mathbb{Q}_3}(\vartheta) = \begin{bmatrix} \frac{15}{16}e^{-\hat{i}\vartheta} & 1 - \frac{5}{16}e^{-\hat{i}\vartheta} & \frac{1}{16}e^{-\hat{i}\vartheta} + \frac{5}{16}e^{\hat{i}\vartheta} \\ e^{-\hat{i}\vartheta} - \frac{5}{16} & \frac{15}{16} & \frac{5}{16} + \frac{1}{16}e^{2\hat{i}\vartheta} \\ \frac{9}{16}e^{-\hat{i}\vartheta} & \frac{9}{16}e^{-\hat{i}\vartheta} & 1 - \frac{1}{16}(e^{\hat{i}\vartheta} + e^{-\hat{i}\vartheta}) \end{bmatrix}. \quad (4.15)$$

A trivial computation shows again that there is a zero of fourth order in the mirror point $\vartheta = \pi$, being

$$\det(\mathbf{p}_{\mathbb{Q}_3}(\vartheta)) = \frac{1}{64}e^{-3\hat{i}\vartheta}(e^{\hat{i}\vartheta} + 1)^4.$$

However, the main goal is to verify the conditions in Equations (4.9) and (4.10): we have explicitly formed the matrices involved and computed their eigenvalues for $\vartheta \in [0, 2\pi]$. The results are in perfect agreement with the theoretical requirements,

(see Figure 4.4). This analysis links the geometric approach proposed in [13, 48, 49] to the novel algebraic multigrid methods for block-Toeplitz matrices.

In the third panel of Table 4.1, we report the number of iterations needed for achieving the predefined tolerance 10^{-6} , when increasing the matrix size in the setting of the current subsection. Indeed, we use $A_{m_s}(p_{\mathbb{Q}_3})(K_{m_s+1 \times m_s})^T$ and its transpose as restriction and prolongation operators and Gauss–Seidel as a smoother (one iteration of pre-smoothing and one iteration of post-smoothing).

As expected, we observe that the number of iterations needed for the two-grid convergence remains constant, when we increase the matrix size, numerically confirming the optimality of the method. In analogy to the \mathbb{Q}_2 case, we notice that the V-cycle methods show the same optimal convergence properties.

Comparing the three panels in Table 4.1, we also notice a mild dependency of the number of iterations on the polynomial degree k . In addition, we can see in Tables 4.2 and 4.3 that the optimal behaviour of the two-grid and V-cycle methods for $k = 2, 3$ remains unchanged if we test different tolerance values.

Table 4.2: Number of iterations needed for the convergence of the two-grid and V-cycle methods for $k = 2$ in one dimension with $a(x) \equiv 1$ and $\text{tol} = 1 \times 10^{-2}, 1 \times 10^{-4}$, and 1×10^{-8} .

# Subintervals	$\text{tol} = 1 \times 10^{-2}$		$\text{tol} = 1 \times 10^{-4}$		$\text{tol} = 1 \times 10^{-8}$	
	TGM	V-Cycle	TGM	V-Cycle	TGM	V-Cycle
8	3	3	5	5	8	8
16	3	3	5	5	9	9
32	3	3	5	5	9	10
64	3	3	5	5	9	10
128	3	3	5	5	9	10
256	3	3	5	5	9	10
512	3	3	5	5	9	10

Table 4.3: Number of iterations needed for the convergence of the two-grid and V-cycle methods for $k = 3$ in one dimension with $a(x) \equiv 1$ and $\text{tol} = 1 \times 10^{-2}, 1 \times 10^{-4}$, and 1×10^{-8} .

# Subintervals	$\text{tol} = 1 \times 10^{-2}$		$\text{tol} = 1 \times 10^{-4}$		$\text{tol} = 1 \times 10^{-8}$	
	TGM	V-Cycle	TGM	V-Cycle	TGM	V-Cycle
8	3	3	6	6	12	12
16	3	3	6	6	12	12
32	3	3	6	6	12	12
64	3	3	6	6	12	12
128	3	3	6	6	12	12
256	3	3	6	6	12	12
512	3	3	6	6	12	12

Remark 4.3.1. *From the cases analysed in this section, we notice that, even though $\mathbf{p}(0)$ and $\mathbf{p}(\pi)$ do not commute, the two-grid method is still convergent and optimal. The latter commutation property, along with Conditions (A) and (B) reported in Remark 4.1.1, is sufficient to have optimal convergence of the two-grid method. This analysis reveals that commutativity is not a necessary property. Indeed, in our examples, we show that the operator $R(\vartheta)$ is uniformly bounded in the spectral norm.*

However, we notice that in all cases the commutator $S_{\mathbb{Q}_k}(\vartheta) = \mathbf{P}_{\mathbb{Q}_k}(\vartheta)\mathbf{P}_{\mathbb{Q}_k}(\vartheta + \pi) - \mathbf{P}_{\mathbb{Q}_k}(\vartheta)\mathbf{P}_{\mathbb{Q}_k}(\vartheta + \pi)$ computed in θ is a singular matrix. In particular, computing our commutator matrix $S_{\mathbb{Q}_k}(\vartheta)$ in $\vartheta = 0$, we obtain:

$$S_{\mathbb{Q}_2}(0) = \frac{1}{2} \begin{pmatrix} -1 & 1 \\ -1 & 1 \end{pmatrix}, \quad S_{\mathbb{Q}_3}(0) = \frac{1}{256} \begin{pmatrix} -462 & 330 & 132 \\ -438 & 354 & 84 \\ -378 & 270 & 108 \end{pmatrix},$$

which are indeed singular matrices.

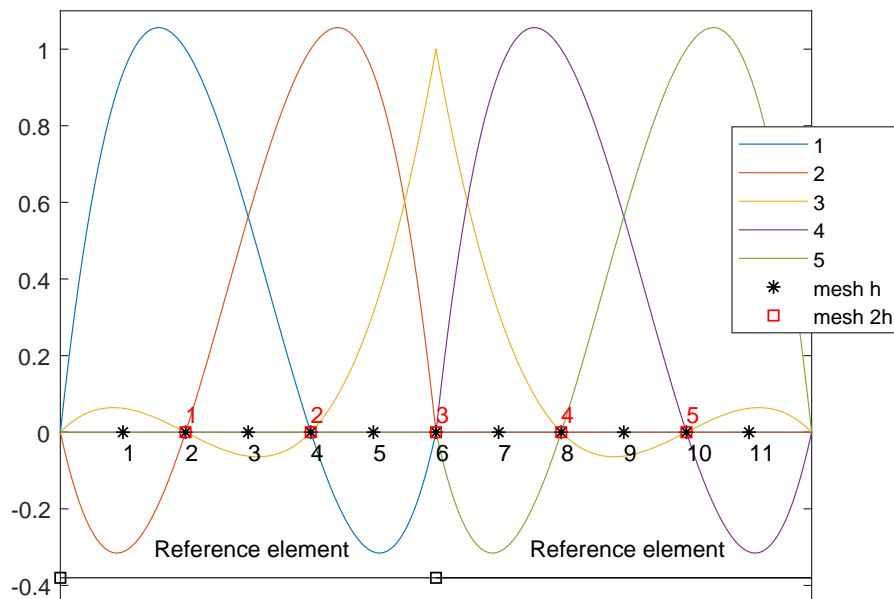


Figure 4.3: Construction of the \mathbb{Q}_3 prolongation operator: basis functions on the reference element.

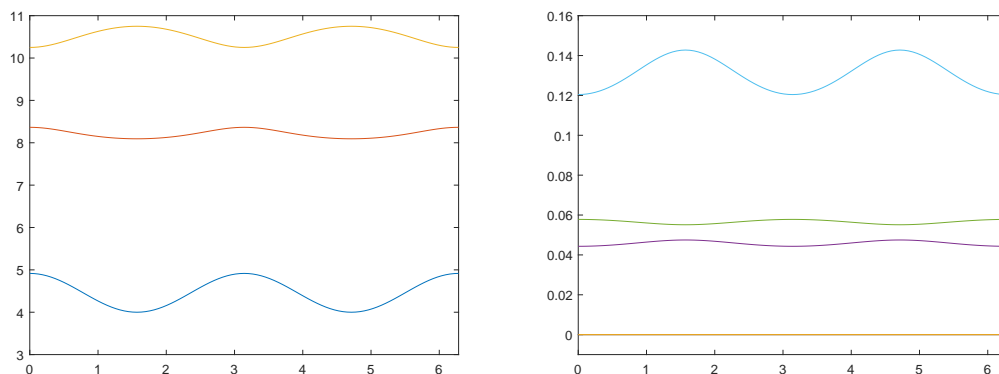


Figure 4.4: Check of conditions for \mathbb{Q}_3 prolongation: **(left)** the plot of the eigenvalues of $p(\vartheta)^H p(\vartheta) + p(\vartheta + \pi)^H p(\vartheta + \pi)$ for $\vartheta \in [0, 2\pi]$; and **(right)** the plot of the eigenvalues of $R(\vartheta)$ for $\vartheta \in [0, 2\pi]$.

Remark 4.3.2. *It is worth stressing that the results hold also in dimension $d \geq 2$. In fact, interestingly, we observe that the dimensionality d does not affect the efficiency of the proposed method, as well shown in Table 4.4 for the case $d = 2$. We finally remind that the tensor structure of the resulting matrices highly facilitates the generalization and extension of the numerical code to the case of $d \geq 2$. Indeed,*

the prolongation operators in the multilevel setting are constructed by a proper tensorization of those in 1D.

Table 4.4: Number of iterations needed for the convergence of the two-grid and V-cycle methods for $k = 1, 2, 3$ in dimension $d = 2$ with $a(\mathbf{x}) \equiv 1$.

$k = 1$			$k = 2$			$k = 3$		
# Nodes	Two Grid	V-Cycle	# Nodes	Two Grid	V-Cycle	# Nodes	Two Grid	V-Cycle
7^2	5	5	15^2	6	6	23^2	7	7
15^2	5	6	31^2	6	6	47^2	7	7
31^2	5	6	63^2	6	6	95^2	7	7
63^2	5	6	127^2	6	6	191^2	7	7
127^2	5	6	255^2	6	6	383^2	7	7

Furthermore, we highlight that the presented analysis for $a \equiv 1$ can be easily extended to the case on non-constant coefficients $a(x) \neq 1$ in 1D and $a(x, y) \neq 1$ in 2D, since, following a geometric approach, the prolongation operators for the general variable coefficients remain unchanged. In Tables 4.5 and 4.6, we show the number of iterations needed for the convergence of the two-grid and V-cycle methods for $k = 2$ in one and two dimensions for different values of $a \neq 1$.

Table 4.5: Number of iterations needed for the convergence of the two-grid and V-cycle methods for $k = 2$ in one dimension with $a(x) = e^x$, $a(x) = 10x + 1$, $a(x) = |x - 1/2| + 1$, and $\text{tol} = 1 \times 10^{-6}$.

# Subintervals	$a(x) = e^x$		$a(x) = 10x + 1$		$a(x) = x - 1/2 + 1$	
	TGM	V-Cycle	TGM	V-Cycle	TGM	V-Cycle
8	7	7	11	11	7	7
16	7	7	9	12	7	7
32	7	8	7	14	7	7
64	7	8	7	14	7	7
128	7	8	7	15	7	7
256	7	8	7	15	7	7
512	7	8	7	14	7	7

Table 4.6: Number of iterations needed for the convergence of the two-grid and V-cycle methods for $k = 2$ in two dimensions with $a(x, y) = e^{(x+y)}$, $a(x, y) = 10(x + y) + 1$, $a(x, y) = |x - 1/2| + |y - 1/2| + 1$, $a(x, y) = 1$ if $x \leq 1/2$ and $y \leq 1/2$, 5000 otherwise, and $\text{tol} = 1 \times 10^{-6}$.

# Nodes	$a(x, y) = e^{(x+y)}$		$10(x + y) + 1$		$ x - 1/2 + y - 1/2 + 1$		$\begin{cases} 1 & x, y \leq 1/2 \\ 5000 & \text{otherwise} \end{cases}$	
	Two Grid	V- Cycle	Two Grid	V- Cycle	Two Grid	V- Cycle	Two Grid	V- Cycle
7^2	6	6	6	6	6	6	6	6
15^2	6	6	6	6	6	6	6	6
31^2	6	6	6	6	6	6	6	6
63^2	6	6	6	6	6	6	6	6
127^2	6	6	6	6	6	6	6	6

CONCLUSION AND PERSPECTIVES

The purpose of this thesis relied in showing the crucial role played the symbol of the matrix-sequence arising from the discretization of PDEs in providing the necessary information for analysing the spectra of this sequence of matrices and in developing an appropriate fast method to solve the linear problem associated. Now, we will take a quick look at what we have done in this thesis and then we will mention some of open problems.

- **Chapter 2:** We provided the basic tools in order to deal with Toeplitz matrices sequences. In particular we defined the asymptotic distribution of matrix sequence in the sense of eigenvalues and singular values, followed by the notion of zero-distributed sequence. Furthermore, we introduced the concept of Toeplitz and Circulant structures and we concluded with the asymptotic notion of GLT-sequences.
- **Chapter 3:** We considered a class of elliptic partial differential equations with Dirichlet boundary conditions, where the operator was $\operatorname{div}(-a(\mathbf{x})\nabla\cdot)$ with a continuous and positive on $\bar{\Omega}$. For the numerical approximation, we employed the classical \mathbb{P}_k Finite Element Method, in the case of Friedrichs-Keller triangulations, which led to a sequence of matrices of increasing size. In order to analyse the spectral properties of the resulting matrices, we determined the associated spectral symbol, which is a function describing the spectral distribution (in the Weyl sense) when the matrix-size tends to infinity. We studied in detail the case of constant coefficients and we have given

a brief account in the more involved case of variable coefficients. The mathematical tools stem out from the Toeplitz technology and from the rather new theory of GLT matrix-sequences. Numerical results are shown for a practical evidence of the theoretical findings.

- **Chapter 4:** We considered multigrid strategies for the resolution of linear systems arising from the \mathbb{Q}_k Finite Elements approximation of one- and higher-dimensional elliptic partial differential equations with Dirichlet boundary conditions and where the operator is $\operatorname{div}(-a(\mathbf{x})\nabla\cdot)$, with a continuous and positive over $\bar{\Omega}$, Ω being an open and bounded subset of \mathbb{R}^d . While the analysis is in one dimension, the numerics are displayed in a higher dimension $d \geq 2$, showing an optimal behaviour in terms of the dependency on the matrix size and a substantial robustness with respect to the dimensionality d and to the polynomial degree k , (see Remark 4.3.2).

Now, we list some perspectives that will be considered in the future researches:

1. It would be valuable to find a unified formula for the symbols of the \mathbb{P}_k over a d dimensional cube for every k, d presented in Chapter 3 as done for the case of \mathbb{Q}_k discretizations [40].
2. In Chapter 4, we noticed that the symbol of our projector $\mathbf{p}_{\mathbb{Q}_k}$ satisfies the conditions set in Items (A) and (B), while Condition (C) is violated. We can see from the mathematical derivations in [24] that the latter condition is, in fact, a technical one. We believe that condition (C) can be replaced with a less restricted one, presumably in accordance with Remark 4.3.1.
3. More in general, our GLT tools are quite broad and show a remarkable versatility. Thus as a general claim, we think that the same techniques could be used in imaging and inverse problems, since also in this context the spectral analysis and the study of ill-conditioned subspaces are of key importance, (see [70]).

BIBLIOGRAPHY

- [1] ARICO, A., DONATELLI, M., AND CAPIZZANO-SERRA, S. V-cycle optimal convergence for certain (multilevel) structured linear systems. *SIAM Journal on Matrix Analysis and Applications* 26, 1 (2004), 186–214.
- [2] BARBARINO, G., BIANCHI, D., AND GARONI, C. Constructive approach to the monotone rearrangement of functions. *Expositiones Mathematicae* 40, 1 (2022), 155–175.
- [3] BARBARINO, G., GARONI, C., AND SERRA-CAPIZZANO, S. Block generalized locally Toeplitz sequences: theory and applications in the multidimensional case. *Electronic Transactions on Numerical Analysis* 53 (2020), 113–216.
- [4] BARBARINO, G., GARONI, C., AND SERRA-CAPIZZANO, S. Block generalized locally Toeplitz sequences: theory and applications in the unidimensional case. *Electronic Transactions on Numerical Analysis* 53 (2020), 28–112.
- [5] BECKERMANN, B., AND KUIJLAARS, A. B. Superlinear convergence of conjugate gradients. *SIAM Journal on Numerical Analysis* 39, 1 (2001), 300–329.
- [6] BECKERMANN, B., AND SERRA-CAPIZZANO, S. On the asymptotic spectrum of finite element matrix sequences. *SIAM Journal on Numerical Analysis* 45, 2 (2007), 746–769.

- [7] BENEDUSI, P., GARONI, C., KRAUSE, R., LI, X., AND SERRA-CAPIZZANO, S. Space-time FE-DG discretization of the anisotropic diffusion equation in any dimension: the spectral symbol. *SIAM Journal on Matrix Analysis and Applications* 39, 3 (2018), 1383–1420.
- [8] BHATIA, R. *Matrix Analysis*. Springer-Verlag New York, 1997.
- [9] BINI, D. A., IANNAZZO, B., AND MEINI, B. *Numerical solution of algebraic Riccati equations*. SIAM, 2011.
- [10] BINI, D. A., LATOUCHE, G., AND MEINI, B. *Numerical methods for structured Markov chains*. Oxford University Press, 2005.
- [11] BÖTTCHER, A., AND GRUDSKY, S. M. *Toeplitz matrices, asymptotic linear algebra and functional analysis*, vol. 67. Springer, 2000.
- [12] BÖTTCHER, A., AND SILBERMANN, B. *Introduction to Large Truncated Toeplitz Matrices*. Springer Science & Business Media, 1999.
- [13] BRANDT, A. Multi-level adaptive solutions to boundary-value problems. *Mathematics of Computation* 31, 138 (1977), 333–390.
- [14] BRIGGS, W. L., HENSON, V. E., AND MCCORMICK, S. F. *A multigrid tutorial*. SIAM, 2000.
- [15] BUNCH, J. R. Stability of methods for solving Toeplitz systems of equations. *SIAM Journal on Scientific and Statistical Computing* 6, 2 (1985), 349–364.
- [16] CHAN, R. H., AND NG, M. K. Conjugate Gradient methods for Toeplitz systems. *SIAM Review* 38, 3 (1996), 427–482.
- [17] CHAN, R. H., AND YEUNG, M.-C. Circulant preconditioners for Toeplitz matrices with positive continuous generating functions. *Mathematics of Computation* 58, 197 (1992), 233–240.
- [18] CIARLET, P. G. *Introduction a l'analyse numerique matricielle et a l'optimisation PG Ciarlet*. masson, 1988.
- [19] CIARLET, P. G. *The finite element method for elliptic problems*. SIAM, 2002.

- [20] COTTRELL, J. A., HUGHES, T. J., AND BAZILEVS, Y. *Isogeometric analysis: toward integration of CAD and FEA*. John Wiley & Sons, 2009.
- [21] COTTRELL, J. A., REALI, A., BAZILEVS, Y., AND HUGHES, T. J. Isogeometric analysis of structural vibrations. *Computer Methods in Applied Mechanics and Engineering* 195, 41-43 (2006), 5257–5296.
- [22] DEL PRETE, V., DI BENEDETTO, F., DONATELLI, M., AND SERRA-CAPIZZANO, S. Symbol approach in a signal-restoration problem involving block Toeplitz matrices. *Journal of Computational and Applied Mathematics* 272 (2014), 399–416.
- [23] DI BENEDETTO, F., FIORENTINO, G., AND SERRA-CAPIZZANO, S. CG preconditioning for Toeplitz matrices. *Computers & Mathematics with Applications* 25, 6 (1993), 35–45.
- [24] DONATELLI, M., FERRARI, P., FURCI, I., SERRA-CAPIZZANO, S., AND SESANA, D. Multigrid methods for block-Toeplitz linear systems: convergence analysis and applications. *Numerical Linear Algebra with Applications* 28, 4 (2021), e2356.
- [25] DONATELLI, M., GARONI, C., MANNI, C., SERRA-CAPIZZANO, S., AND SPELEERS, H. Robust and optimal multi-iterative techniques for IgA collocation linear systems. *Computer Methods in Applied Mechanics and Engineering* 284 (2015), 1120–1146.
- [26] DONATELLI, M., GARONI, C., MANNI, C., SERRA-CAPIZZANO, S., AND SPELEERS, H. Robust and optimal multi-iterative techniques for IgA Galerkin linear systems. *Computer Methods in Applied Mechanics and Engineering* 284 (2015), 230–264.
- [27] DONATELLI, M., GARONI, C., MANNI, C., SERRA-CAPIZZANO, S., AND SPELEERS, H. Spectral analysis and spectral symbol of matrices in isogeometric collocation methods. *Mathematics of Computation* 85, 300 (2016), 1639–1680.

- [28] DONATELLI, M., GARONI, C., MANNI, C., SERRA-CAPIZZANO, S., AND SPELEERS, H. Symbol-based multigrid methods for Galerkin B-spline isogeometric analysis. *SIAM Journal on Numerical Analysis* 55, 1 (2017), 31–62.
- [29] DONATELLI, M., MOLTENI, M., PENNATI, V., AND SERRA-CAPIZZANO, S. Multigrid methods for cubic spline solution of two point (and 2D) boundary value problems. *Applied Numerical Mathematics* 104 (2016), 15–29.
- [30] DOROSTKAR, A., NEYTCHIEVA, M., AND SERRA-CAPIZZANO, S. Spectral analysis of coupled PDEs and of their Schur complements via generalized locally Toeplitz sequences in 2D. *Computer Methods in Applied Mechanics and Engineering* 309 (2016), 74–105.
- [31] ENGL, H. W., HANKE, M., AND NEUBAUER, A. *Regularization of Inverse Problems*, vol. 375. Springer Science & Business Media, 2000.
- [32] ESTATICO, C., AND SERRA-CAPIZZANO, S. Superoptimal approximation for unbounded symbols. *Linear Algebra and its Applications* 428, 2-3 (2008), 564–585.
- [33] FERRARI, P., RAHLA, R. I., TABLINO-POSSIO, C., BELHAJ, S., AND SERRA-CAPIZZANO, S. Multigrid for \mathbf{Q}_k Finite Element Matrices using a (block) Toeplitz symbol approach. *Mathematics* 8, 1 (2020), 5.
- [34] FIORENTINO, G., AND SERRA-CAPIZZANO, S. Multigrid methods for Toeplitz matrices. *Calcolo* 28, 3-4 (1991), 283–305.
- [35] FORTIN, M., AND BREZZI, F. *Mixed and hybrid finite element methods*. New York: Springer-Verlag, 1991.
- [36] GARONI, C. *Structured matrices coming from PDE approximation theory: spectral analysis, spectral symbol and design of fast iterative solvers*. PhD thesis, Università degli Studi dell’Insubria, 2014.
- [37] GARONI, C., MANNI, C., PELOSI, F., SERRA-CAPIZZANO, S., AND SPELEERS, H. On the spectrum of stiffness matrices arising from isogeometric analysis. *Numerische Mathematik* 127, 4 (2014), 751–799.

- [38] GARONI, C., AND SERRA-CAPIZZANO, S. *Generalized Locally Toeplitz sequences: Theory and applications*, vol. 1. Springer, 2017.
- [39] GARONI, C., AND SERRA-CAPIZZANO, S. *Generalized Locally Toeplitz sequences: Theory and applications*, vol. 2. Springer, 2018.
- [40] GARONI, C., SERRA-CAPIZZANO, S., AND SESANA, D. Spectral analysis and spectral symbol of d -variate \mathbf{Q}_p lagrangian FEM stiffness matrices. *SIAM Journal on Matrix Analysis and Applications* 36, 3 (2015), 1100–1128.
- [41] GARONI, C., SERRA-CAPIZZANO, S., AND SESANA, D. Tools for determining the asymptotic spectral distribution of non-Hermitian perturbations of Hermitian matrix-sequences and applications. *Integral Equations and Operator Theory* 81, 2 (2015), 213–225.
- [42] GARONI, C., SERRA-CAPIZZANO, S., AND SESANA, D. Block Generalized Locally Toeplitz sequences: topological construction, spectral distribution results, and star-algebra structure. In *Structured Matrices in Numerical Linear Algebra*. Springer, 2019, pp. 59–79.
- [43] GARONI, C., SERRA-CAPIZZANO, S., AND SESANA, D. Block Locally Toeplitz sequences: construction and properties. In *Structured Matrices in Numerical Linear Algebra*. Springer, 2019, pp. 25–58.
- [44] GARONI, C., SPELEERS, H., EKSTRÖM, S.-E., REALI, A., SERRA-CAPIZZANO, S., AND HUGHES, T. J. Symbol-based analysis of finite element and isogeometric B-spline discretizations of eigenvalue problems: Exposition and review. *Archives of Computational Methods in Engineering* 26, 5 (2019), 1639–1690.
- [45] GOLINSKII, L., AND SERRA-CAPIZZANO, S. The asymptotic properties of the spectrum of nonsymmetrically perturbed Jacobi matrix sequences. *Journal of Approximation Theory* 144, 1 (2007), 84–102.
- [46] GOLUB, G., AND VAN LOAN, C. Matrix computations 4th edition the johns hopkins university press. *Baltimore, MD* (2013).
- [47] GRENANDER, U. *Toeplitz Forms and Their Applications*, 2 ed. Chelsea Pub Co, 1984.

- [48] HACKBUSCH, W. *Multi-grid methods and applications*. Springer Series in Computational Mathematics. Springer, 1985.
- [49] HACKBUSCH, W. *Iterative solution of large sparse systems of equations*, vol. 95. Springer, 1994.
- [50] HANSEN, P. C., NAGY, J. G., AND O’LEARY, D. P. *Deblurring images: matrices, spectra, and filtering*. SIAM, 2006.
- [51] HUGHES, T. J., EVANS, J. A., AND REALI, A. Finite element and NURBS approximations of eigenvalue, boundary-value, and initial-value problems. *Computer Methods in Applied Mechanics and Engineering* 272 (2014), 290–320.
- [52] HUGHES, T. J., REALI, A., AND SANGALLI, G. Duality and unified analysis of discrete approximations in structural dynamics and wave propagation: comparison of p-method finite elements with k-method NURBS. *Computer Methods in Applied Mechanics and Engineering* 197, 49-50 (2008), 4104–4124.
- [53] HWANG, S.-G. Cauchy’s interlace theorem for eigenvalues of Hermitian matrices. *The American Mathematical Monthly* 111, 2 (2004), 157–159.
- [54] MAZZA, M., RATNANI, A., AND SERRA-CAPIZZANO, S. Spectral analysis and spectral symbol for the 2d curl-curl (stabilized) operator with applications to the related iterative solutions. *Mathematics of Computation* 88, 317 (2019), 1155–1188.
- [55] MOROZOV, S., SERRA-CAPIZZANO, S., AND TYRTYSHNIKOV, E. Computation of asymptotic spectral distributions for sequences of grid operators. *Computational Mathematics and Mathematical Physics* 60, 11 (2020), 1761–1777.
- [56] NG, M. K. *Iterative methods for Toeplitz systems*. Numerical Mathematics and Scie, 2004.
- [57] QUARTERONI, A. *Numerical Models for Differential Problems*, vol. 16. Springer, 2017.

- [58] RAHLA, R. I., SERRA-CAPIZZANO, S., AND TABLINO-POSSIO, C. Spectral analysis of \mathbb{P}_k Finite Element matrices in the case of Friedrichs–Keller triangulations via Generalized Locally Toeplitz technology. *Numerical Linear Algebra with Applications* 27, 4 (2020), e2302.
- [59] REALI, A. An isogeometric analysis approach for the study of structural vibrations. *Journal of Earthquake Engineering* 10, spec01 (2006), 1–30.
- [60] RUGE, J. W., AND STÜBEN, K. Algebraic multigrid. In *Multigrid methods*. SIAM, 1987, pp. 73–130.
- [61] RUSSO, A., SERRA-CAPIZZANO, S., AND TABLINO-POSSIO, C. Quasi-optimal preconditioners for finite element approximations of diffusion dominated convection–diffusion equations on (nearly) equilateral triangle meshes. *Numerical Linear Algebra with Applications* 22, 1 (2015), 123–144.
- [62] SAAD, Y. *Iterative methods for sparse linear systems*. SIAM, 2003.
- [63] SCHWAB, C. *p- and hp-Finite Element Methods - Theory and Applications in solid and fluid mechanics*. Oxford Univ. Press, 1998.
- [64] SERRA-CAPIZZANO, S. Multi-iterative methods. *Computers & Mathematics with Applications* 26, 4 (1993), 65–87.
- [65] SERRA-CAPIZZANO, S. Asymptotic results on the spectra of block Toeplitz preconditioned matrices. *SIAM Journal on Matrix Analysis and Applications* 20, 1 (1998), 31–44.
- [66] SERRA-CAPIZZANO, S. On the extreme eigenvalues of Hermitian (block) Toeplitz matrices. *Linear Algebra and its Applications* 270, 1-3 (1998), 109–129.
- [67] SERRA-CAPIZZANO, S. A Korovkin-type theory for finite Toeplitz operators via matrix algebras. *Numerische Mathematik* 82, 1 (1999), 117–142.
- [68] SERRA-CAPIZZANO, S. Superlinear PCG methods for symmetric Toeplitz systems. *Mathematics of Computation* 68, 226 (1999), 793–803.

- [69] SERRA-CAPIZZANO, S. Generalized Locally Toeplitz sequences: spectral analysis and applications to discretized partial differential equations. *Linear Algebra and its Applications* 366 (2003), 371–402.
- [70] SERRA-CAPIZZANO, S. A note on antireflective boundary conditions and fast deblurring models. *SIAM Journal on Scientific Computing* 25, 4 (2004), 1307–1325.
- [71] SERRA-CAPIZZANO, S. The GLT class as a Generalized Fourier analysis and applications. *Linear Algebra and its Applications* 419, 1 (2006), 180–233.
- [72] SERRA-CAPIZZANO, S., AND TABLINO-POSSIO, C. Finite element matrix sequences: the case of rectangular domains. *Numerical Algorithms* 28, 1 (2001), 309–327.
- [73] SERRA-CAPIZZANO, S., AND TABLINO-POSSIO, C. Multigrid methods for multilevel circulant matrices. *SIAM Journal on Scientific Computing* 26, 1 (2004), 55–85.
- [74] STRANG, G. A proposal for Toeplitz matrix calculations. *Studies in Applied Mathematics* 74, 2 (1986), 171–176.
- [75] TILLI, P. A note on the spectral distribution of Toeplitz matrices. *Linear and Multilinear Algebra* 45, 2-3 (1998), 147–159.
- [76] TOEPLITZ, O. Zur theorie der quadratischen und bilinearen formen von unendlichvielen veränderlichen. *Mathematische Annalen* 70, 3 (1911), 351–376.
- [77] TYRTYSHNIKOV, E. A unifying approach to some old and new theorems on distribution and clustering. *Linear Algebra and its Applications* 232 (1996), 1–43.